Observing giant panda habitat and forage abundance from space

Wang, Tiejun

Observing giant panda habitat and forage abundance from space

Wang, Tiejun

Table of contents

Summary

Giant pandas are obligate bamboo grazers. The bamboos favoured by giant pandas are typical forest understorey plants. Therefore, the availability and abundance of understorey bamboo is a key factor in determining the quantity and quality of giant panda food resources. However, there is little or no information about the spatial distribution or abundance of bamboo underneath the forest canopy, due to the limitations of traditional ground survey and remote sensing classification techniques. In this regard, the development of methods that can predict the understorey bamboo spatial distribution and cover abundance is critical for an improved understanding of the habitat, foraging behaviour and distribution of giant pandas, as well as facilitating an optimal conservation strategy for this endangered species.

The objectives of this study were to develop innovative methods in remote sensing and GIS for estimating the giant panda habitat and forage abundance, and to explain the altitudinal migration and the spatial distribution of giant pandas in the fragmented forest landscape.

It was concluded that 1) the vegetation indices derived from winter (leaf-off) satellite images can be successfully used to predict the distribution of evergreen understorey bamboo in a deciduous-dominated forest, 2) winter is the optimal season for quantifying the coverage of evergreen understorey bamboo in a mixed temperate forest, regardless of the classification methods used, 3) a higher mapping accuracy for understorey bamboo in a coniferous-dominated forest can be achieved by using an integrated neural network and expert system algorithm, 4) the altitudinal migration patterns of sympatric giant pandas and golden takins are related to satellite-derived plant phenology (a surrogate of food quality) and bamboo abundance (a surrogate of food quantity), 5) the driving force behind the seasonal vertical migration of giant pandas is the occurrence of bamboo shoots and the temperature variation along an altitudinal gradient, 6) the satellite-derived forest patches occupied by giant pandas were significantly larger and more contiguous than patches where giant pandas were not recorded, indicating that giant pandas appear sensitive to patch size and isolation effects associated with forest fragmentation.

Overall, the study has been shown the potential of satellite remote sensing to map giant panda habitat and forage (i.e., understorey bamboo) abundance. The results are important for understanding the foraging behaviour and the spatial distribution of giant pandas, as well as the evaluation and modelling of giant panda habitat in order to guide decision-making on giant panda conservation.

Samenvatting

Het hoofdvoedsel van de reuzenpanda is bamboe, normaal gesproken te vinden in de bosondergroei. Daarom is de beschikbaarheid en overvloed van de bamboe hier van groot belang voor het vaststellen van de hoeveelheid en kwaliteit van de voedselreserves. Er is echter nauwelijks informatie beschikbaar over de spatiale verdeling en overvloed van bamboe op de bosvloer; dit is te wijten aan beperkingen van de traditionele kartering en remote sensing classificatietechnieken. Hierop gelet is het ontwikkelen van methoden voor het voorspellen van de bamboeverspreiding in de ondergroei cruciaal voor het beter begrijpen van de habitat, het voedselzoekgedrag en de verspreiding van reuzenpanda's. De methoden helpen ook bij het ontwikkelen van een optimale beheersstrategie voor deze bedreigde diersoort.

Doelen van deze studie zijn het ontwerpen van innovatieve methoden voor het bepalen van de habitat en voedselvoorraad van reuzenpanda's met behulp van remote sensing en GIS, alsook het vinden van een verklaring voor de hoogte migratie en de spatiale verdeling van de reuzenpanda in gefragmenteerd bos.

Geconcludeerd wordt dat 1) de vegetatie indices (satelliet) uit het winterseizoen (bladvrij) met succes kunnen worden gebruikt om de bamboeondergroei verdeling in loofrijke bossen te voorspellen, 2) het winterseizoen optimaal geschikt is om de bamboe in gematigd, gemengd bos te bepalen ongeacht de classificatiemethode, 3) een grotere karteringnauwkeurigheid kan worden bereikt van ondergroei bamboe in een naaldbos door een algoritme waarin een neuraal netwerk en expertsysteem worden geïntegreerd, 4) de hoogtemigratiepatronen van de sympatrische reuzenpanda en gouden rundergems verband houden met de van de satellietbeelden afgeleide plantfenologie (voedsel kwaliteit) en de bamboe (voedsel kwantiteit), 5) de drijvende kracht achter de seizoensbepaalde hoogtemigratie van de reuzenpanda wordt bepaald door de aanwezigheid van bamboescheuten en de verticale temperatuurgradiënt, 6) satelliet bepaalde stukken bos met panda's significant groter en minder fragmentarisch zijn dan die zonder, wat op een gevoeligheid voor grootte van de stukken bos en isoleringeffecten door fragmentatie duidt.

Algemeen heeft de studie de kracht van remote sensing (satelliet) aangetoond bij het in kaart brengen van de panda habitat en bamboe. De resultaten zijn belangrijk voor begrip van het voedselzoekgedrag en de spatiale verdeling van de reuzenpanda en voor de evaluatie en modellering van de reuzenpanda habitat om te komen tot een beleidsontwikkeling voor milieubeheer van de reuzenpanda.

To all the rangers
who dedicate their life
towards the conservation of giant pandas in China

Acknowledgements

Chapter 1

General introduction

BACKGROUND

There are probably no more than a dozen of the approximately 4,000 mammals that are recognized by the vast majority of people, regardless of where they live and what language they speak. Most people, if ever exposed, remember and are able to name elephants, tigers, bears, rhinoceroses and gorillas. The giant panda (*Ailuropoda melanoleuca*) probably tops this list of charismatic mega-fauna in terms of attractiveness and mass appeal. Unfortunately, nowadays the giant panda is listed as one of the most endangered mammals in the world due to its small population size and continued decline of its habitat (IUCN 2007).

Fossil remains show that the giant panda originally occurred throughout most of southern and eastern China, northern Myanmar, and northern Vietnam (Thue 1984, Pan et al., 1988). Historical records from ancient China suggest that as recently as 2000 years ago giant pandas still inhabited an area covered by five modern Chinese provinces (Henan, Hubei, Hunan, Guizhou and Yunnan) where they do not occur today (Wen and He 1981). By 1900, giant pandas occurred only in the Qinling Mountains and along the eastern edge of the Tibetan plateau. Soon afterwards the expansion of agriculture upstream along principal river valleys divided this pattern of occupancy further into regions in five mountain ranges (i.e., Minshan, Qionglai, Liangshan, Xiangling and Qinling) in China's Gansu, Shaanxi and Sichuan provinces (Hu 1985).

In order to assess the status of giant panda population and its habitat, three national-level ground surveys were conducted by the Chinese government in 1974-1977, 1985-1988 and 1999-2002, respectively (State Forestry Administration 2006). In addition, a number of local surveys were also carried out at different levels. As a result, large amounts of money and labour have been invested in these surveys. For instance, 3,000 people were involved in the first national panda survey, and more than two million dollars were spent in the third national panda survey. The survey results showed a dramatic change in giant panda population and its habitat. For instance, the first national survey in 1970s showed that there were roughly 2,500 wild pandas living in 29,500 km^2 of forest; the second national survey in 1980s estimated that between 1,000 and 1,100 animals were alive in an area of 14,000 km^2 of forest; and the third national survey in 1990s estimated that there were approximately 1,600 pandas living in the wild, and the total giant panda habitat is about 23,000 km^2. The results of the three national panda surveys are incomparable due to different survey extent, intensity, techniques as well as political reasons (State Forestry Administration 2006). For example, the first survey covered an area of 43 counties; the second survey only sampled 34 counties; and the third survey investigated an area of 45 counties. Despite plausible panda numbers and its

habitat size, one thing the surveys have confirmed that the range of today's giant pandas is subdivided into about 24 small populations separated by mountain ranges, rivers, roads, forest clearings and human settlements. Some populations have fewer than 20 pandas, making them demographically and genetically vulnerable (Mackinnon et al., 1989, O'Brien et al., 1994, Pan et al., 2001, State Forestry Administration 2006).

PROBLEM DEFINITION

Challenges in mapping giant panda forage distribution and cover abundance – Giant pandas are obligate bamboo grazers and they select habitat primarily on the basis of suitability for foraging (Schaller et al., 1985). Additionally, the bamboos favoured by giant pandas are typical forest understorey plants. Therefore, the availability and abundance of understorey bamboo is a key factor in determining the quantity and quality of panda habitat. However, our understanding of understorey bamboo spatial distribution at local and national levels is limited, as previous studies focused on ground surveys executed over small and intensively studied sites. In addition the complexity of bamboo distribution, influenced by human activities (clear cutting and fire), as well as periodical mass flowering and die-off (Reid et al., 1989), makes the up-scaling to large areas through conventional point-based environmental modelling extremely difficult. Although many studies have been conducted in the past several decades to map and assess the giant panda habitat using traditional ground survey and remote sensing techniques (De Wulf et al., 1988, Liu et al., 2001, Loucks et al., 2003), in these studies, the researchers assumed that the distribution of understorey bamboo has a constant spatial cover. All authors noted that the unsuitable habitat would be underestimated, because critical information (i.e., bamboo distribution) affecting giant panda habitat was not available for the entire region. Linderman et al., (2005) estimated that in the Wolong Nature Reserve (one of the largest panda reserves in China) the potential panda habitat decreased by 29-52% after information about bamboo distribution was incorporated in the analyses. The scarcity of extensive, detailed, as well as reliable information about bamboo distribution and its abundance impedes the implementation of panda conservation strategies such as habitat restoration, simply because managers do not know 'what is where'. Consequently, a practical approach to predict the understorey bamboo from remote sensing data is needed for more accurate habitat analysis.

Understanding of the underlying causes of the altitudinal migration of giant pandas – Animal migration is one of nature's most visible and widespread phenomena (Baker 1978). Understanding of the causes of animal migration can

yield valuable insights into the variables that determine their life histories, habitat requirements, and foraging strategies (Richter and Cumming 2006). Giant pandas and golden takins (*Budorcas taxicolor bedfordi*) are both large "IUCN red-listed" mammals, and occur sympatrically throughout the southern part of the Qinling Mountains in China (Pan et al., 1988, Wu et al., 1990). Many observers have reported that both species have the habit of altitudinal migration in a mixed forest-bamboo landscape (Liu et al., 2002, Zeng et al., 2008). Although previous studies have indicated that the migration patterns of giant pandas and golden takins appear different, little is known about these differences in relation to the environmental factors. Three drivers of the altitudinal migration of these two species have been suggested (Pan et al., 1988, Yong et al., 1994, Zeng et al., 2008): (1) to seek more abundant or nutritious forage, (2) to search for optimum temperature conditions, or (3) to escape insect harassment. However, there is no quantitative research testing of these hypotheses, as continuous field observations of environmental conditions are not easily available. We were interested in how ecological factors affect patterns of altitudinal migration. In particular, we focused on how food availability (i.e., food quality and quantity) might cause differences in migration patterns between species.

Understanding the spatial distribution of giant pandas in relation to forest fragmentation – Knowledge of the giant panda distribution is fundamental to conserve this endangered species and ensure its long-term survival. However, little is known about the distribution pattern of the giant pandas at a regional scale, as previous studies have focused on the relationship of giant panda occurrence and micro-environmental factors at the site-based level. Moreover, although habitat loss and fragmentation have already been recognized as major threats that pose a great danger for giant panda population (Hu 2001, Pan et al., 2001), no quantitative and systematic research has been undertaken due to the low effectiveness of conventional methods in generalization of relationships between habitat fragmentation and giant panda population. In other words, to date no studies have attempted to address the giant panda distribution with relation to the spatial configuration of forested landscapes, e.g., forest patch size, patch isolation and aggregation. There is a need to uncover the underlying relationship between the heterogeneity of the forest landscape and the distribution pattern of giant pandas for more effective conservation of the wild giant panda population.

RESEARCH OBJECTIVES AND QUESTIONS

The objectives of this study were to develop innovative methods in remote sensing and GIS for estimating the giant panda habitat and forage abundance, and to explain the altitudinal migration and the spatial distribution of giant pandas in the fragmented forest landscape. In order to achieve the objectives of this study, the following research questions are formulated:

1) Can vegetation indices derived from winter (leaf-off) satellite images be successfully used to predict evergreen understorey bamboo in a deciduous-dominated or mixed forest? If so, does a statistically significant difference exist in bamboo mapping accuracy between the vegetation index thresholds-based decision tree approach and the traditional multispectral bands-based classifiers?

2) Is it possible to develop a new approach, an integrated neural network and expert system algorithm, based on remote sensing and GIS in order to achieve a higher accuracy for mapping evergreen or semi-evergreen understorey bamboo species in a coniferous-dominated forest?

3) Does the seasonal movement or altitudinal migration of giant pandas correlate with satellite (MODIS NDVI)-derived plant phenology?

4) Can satellite-derived plant phenology (a surrogate of food quality) and bamboo abundance (a surrogate of food quantity) explain the difference in altitudinal migration patterns between the giant pandas and the golden takins?

5) Which landscape metrics characterize fragmentation of forests occupied by giant pandas? What are the relationships between the distribution of giant pandas and the forest fragmentation?

THE STUDY AREA

Considering the specific research questions and the availability of material, the study was conducted at three different landscape levels, from local (Foping Nature Reserve), to regional (Qinling Mountains), and to national (China).

The Foping National Nature Reserve is located between 33°32´-33°45´N, 107°40´-107°55´E on the south slope of the Qinling Mountains. The reserve was established in 1978, and is dedicated to the conservation of the giant panda and its habitat. The reserve covers an area of 294 km² and with elevation ranges from about 1,000 to 2,900 m. It is one of the few Chinese reserves with intact ecosystems, and is renowned for having the highest density of giant pandas in China, and thus of the world. An estimated 76 giant pandas live in the reserve.

The cool, wet climate and fertile soils in Foping Nature Reserve provides ideal conditions for bamboo to thrive in the understorey of multiple vegetation types. Two bamboo species, *Bashania fargesii* (below 2,000 m) and *Fargesia qinlingensis* (above 2,000 m), dominate the forest understorey and form the principle food source for the giant pandas in the reserve.

Figure 1 Map showing the present giant panda habitats in Shaanxi, Gansu and Sichuan provinces of China. Location of study area of the Qinling Mountains is indicated with a rectangle box.

The Qinling Mountain Range forms a natural boundary between northern and southern China. The north-facing slopes drain to the Yellow River and the south-facing slopes into Yangtze. The current study focus on a region between 33°3′-34°4′N, 106°4′-108°8′E in the western part of the Qinling Mountains. It covers an area of 20,000 km² and with elevation ranges from about 560 to 3,700 m. According to the latest national panda survey, the Qinling Mountains harbour approximately 300 giant pandas which account for almost 20% of the total populations in China. There are three major vegetation zones in the Qinling Mountains. Lower elevations are subtropical evergreen and deciduous broadleaf forests. At mid-elevation are temperate deciduous broadleaf and subalpine needleleaf forests. The highest elevations are subalpine scrub meadow. In the absence of humans, bamboo would be distributed between 500 and 3,100 m elevation mainly on the south-facing slopes and partly on the

north-facing slopes. Five major roads have been constructed passing through the panda distribution area in the Qinling Mountains.

The entire giant panda distribution area is located between 28°12´-34°1´N, 106°4´-108°8´E, which incorporates 45 administrative counties in the provinces of Shaanxi, Gansu and Sichuan in China. The total area encompasses about 160,000 km², with an elevation of 560 to 6,500 m. The study area includes five mountain ranges along the eastern edge of the Qinghai-Tibetan Plateau: Qinling, Minshan, Qionglai, Xiangling, and Liangshan. The northernmost area where the giant panda occurs at present is the Qinling region, which is covered with deciduous broadleaf and subalpine coniferous forests. The density of giant pandas is highest in the Qinling Mountains. The Minshan and Qionglai regions, with a cool and humid climate, include the largest extant panda habitat in China. The Xiangling and Liangshan regions form the southernmost panda distribution area, dominated by evergreen broadleaf and coniferous forests.
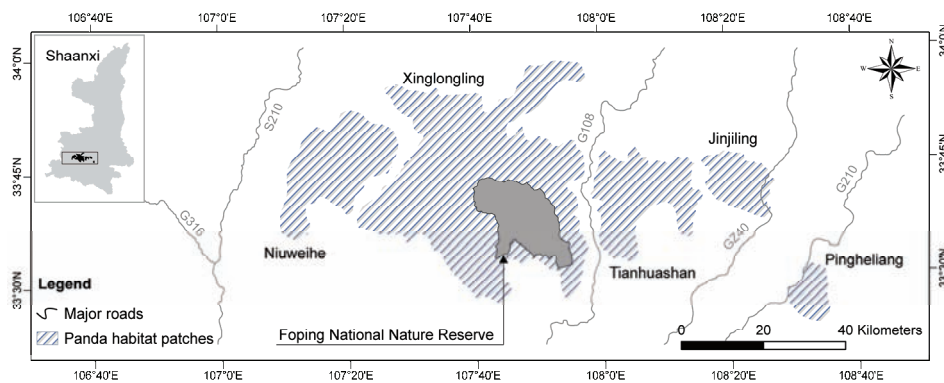
Figure 2 Map showing the location of the Foping National Nature Reserve (dark grey) in the Qinling Mountains. Five habitat patches of the giant panda and five major roads in the Qinling Mountains are displayed.

OUTLINE OF THESIS

This thesis constitutes a collection of 5 papers that have been submitted to peer-reviewed international journals. Out of these 5 papers, 3 papers have been accepted for publication and the remaining 2 papers are under review. Each paper has been presented as a stand-alone chapter and deals with one specific research question. To maintain a consistent style throughout the thesis, the abbreviations, names and referencing style were standardized, and may be

different from the published or submitted papers. However, deviations from the submitted papers were minimized, and no sections were removed, revised, or added to the chapters. Chapter 1 provides a brief research background, clarifies the research problems, then formulates the objectives and questions of research, and describe the study area. Chapter 2 presents a new approach that combines forest phenology and Landsat vegetation indices to estimate evergreen understorey bamboo coverage in a deciduous-dominated forest. Chapter 3 develops an integrated neural network and expert system algorithm to improve the mapping accuracy for evergreen or semi-evergreen understorey bamboo species in a coniferous-dominated forest. Chapter 4 presents a method to display vegetation dynamics as captured by the MODIS NDVI along natural gradients and to visualise and test correlations between vegetation phenology and animal movement. Chapter 5 examines the altitudinal migration of sympatric giant pandas and golden takins in relation to satellite-derived plant phenology (a surrogate of food quality) and bamboo abundance (a surrogate of food quantity). Chapter 6 characterise the spatial distribution of giant pandas in the fragmented forest landscape of south-western China using MODIS data and landscape matrices. Finally, chapter 7 provides an overview of the research findings relevant to specific research questions stated in Chapter 1, and discuss the practical relevance of these results in the light of the development and implementation of giant panda conservation strategies.

REFERENCES

Baker, R. R. 1978. The evolutionary ecology of animal migration. Hodder and Stoughton, London.

De Wulf, R. R., R. E. Goossens, J. R. Mackinnon, and S. C. Wu. 1988. Remote Sensing for wildlife management: giant panda habitat mapping from LANDSAT MSS images. Geocarto International **1**:41-50.

Hu, J. C. 1985. Geographic and ecological distribution of the giant panda. Journal of Sichuan Normal College **6**:7-15 (in Chinese).

Hu, J. C. 2001. Research on the Giant Panda. Shanghai Scientific & Technological Education Publishers, Shanghai (in Chinese).

IUCN. 2007. 2007 IUCN Red List of Threatened Species. World Conservation Union, Gland, Switzerland.

Linderman, M., S. Bearer, L. An, Y. C. Tan, Z. Y. Ouyang, and J. G. Liu. 2005. The effects of understorey bamboo on broad-scale estimates of giant panda habitat. Biological Conservation **121**:383-390.

Liu, J. G., M. Linderman, Z. Y. Ouyang, L. An, J. Yang, and H. M. Zhang. 2001. Ecological degradation in protected areas: the case of Wolong Nature Reserve for giant pandas. Science **292**:98-101.

Liu, X. H., A. K. Skidmore, T. J. Wang, Y. G. Yong, and H. H. T. Prins. 2002. Giant panda movements in Foping nature reserve, China. Journal of Wildlife Management **66**:1179-1188.

Loucks, C. J., Z. Lu, E. Dinerstein, D. J. Wang, D. L. Fu, and H. Wang. 2001. The giant pandas of the Qinling Mountains, China: a case study in designing conservation landscapes for elevational migrants. Conservation Biology **17**:558-565.

Mackinnon, J. R. and R. R. D. Wulf. 1994. Designing protected areas for giant pandas in China. Pages 127-142 *in* R. I. Miller, editor. Mapping the diversity of nature. Chapman & Hall, London.

O'Brien, S. J., W. S. Pan, and Z. Lu. 1994. Pandas, people, and policy. Nature **369**:179-180.

Pan, W. S., Z. S. Gao, and Z. Lu. 1988. The giant panda's natural refuge in the Qinling Mountains. Peking University Press, Beijing (in Chinese).

Pan, W. S., Z. Lu, X. J. Zhu, D. Wang, H. Wang, Y. Long, D. L. Fu, and X. Zhou. 2001. The opportunity for the giant panda to exist. Peking University Press, Beijing (in Chinese).

Reid, D. G., J. C. Hu, S. Dong, W. Wang, and Y. Huang. 1989. Giant panda Ailuropoda melanoleuca behaviour and carrying capacity following a bamboo die-off. Biological Conservation **49**:85-104.

Richter, H. V. and G. S. Cumming. 2006. Food availability and annual migration of the straw-colored fruit bat (Eidolon helvum). Journal of Zoology **268**:35-44.

Schaller, G. B., J. C. Hu, W. S. Pan, and J. Zhu. 1985. The giant pandas of Wolong. University of Chicago, Chicago.

State Forestry Administration. 2006. The third national survey report on giant pandas in China. Science Press, Beijing (in Chinese).

Thue, L. V. 1984. On the distribution of Pleisticene giant panda in Vietnam. Inqua **11**:146 (in Chinese).

Wu, J. Y., Y. P. Han, H. Qu, S. X. Liu, X. M. Zhu, J. X. Jia, J. Y. Liu, and L. Zhang. 1990. The Chinese Takin. China Forestry Publishing House, Beijing (in Chinese).

Yong, Y. G., K. W. Wang, and T. J. Wang. 1994. Movement habits of the giant pandas in Foping. Acta Theriologica Sinica **14**:9-14 (in Chinese).

Zeng, Z. G., A. K. Skidmore, Y. L. Song, T. J. Wang, and H. S. Gong. 2008. Seasonal altitudinal movements of golden takin in the Qinling Mountains of China. Journal of Wildlife Management **72**:611-617.

Chapter 2

Understorey bamboo discrimination using a winter image

ABSTRACT

In this study, a new approach is presented that combines forest phenology and Landsat vegetation indices to estimate evergreen understorey bamboo coverage in a mixed temperate forest. It was found that vegetation indices, especially the normalized difference vegetation index (NDVI) derived from leaf-off (winter) images were significantly correlated with percent understorey bamboo cover for both deciduous and mixed coniferous/deciduous forests. Winter NDVI was used to map bamboo coverage using a binary decision tree classifier. A high mapping accuracy for understorey bamboo presence/absence was achieved with an overall accuracy of 89 percent (kappa=0.59). In addition, for the first time, we successfully classified three density classes of bamboo with an overall accuracy of 68 percent (kappa=0.48). These results were compared to three traditional multispectral bands-based methods (mahalanobis distance, maximum likelihood, and artificial neural networks). The highest mapping accuracy was again obtained from winter images. However, the kappa z-test showed that there was no statistical difference in accuracy between the methods. The results suggest that winter is the optimal season for quantifying the coverage of evergreen understorey bamboos in a mixed forest area, regardless of the classification methods used.

INTRODUCTION

Understorey plants are important elements of forest structure and composition, providing habitat and forage for wildlife, and contributing to flora diversity (Mckenzie and Halpern 1999, Rettie et al., 1997). Bamboos are typical understorey tree-grasses in Japanese, Chilean, and Chinese temperate and subalpine forests where they achieve a high degree of dominance (Franklin et al., 1979, Taylor and Qin 1988, Veblen 1982). Many mammals and birds rely on this special niche as sites for foraging and nesting, in which the most famous are giant panda (*Ailuropoda melanoleuca*), red panda (*Ailurus fulgens*), and golden pheasant (*Chrysolophus pictu*) (Gong et al., 2006, Reid et al., 1991, Reid et al., 2004, Schaller et al.,1985). Knowledge of understorey bamboo presence/absence and its abundance would enable wildlife managers to identify areas of suitable habitat for dependent animals and birds (Borkowski and Furubayashi 1998, Diaz et al., 2005, Liu et al., 2005, Reid et al., 2004, Warner 2002). However, our understanding of understorey bamboo spatial distribution at local and national levels is limited, as previous studies focused on ground surveys executed over small and intensively studied sites. In addition the complexity of bamboo distribution, influenced by human activities (clear cutting and fire), as well as periodical mass flowering and die-off (Reid et al., 1989), makes the up-scaling to large areas through conventional point-based environmental modelling extremely difficult. A few studies have been conducted at large landscape level. For example, the panda habitat assessment in the Wolong Nature Reserve of Sichuan (Liu et al., 2001) and the Qinling Mountains of Shaanxi (Loucks et al., 2003) in China assumed that the distribution of understorey bamboo has a constant spatial cover. In these studies the authors noted that the unsuitable habitat would be underestimated, because critical information affecting panda habitat, such as bamboo distribution, was not available for the entire region.

Remote sensing may be suitable for mapping forest understorey across large areas. For example, Morain (1986) conducted a primary investigation on understorey bamboo assessment in a Chinese panda reserve using 35 mm colour infrared air photographs (scale 1:12,000) acquired in April (leaf-off season). He reported that three types of understorey bamboo status (mixed with deciduous trees, mixed with coniferous trees, and mainly deciduous vegetation without bamboo) may be visually distinguished. By utilizing summer TM image and an unsupervised classification approach, Stenback and Congalton (1990) detected presence and absence of vegetated understorey for different canopy closures in the Sierran mixed conifer zone with an overall accuracy range from 55 to 69 percent and kappa coefficient (κ) range from 0.08 to 0.38. Linderman et al., (2004) mapped the presence and absence of understorey bamboos in a Chinese mixed temperate forest using leaf-on Landsat image and

an artificial neural network algorithm, achieving an overall mapping accuracy of 80 percent (κ value not stated). More recently, Joshi et al., (2006) developed a remotely sensed data and understorey light climate based model to predict the presence and absence of an understorey invasive species (*Chromolaena odorata*) in Nepal, and obtained an overall mapping accuracy of 74 percent (κ=0.56). These studies demonstrate that remote sensing methods can quantify understorey species. However, there are conflictive definitions of understorey species for presence and absence that make comparisons difficult, and may have biased the quality of results for particular studies. For example, the research of Stenback and Congalton (1990) defined 'presence' as greater than 50 percent vegetated cover, Linderman et al., (2004) defined "presence" as greater than 10 percent, and Joshi et al., (2006) defined an absolute presence or absence of understorey invasive species. In this study, we defined a priori three cover classes densities, viz. the bamboo absence (<1%), low bamboo cover (1-50%), and high bamboo cover (>50%). Furthermore, the phenological difference between overstorey and understorey and its impact on understorey detection has not been examined in previous studies. Our research complements and extends these analyses by comparing the difference in understorey mapping accuracy as influenced by image acquisition time i.e., phenology.

Vegetation indices (VIs) are a popular tool to relate remotely sensed data to many biophysical parameters of vegetation such as leaf area index (LAI), fractional absorption of photosynthetically active radiation (FPAR), percent green cover (Turner et al., 1999, Huete et al., 2002, Myneni et al., 2002). The cover class densities of green vegetation have been linked to vegetation indices (Dymond et al., 1992, Purevdorj et al., 1998, Wittich and Hansing 1995). Vegetation indices are physically based on the differential scattering and absorption of a green leaf, and specifically the absorption of incident red light by plant chlorophyll and scattering of incident near-infrared (NIR) radiation by plant leaves (Myneni 1995). Most of the VIs is so-called 'broadband' vegetation indices because they capture this contrast through algebraic combinations of these two spectral bands. These various combinations have been claimed to minimize and normalize the effect of external influences, such as solar irradiance changes due to the atmospheric effect (Kaufman and Tanré 1992), or variations in soil background (Huete 1988), illumination and topographic (Colby 1991, Huete 1988, Kaufman and Tanré 1992). Vegetation indices are simple and easy to use and allow operational monitoring of the Earth's vegetative cover at local, regional and global scale biomes (Townshend et al., 1991, Tucker et al., 1985).

As dense overstorey forest and co-occurrence of other understories significantly contribute to remote sensing derived vegetation indices during the growing

season, the first hypothesis for this study is that vegetation indices derived from winter (leaf-off) imagery can be used to detect the presence and absence of bamboo as well as to quantify the cover degree of evergreen understorey bamboo species.

Seasonal change is a common natural phenomenon in forested landscapes occurring on an annual basis. By considering the seasonal variation of vegetation (phenology), more accurate vegetation maps have been obtained. For example, Goodenough et al., (2001) compared classification accuracies achieved for forest classes with single leaf-on date and paired image sets of leaf-on and leaf-off condition. They concluded that the inclusion of the leaf-off data sharply delineates the signatures of the deciduous components in the imagery, resulting in increased overall classification accuracy. Townsend and Walsh (2001) classified forest wetland communities in the southeast US using a multi-temporal approach with leaf-off and leaf-on images to successfully identify mixes of deciduous and evergreen species. This approach was also used by Flores et al., (2003) to effectively estimate LAI of evergreen overstorey and the deciduous understorey component. However, such approaches have not been previously used to map and quantify evergreen understorey species. A second hypothesis for this study is that compared to the leaf-on, partial leaf-on, and partial leaf-off images, the leaf-off image consistently yields the most accurate results for mapping evergreen understorey bamboo, regardless of the classification method used.

Based on the above hypotheses, the objectives of this study were to: 1) assess whether vegetation indices derived from winter (leaf-off) imagery may successfully map understorey bamboo cover in a mixed temperate forest and, if so, then 2) to compare the mapping accuracies of the vegetation index thresholds-based decision tree approach with the traditional multispectral bands-based classifiers.

STUDY AREA

The study area, Foping Biosphere Reserve is located on the south slope of the Qinling Mountains in China (33°32´-33°45´N, 107°40´-107°55´E). The reserve covers an area of 294 km² and with elevation ranges from about 1,000 to 2,900 m (Figure 1). It is one of the few reserves for intact ecosystems, as well as the most populated giant panda habitat in China. The current research focuses on the lower elevation areas below 2,000 m. A digital elevation model (DEM) of the study area was used to mask all the images used in the study.

Forest is the major land cover and accounts for 98 percent of total land area in this reserve. The vegetation (below 2,000 m) is principally dominated by deciduous broadleaf forest, with some interspersed areas of mixed coniferous and deciduous broadleaf forests (Yue et al., 1999). The dominant deciduous broadleaf tree species are oaks (*Quercus* spp.), poplars (*Populus* spp.), and birches (*Betula* spp.) while the most common evergreen needle leaf tree species are pines (*Pinus* spp.) and fir (*Tsuga chinensis*). Canopy trees in this area leaf-out in mid April to late May, while leaf-fall is complete by mid October to early November. The midstorey and understorey layers (shrubs and saplings) are dominated by *Bashania fargesii*, *Abelia engleriana*, *Lespedeza bicolor*, and *Listea pungens*. The dominant forest floor layer (herbs) is *Carex lanceolata*. However, there are no preponderant shrubs and herbs once the bamboo dominates the forest understorey (Ren et al., 1998). The co-occurrence of other understories is depended on the cover of bamboo *Bashania fargesii*.
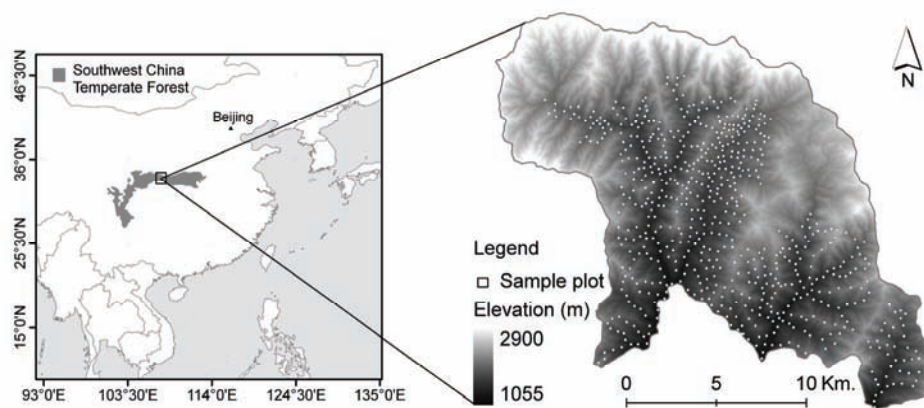
Figure 1 Location of study area in China, and the distribution of sample plots (< 2,000 m) on the DEM map of Foping Nature Reserve

The cool, wet climate and fertile soils in Foping reserve provides ideal conditions for bamboo to thrive in the understorey of multiple vegetation types. *Bashania fargesii*, a typical evergreen understorey bamboo species dominates the study area. It grows in an elevation belt between 1,000–2,000 m, where the pandas usually spend three quarters of the year (Liu et al., 2002). *B. fargesii* establish new shoots in May. Culms vary in basal diameter from 1 to 2 cm, and grow to an average height of 2.5 m. The undulating topography provides for a broad range of microclimates, which influences different growth phases of bamboo over relatively short distances. In forested areas, *B. fargesii* is

distributed in patches, ranging in size from single plants to hundreds of meters across.

METHODS

Ground Survey Data

The data used in this study were collected during field campaigns conducted as part of missions for China's Third National Giant Panda Survey between 1999 and 2000 in Foping Nature Reserve. As noted in the Introduction, evergreen bamboo is a resilient perennial which changes in area or cover very little over a period of a few years (Taylor et al., 1987). In contrast, the overstorey in this area is deciduous and exhibits dramatic seasonal variation due to leaf senescence and flush (Pan et al., 1988), with these seasonal leaf-on and leaf-off phenomena being obvious on summer and winter images respectively. In other words, the seasonal state of a pixel may be inferred from the change in the overstorey forest cover. As a consequence, there was no attempt to sample each individual (seasonal) image in the field; as such an effort would be redundant in terms of ground checking land cover. In general, the study area is inaccessible, especially due to snow in the winter months. A total of 646 sample plots (65 plots in 1999 and 581 plots in 2000) were carefully selected from the survey database based on three criteria: 1) the position of plots was below 2,000 m; 2) the horizontal distance between adjacent plots was at least 300 m; 3) a strong satellite signal was received by Garmin 12XL GPS unit, which means at least four satellites were located well above the horizon. Using the method of Ardö and Pilesjö (1992) we tested that the GPS precision was less than 10 meters for 95% of observations. A stratified random sampling based on the terrain position (i.e., valley, mid-slope, and ridge) was adopted in both surveys to ensure the representative habitat types can be collected over the mountains terrain. The sample plots were 20 m × 20 m, and were recorded where bamboo coverage was relatively homogeneous over a 60 m × 60 m area. Within the plots, many biotic and abiotic variables were measured such as location, slope aspect, slope gradient, slope position, distance to water source, tree species, average tree height, percent bamboo cover and panda signs etc. Furthermore, five subplots (2 m × 2 m) were also established within each 20 m × 20 m plot to measure the bamboo characteristics in detail, such as total culm density and proportion of old shoots, average height and basal diameter. In this study, only three variables were used which are GPS position, tree species (presence/absence of conifer), and percent bamboo cover. The bamboo cover was visually estimated in the field and assigned to one of the following classes: <1%, 1-24%, 25- 49%, 50 -74% and >74% following the methods described by (Kent and Coker 1992, Taylor and Qin 1988, State Forestry Administration 2006).

(a)

(b)

(c)

(d)

(e)
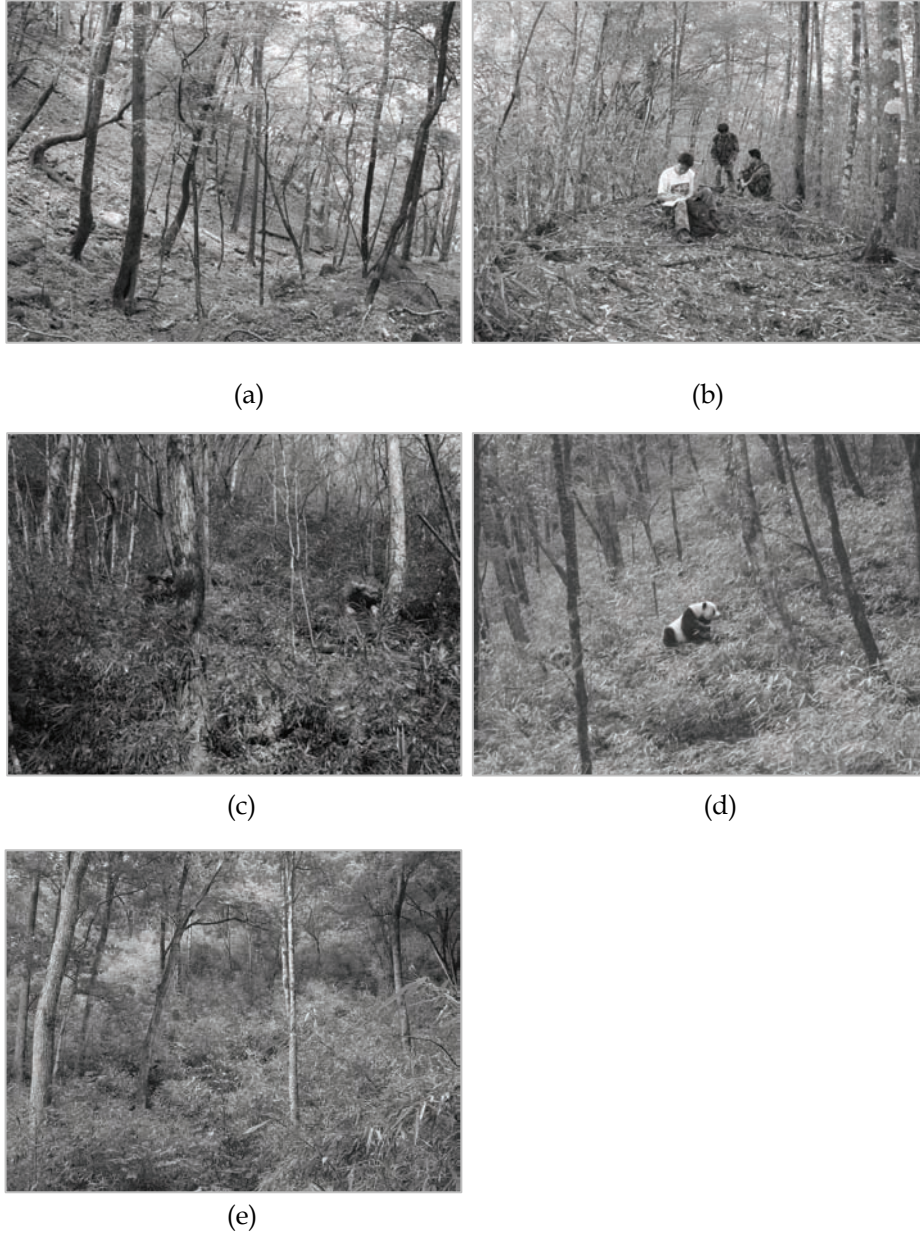
Figure 2 Examples of the bamboo (*B. fargesii*) coverage (a): No bamboo (<1 %), (b): Very low cover (1-24%), (c): Low cover (25-49%), (d): High cover (50-74%), and (e): Very high cover (>74 %) beneath overstorey forest in the Foping Nature Reserve

Note that the visual estimation of understorey bamboo coverage was based on two factors: the proportion of gap size between the bamboo patches and abundance of bamboo culms within the field plot. In the field, measurement crews used photographs of different canopy densities as templates to calibrate and standardize estimates of bamboo cover (between crews as well as over time). Typical photographs of bamboo density ranging from no bamboo (<1%) to very high cover (>74%) are shown in Figure 2a through 2e.

Landsat TM/ETM+ Images and Pro-processing
Four seasons of clear and systematically corrected (Level 2) Landsat images were purchased from the China Remote Sensing Satellite Ground Station (Table 1). Considering that the study area has been well protected over the past 30 years and the bamboo density change is relatively slow underneath the mature forest (Tian and Liu 1985), the dominant cover of understorey bamboo associated with the different images remained similar. These images were projected to a UTM projection with the WGS84 datum. Co-registration was conducted based on an independent orthorectified Landsat 7 ETM+ product (http://glcfapp.umiacs.umd.eud). This product was selected as the master image because 1) it is an orthorectified image and the relief displacement was corrected. 2) It contained the highest positional accuracy with respect to the ground measurements after a slight geometric modification using an additional 20 local ground control points (GCPs) located uniformly across the image at clear features including river junctions, roads and rock outcrops. The GCPs were collected using a Trimble Pro XRS differential GPS in 2005. A second order polynomial transformation model with bilinear interpolation was used for the geometric correction of the orthorectified image within the ERDAS Imagine software package. The resulting images had a spatial resolution of 28.5 m, and all images had a RMSE of less than 0.5 pixels (<14 m). Because this study involved analysis of biophysical parameters derived from multi-seasonal images in a mountains terrain, it was necessary to perform atmospheric, topographic and radiometric correction to convert digital numbers to surface reflectance values. It is well known that winter images are difficult to process with respect to shading problems in areas of high terrain. We therefore made atmospheric and terrain corrections using ATCOR (Atmospheric and Topographic CORrection), an algorithm written by DLR (German Aerospace Agency) for mountainous terrain which is an add-on module to ERDAS Imagine and uses look-up tables computed with the MODTRAN 4 radiative transfer code (Richter 1996, 1998) and applied Stefanov et al., (2001) and Greeberg et al., (2005). The ATCOR algorithm was run using parameters found within the image metadata as well as partially provided and calculated by the package itself such as the sensor pre-launch calibration file and sun position. Information about elevation, slope, aspect, skyview and shadow derived from a

DEM was employed to correct terrain effects. The DEM was obtained from a 1:50,000 scale contour map with 20 m contours, developed by the State Bureau of Surveying and Mapping of China (1987). A mid-latitude, rural aerosol concentration model with 30 km estimated visibility (the estimation is based on actual observations from Hanzhong airport located 60 km from the study area) therefore was used as input to the radiative transfer code respectively. Each image (spring, summer, autumn, winter) was individually processed. Thus, the output from ATCOR is a reflectance image corrected for radiometric and terrain effects.

Table 1 Characteristics of Landsat TM/ETM+ images used in this study

Acquisition date	Landsat satellite	Path/Row	Season	Phenology	Note
22 May 2001	7 ETM+	128/37	Spring	Partly leaf-on	Master image
19 May 2000	7 ETM+	128/37	Spring	Partly leaf-on	Co-registration
30 July 2000	5 TM	128/37	Summer	Leaf-on	Co-registration
19 October 1997	5 TM	127/37	Autumn	Partly leaf-off	Co-registration
20 March 2001	5 TM	127/37	Winter	Leaf-off	Co-registration

Calculating Vegetation Indices

It is impractical to test all available vegetation indices. Therefore, three key indices were used (Table 2), selected because their design represents three important improvements in VI development to minimize the effect of topographic, soil background and atmospheric variations.

Table 2 Categories of vegetation indices used in the study

VI	Formula	Reference	Note
NDVI	$\dfrac{\rho_{nir} - \rho_{red}}{\rho_{nir} + \rho_{red}}$	Rouse *et al.*, (1973)	Reduce terrain effect and sensitive to green vegetation
SAVI	$\dfrac{\rho_{nir} - \rho_{red}}{\rho_{nir} + \rho_{red} + L}(1 + L)$	Huete, (1988)	Reduce non-canopy background effect and better in low biomass situation
EVI	$G * \dfrac{\rho_{nir} - \rho_{red}}{\rho_{nir} + C_1 * \rho_{red} - C_2 * \rho_{blue} + L}$	Liu and Huete, (1995)	Reduce atmospheric influence and improved performance in high biomass

The ρ_{blue}, ρ_{red}, ρ_{nir} in NDVI, SAVI, and EVI are the surface reflectance factors for their respective TM and ETM+ bands; L is a canopy background adjustment factor, which adopted in SAVI is a constant soil line of 0.5. C_1 and C_2 are the coefficients of the aerosol resistance term, which uses the blue band to correct

for aerosol influences in the red band. The coefficients adopted in the EVI algorithm are, $L = 1$, $C_1 = 6$, $C_2 = 7.5$, and G (gain factor) = 2.5.

Determining Optimal Season and Vegetation Index

The original 646 sample plots of five cover classes of bamboo estimated in the field were combined into three broad cover classes, which are bamboo absence (<1%), low bamboo cover (1-50%), and high bamboo cover (>50%). Additionally, the occurrence of evergreen conifers in our study site is a major problem because conifers mix with the evergreen understorey bamboo in the leaf-off season. Therefore, the datasets were split into two groups according to the presence (317 samples) and absence (329 samples) of evergreen conifers in each plot. Training and testing samples were randomly selected (321 samples for training and 325 samples for testing). The three vegetation indices values were extracted for each training sample for images of the four seasons. Correlation analysis between the three vegetation indices and the three classes of bamboo coverage, for the four seasons, was performed using a multiple R-square tests (StatSoft, Inc., 2001). The results were used to identify which season image, and which vegetation index is most suitable for mapping evergreen understorey bamboo coverage.

Mapping the Presence/absence of Conifer Overstorey

In order to achieve the highest mapping accuracy for classification of conifer overstorey, three commonly used classification methods, mahalanobis distance classifier (MDC), maximum likelihood classifier (MLC), and artificial neural networks (ANN) were tested on the four seasonal Landsat images. In this study, a three-layer feedforward error-backpropagation artificial neural networks implemented in Interactive Data Language (IDL) was used (Skidmore et al., 1997). Both MDC and MLC classifiers were implemented in ENVI version 4.2. The sample plots of the presence/absence of conifer were randomly divided into two equal groups, a training set (323 samples) and a test set (323 samples). Six Landsat TM/ETM+ bands (1-5, and 7) were included in the classification. The highest accuracy map for the presence/absence of conifer was then used as an input layer for the vegetation index thresholds-based decision tree approach.

Linking Vegetation Index to Bamboo Presence and Coverage

Once the optimal season image and vegetation index were determined, the midpoint between the mean vegetation indexes values derived from three classes of bamboo coverage were selected. A decision tree classifier (DTC) was employed to link bamboo presence and coverage to the vegetation indices. The DTC is a multistage classifier made up of a series of binary decisions that are used to determine the correct category for each pixel. The details of DTC is described in Hansen et al., (1996) and ENVI version 4.2 (Research Systems, Inc.,

2005). In recent years, the DTC techniques have been successfully used for a wide range of classification problems and are becoming an important tool for the classification of remotely sensed data (Pal and Mather 2003, Pavuluri et al., 2002, Simard et al., 2000, Xu et al., 2005). These techniques have advantages for land use and land cover classification because of their flexibility, nonparametric nature, and ability to handle non-liner relations between features and classes. The decisions can be based on any available characteristic of the dataset, while the tree structure gives easily understandable and interpretable information regarding the predictive or generalization ability of the data. In this study, for example, the DTC is based on a set of vegetation index thresholds, a vegetation index map, a DEM used to mask the specific study areas below 2,000 m, and a land cover map of presence/absence of conifer overstorey. Figure 3 presents the structure and parameters of decision tree which used to classify three classes of bamboo coverage.
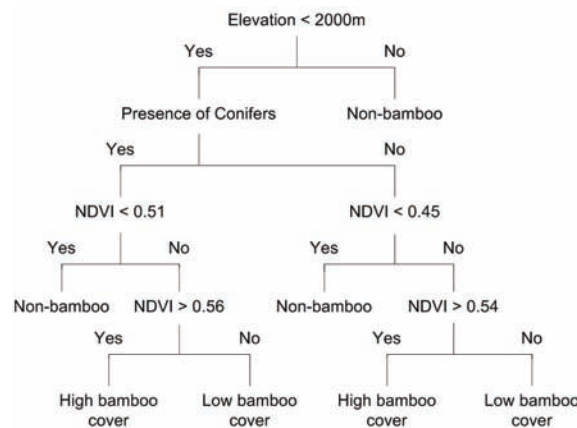
Figure 3 The structure of decision tree classifier and its parameters for three classes of bamboo coverage

Mapping Bamboo Coverage Using Multispectral Bands-based Approach
The three classifiers (MDC, MLC, and ANN) applied to classify conifers were further used to map the understorey bamboo presence/absence and coverage using four seasons of Landsat imagery. Only six TM/ETM+ bands (excluding the thermal and panchromatic bands) were used by these classifiers. In order to compare the results, the same training and test datasets as used for the vegetation index-based decision tree approach were also applied to these three multispectral bands-based classifiers. The overall mapping accuracy and kappa coefficient (Cohen 1960) were calculated, and a widely applied kappa z-test

(Congalton 1983) is used to test for statistically significant differences in output images.

RESULTS

Determining the Optimal Season and Vegetation Index

Table 3 results highlights that the highest correlations between vegetation index and bamboo cover were observed in leaf-off season (winter) with the R^2-value ranging from 0.47 to 0.65. The weakest relationships were found in leaf-on or partly leaf-on seasons (spring, summer and autumn) with the R^2-value ranging from 0.01 to 0.13. Winter NDVI appeared to give higher R^2-values than SAVI and EVI, which explained respectively 65% and 52% of variation in bamboo coverage for the areas without and with conifers. This relationship suggests that three classes of bamboo cover can be quantified adequately by using winter TM-derived NDVI (Table 3).

Table 3 R^2-values for the relationship between the three vegetation indices and three classes of bamboo coverage in four seasons in areas with and without conifers; Note that the values followed by * are significant at 0.01 confidence level

VI	Bamboo in the area without conifer				Bamboo in the area with conifer			
	Spring	Summer	Autumn	Winter	Spring	Summer	Autumn	Winter
NDVI	0.13*	0.05*	0.13*	0.65*	0.01	0.01	0.11*	0.52*
SAVI	0.10*	0.06*	0.11*	0.51*	0.03	0.04	0.11*	0.47*
EVI	0.09*	0.06*	0.11*	0.53*	0.03	0.04	0.12*	0.48*

Producing the Highest Accuracy Map for the Presence/absence of Conifer

Table 4 details that the winter image yielded the highest map accuracy. The highest mapping accuracy was achieved by ANN with an overall mapping accuracy of 83 percent (κ=0.64). A kappa z-test for pair-wise comparison in accuracy shows that there was significant difference between winter and other seasons, but no significant difference in accuracy as a result of the method used.

Table 4 Comparison of overall mapping accuracy and kappa coefficient for classification of conifer overstorey from three different classifiers (MDC, MLC and ANN) in four seasons; Note that the OVA = overall accuracy

Seasons	MDC		MLC		ANN	
	OVA (%)	Kappa	OVA (%)	Kappa	OVA (%)	Kappa
Spring	72	0.43	73	0.44	72	0.40
Summer	67	0.33	69	0.33	71	0.39
Autumn	72	0.43	68	0.37	74	0.45
Winter	81	0.61	82	0.63	83	0.64

Mapping Understorey Bamboo Presence and Coverage Using NDVI

Table 5 displays winter NDVI thresholds derived from the previous statistical analyses, that shows differences in mean NDVI values and the thresholds between land cover types. In general, the winter NDVI calculated from the three classes of bamboo in the area with conifers is relatively higher than the area without conifers. Winter NDVI was used to map bamboo coverage using a binary decision tree classifier. A high mapping accuracy for understorey bamboo presence/absence was achieved with an overall accuracy of 89 percent (κ=0.59). In addition, three density classes of bamboo was also successfully classified with an overall accuracy of 68 percent (κ=0.48).

Table 5 Winter NDVI thresholds for three classes of bamboo coverage in areas with and without conifers; Note that the mean NDVI values are at 0.05 confidence level, and "N" represents the number of training samples

Bamboo cover	NDVI in the area without conifer				NDVI in the area with conifer			
	Mean	Std. error	Thresholds	N	Mean	Std. error	Thresholds	N
No-bamboo	0.40	0.011	< 0.45	18	0.47	0.006	< 0.51	33
Low-bamboo	0.50	0.006	0.45 - 0.54	58	0.54	0.005	0.51 - 0.56	56
High-bamboo	0.57	0.005	> 0.54	88	0.59	0.005	> 0.56	68

Comparing the Mapping Accuracy with Multispectral Bands-based Approach

The understorey bamboo presence/absence was classified by using three multispectral bands-based classifiers (MDC, MLC and ANN) in four seasons. The overall mapping accuracy and Kappa coefficient was compared to the results produced by winter NDVI thresholds-based DTC (Table 6), and the maps were shown in Figure 4 (a, b, c, and d). The results show that the highest mapping accuracy was achieved with an overall mapping accuracy of 90 percent (κ=0.63) by using ANN classifier in winter, and then followed by DTC, MLC and MDC. The lower overall mapping accuracies and extremely poor kappa coefficients were obtained in leaf-on and partly leaf-on seasons,

regardless of the methods used. A kappa z-test for pair-wise comparisons proved the leaf-off season (winter) was significantly different to the partly leaf-on and leaf-on seasons (spring, summer, and autumn) (Table 7). We therefore concluded that there was a significant difference on understorey bamboo presence/absence mapping accuracy between the leaf-off and leaf-on as well as partly leaf-on seasons.

Table 6 Comparison of overall mapping accuracies and kappa coefficients for bamboo presence/absence from four different classifiers in four seasons; Note "NC" means "not classified" because there was no significant difference was found between the mean of NDVI and understorey bamboo presence/absence in these seasons

Seasons	MDC		MLC		ANN		NDVI-DTC	
	OVA (%)	Kappa	OVA (%)	Kappa	OVA (%)	Kappa	OVA (%)	Kappa
Spring	69	0.24	76	0.18	81	0.22	NC	NC
Summer	62	0.14	74	0.22	78	0.18	NC	NC
Autumn	62	0.12	63	0.13	84	0.14	NC	NC
Winter	84	0.55	87	0.59	90	0.63	89	0.59

Table 7 Kappa z-test for pair-wise comparison between any two of four seasons (spring, summer, autumn and winter) for bamboo presence/absence from three classifiers (MDC, MLC and ANN); Note the values followed by * are significant at higher than 1.96 at α=0.05

Classifiers	Season	Spring	Summer	Autumn	Winter
MDC	Spring	-			
	Summer	2.88*	-		
	Autumn	3.46*	0.59	-	
	Winter	10.45*	13.53*	14.16*	-
MLC	Spring	-			
	Summer	1.26	-		
	Autumn	1.32	2.54*	-	
	Winter	14.55*	13.00*	15.55*	-
ANN	Spring	-			
	Summer	1.12	-		
	Autumn	0.58	0.58	-	
	Winter	15.44*	16.22*	16.58*	-

The three classes of bamboo coverage were also classified by three methods (MDC, MLC, and ANN) for the winter image. Note that only winter image was employed because the leaf-on images failed to discriminate the bamboo presence/absence according to previous results. The overall accuracies, kappa coefficients and kappa variances from all three multispectral-based methods were compared to NDVI thresholds-based DTC approach (Table 8). The highest mapping accuracy was again achieved with an overall accuracy of 71 percent (κ=0.54) by using ANN classifier, and then followed by MDC, MLC and DTC classifiers, and the maps are shown in Figure 4 (e, f, g, and h). However, the kappa z-test showed that there is no significant difference between the methods used.

Table 8 Overall mapping accuracies, kappa coefficients and kappa variances for three classes of bamboo coverage from four different classifiers in leaf-off season (winter). Note that none of the classifiers have a significant difference in accuracy (kappa z-test parewise comparison, z<1.96 at α=0.05)

Classifiers	OVA (%)	Kappa	Kappa variance
Mahalanobis distance classifier (MDC)	69	0.51	0.00065
Maximum likelihood classifier (MLC)	68	0.49	0.00066
Artificial neural networks (ANN)	71	0.54	0.00062
NDVI-based decision tree classifier (NDVI-DTC)	68	0.48	0.00067

DISCUSSION

Best Season

In this study, it was demonstrated that winter is the best season for predicting an evergreen understorey bamboo species *B. fargesii* in a deciduous-dominated mixed temperate forest, regardless of the classification methods used. There are several reasons which may explain why winter is the most appropriate season for mapping understorey bamboo. The first is because the deciduous canopy trees are leafless and do not block the view of ground features, especially evergreen understorey bamboos. The second is that the leaf-off and die-off of most co-occurring shrubs and grass in winter creates a more uniform ground cover, which may greatly minimize the possibility of miscategorised pixels. However, Linderman et al., (2004) reported that the understorey bamboo misclassification caused by co-occurring grass and shrubs using a leaf-on image is big problem that could not be solved by a neural network classifier. Thirdly,
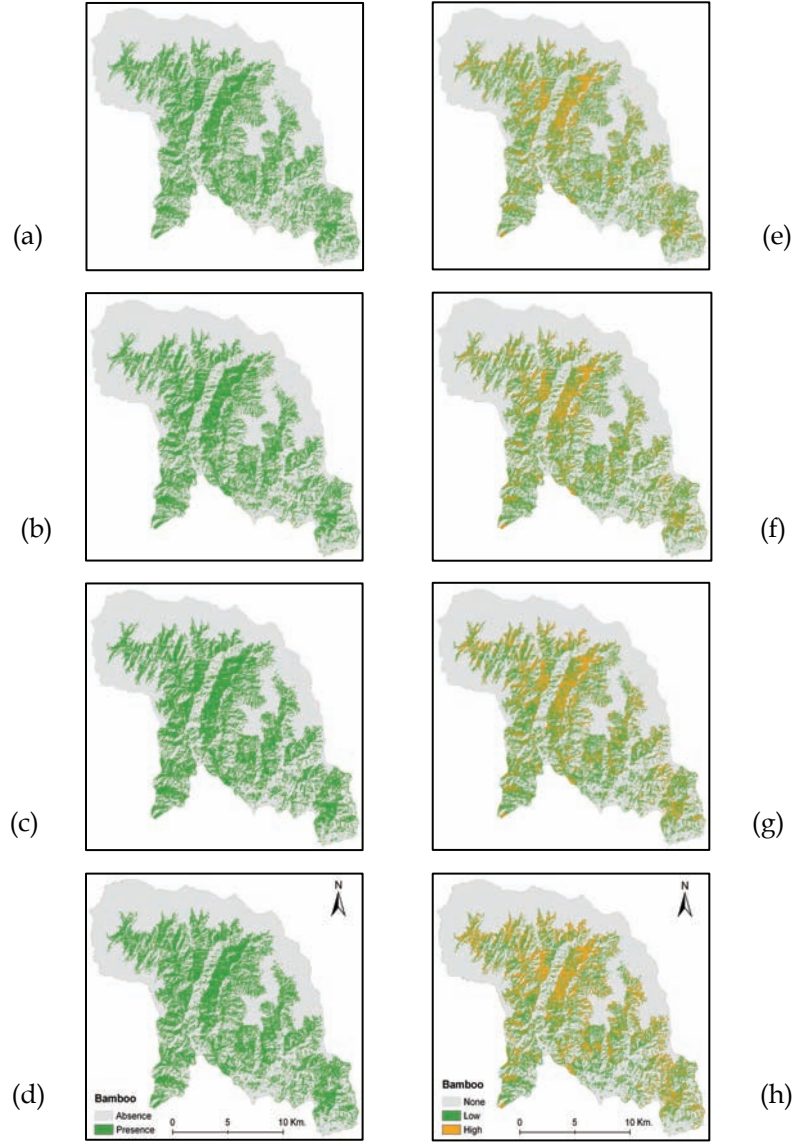
Figure 4 The presence/absence maps of evergreen understorey bamboo (*B. Fargesii*) (a, b, c, and d), as well as the maps of three classes of bamboo coverage (e, f, g, and h) in Foping Nature Reserve produced by four different methods using winter image. Among the maps, a and e is derived from MDC; the map b and f is derived from MLC; the map c and g is produced by ANN, the map d and h is produced by winter NDVI-DTC, respectively

it was believed that the difference in spectral properties between understorey bamboo and overstorey forest, as well as reduced photosynthesis in evergreen coniferous forest in winter, contributed to the higher bamboo mapping accuracy obtained in mixed deciduous/coniferous forests. As Fukui et al., (2004) reported that the spectral reflectance of wild bamboo forests is higher in near infrared than evergreen coniferous forests, but it is much lower than evergreen broadleaf and deciduous broadleaf forests. Moreover, our research complements an earlier study by Stenback and Congalton (1990), who emphasized that the acquisition date of the images is considered to be the critical factor controlling the level of understorey classification obtainable. They therefore suggested that the analysis could be repeated using different acquisition dates selected on the basis of the dominant canopy and understorey phenology.

Optimal Vegetation Index

It was found that NDVI has a relatively stronger relationship with understorey bamboo coverage compared with SAVI and EVI. Because bamboo cover is high in the study area, it is reasonable that SAVI performs poorly relative to NDVI as SAVI is optimized for low vegetation cover (Huete 1988). The EVI was designed to improve sensitivity to high biomass regions and reduce in atmospheric influences (Huete et al., 2002). However, this study showed that there is no saturation problem in winter, as the mean NDVI value (for the high bamboo cover) was 0.59. Moreover, an atmospheric correction was conducted before the calculation of NDVI, further reducing the advantages of EVI compared with NDVI.

Bamboo Presence and Cover Mapping by Using Four Classification Methods

This study tested the effectiveness of a winter NDVI thresholds-based decision tree approach for classifying understorey bamboo coverage. The results were considered good with an overall accuracy of 89 percent (κ=0.59) for bamboo presence/absence, and satisfactory with an overall accuracy of 68 percent (κ=0.48) for three classes of bamboo coverage. To our knowledge, this study is the first attempt at mapping understorey bamboo cover as three classes (instead of presence/absence). As noted above, retrieval of bamboo coverage is important for understanding wildlife distribution patterns and population dynamics based on habitat requirement.

Three traditional multispectral bands-based classifiers (MDC, MLC, and ANN) mapped bamboo coverage, and were compared with NDVI thresholds-based DTC. The kappa z-test showed that there is no significant difference between the methods used. With respect to mapping the three density classes of bamboo, ANN produced the highest accuracy though it is not significantly

higher than NDVI thresholds-based DTC, possibly because the additional spectral information provided by TM band 5 was utilized by the ANN (Stenback and Congalton 1990).

Differences in classification accuracy have been attributed to many factors (Richards and Jia 1999), including how the training data are modelled by the assumption of the parametric or nonparametric classifier (Strahler 1980, Skidmore et al., 1997), the number of training pixels (Foody et al., 2006), the landscape structure and homogeneity of training areas (Hubert-Moy et al., 2002), selection of a classification scheme (Prenzlel and Treitz 2005), the type and quality of the imagery (Underwood et al., 2007), the quality of the ground truth data (Congalton and Green 1999), etc. It has been shown (Richards and Jia 1999) that many of these factors are empirical and vary from case to case, and therefore rely on an analyst's skills in both operating a image processing systems, but also in the 'art' of understanding a classification. In this study, a large dataset was available, the images were carefully corrected for both geometric and radiometric properties, the ground truth data was of high quality and training areas were rather homogeneous because of the use of winter (leaf-off) image. Consequently, these factors resulted in very high accuracy results (especially for a mountainous forested study area) with no statistical difference in the performance of the classifiers.

The problem of estimating bamboo cover in the field is difficult due to poor access, steep terrain and dense understorey. As detailed in the methods, we chose a visual estimation approach. Using instruments to measure incident radiation below and above the forest canopy (and hence infer LAI) may be strictly more objective, but the reality of the forest conditions makes the practical use of these instruments impossible.

CONCLUSIONS

In this paper, the difference in phenological stages between overstorey and understorey, and its impact on evergreen understorey bamboo mapping was investigated. We conclude that: 1) winter imagery significantly improves understorey bamboo cover mapping accuracy regardless of the classification methods used; 2) winter vegetation indices, especially winter NDVI, can be successfully used to map evergreen understorey bamboo coverage. The simplicity, robustness and availability of NDVI have potential to quickly identify the "hot spots" of understorey bamboo over a large region.

The presence and abundance of understorey bamboo is a key factor in giant pandas habitat assessment, but it has normally been assumed to have a constant cover over space and time. The direct result of this research is an improved understanding of the distribution pattern of understorey bamboo abundance at Foping Nature Reserve and other forests in central China. On the basis of these results, a more accurate assessment and modelling for suitable giant panda habitat can be achieved.

REFERENCES

Ardö, J. and P. Pilesjö. 1992. On the accuracy of the global positioning system - A test using a hand-held receiver. International Journal of Remote Sensing **13**:3229-3233.

Borkowski, J. and K. Furubayashi. 1998. Seasonal changes in number and habitat use of foraging Sika deer at the high altitude of Tanzawa Mountains, Japan. Acta Theriologica **43**:95-106.

Cohen, J. 1960. A coefficient of agreement for nominal scales. Educational and Psychological Measurement **20**:37-46.

Colby, J. D. 1991. Topographic normalization in rugged terrain. Photogrammetric Engineering & Remote Sensing **57**:531-537.

Congalton, R. G. and K. Green. 1996. Assessing the Accuracy of Remotely Sensed Data: Principles & Practices. Lewis Publishers, London.

Congalton, R. G., R. G. Oderwald, and R. A. Mead. 1983. Assessing Landsat classification accuracy using discrete multivariate analysis statistical techniques. Photogrammetric Engineering & Remote Sensing **49**:1661-1668.

Diaz, I. A., J. J. Armesto, S. Reid, K. E. Sieving, and M. F. Willson. 2005. Linking forest structure and composition: avian diversity in successional forests of Chiloe' Island, Chile. Biological Conservation **123**:91-101.

Dymond, J. R., P. R. Stephens, P. F. Newsome, and R. H. Wilde. 1992. Percent vegetation cover of a degrading rangeland from SPOT. International Journal of Remote Sensing **13**:1999-2007.

Flores, F. J. 2003. Using hyperspectral remote sensing to estimate leaf area index of loblolly pine plantations. North Carolina State University, Raleigh, North Carolina.

Foody, G. M., A. Mathur, C. Sanchez-Hernandez, and D. S. Boyd. 2006. Training set size requirements for the classification of a specific class. Remote Sensing of Environment **104**:1-14.

Franklin, J. F., T. Maeda, Y. Ohsumi, M. Matsui, H. Yagi, and G. M. Hawk. 1979. Subalpine coniferous forests of central Honshu, Japan. Ecological Monographs **49**:311-334.

Fukui, Y., T. Tachikawa, and Y. Imai. 2004. Mapping bamboo forest expansion in the suburb of Fukuoka city using Aster data.in The 25th Asian

Conference & 1th Asain Space Conference on Remote Sensing. Asian Association on Remote sensing (AARS), Chiang Mai, Thailand.

Gong, H., Z. Zeng, X. Gao, Q. Liang, and Y. Song. 2006. Species of birds and mammals feeding on bamboo in Foping National Nature Reserve. Chinese Journal of Zoology **41**:31-36 (in Chinese).

Goodenough, D. G., A. S. Bhogall, H. Chen, and A. Dyk. 2001. Comparison of methods for estimation of Kyoto Protocol products of forests from multitemporal Landsat. Pages 764-767 in Proceedings of IEEE 2001 International Geoscience and Remote Sensing Symposium. IGARSS'01, July 2001, Sydney, Australia.

Greenberg, J. A., S. Z. Dobrowski, and S. L. Ustin. 2005. Shadow allometry: Estimating tree structural parameters using hyperspatial image analysis. Remote Sensing of Environment **97**:15-25.

Hansen, M., R. Dubayah, and R. DeFries. 1996. Classification trees: an alternative to traditional land cover classifiers. International Journal of Remote Sensing **17**:1075-1081.

Hubert-Moy, L., A. Cotonnec, L. Le Du, A. Chardin, and P. Perez. 2001. A comparison of parametric classification procedures of remotely sensed data applied on different landscape units. Remote Sensing of Environment **75**:174-187.

Huete, A. R. 1988. A soil adjusted vegetation index (SAVI). Remote Sensing of Environment **25**:295-309.

Huete, A. R., K. Didan, T. Miura, E. P. Rodriguez, X. Gao, and L. G. Ferreira. 2002. Overview of the radiometric and biophysical performance of the MODIS vegetation indices. Remote Sensing of Environment **83**:195-213.

Joshi, C., J. D. Leeuw, J. v. Andel, A. K. Skidmore, H. D. Lekhak, I. C. v. Duren, and N. Norbu. 2006. Indirect remote sensing of a cryptic forest understory invasive species. Forest Ecology and Management **225**:245-256.

Kaufman, Y. J. and D. Tanré. 1992. Atmospherically resistant vegetation index (ARVI) for EOS-MODIS. IEEE Transactions on Geoscience and Remote Sensing **30**:261-270.

Kent, M. and P. Coker. 1992. Vegetation Description and Analysis - A Practical Approach. John Wiley, New York.

Linderman, M., J. Liu, J. Qi, L. An, Z. Ouyang, J. Yang, and Y. Tan. 2004. Using artificial neural networks to map the spatial distribution of understory bamboo from remote sensing data. International Journal of Remote Sensing **25**:1685-1700.

Liu, H. and A. Huete. 1995. A feedback based modification of the NDVI to minimize canopy background and atmospheric noise. IEEE Transactions on Geoscience and Remote Sensing **33**:457-465.

Liu, J., M. Linderman, Z. Ouyang, L. An, J. Yang, and H. Zhang. 2001. Ecological degradation in protected areas: The case of Wolong nature reserve for giant pandas. Science **292**:98-101.

Liu, X., A. K. Skidmore, T. Wang, Y. Yong, and H. H. T. Prins. 2002. Giant panda movements in Foping nature reserve, China. Journal of Wildlife Management **66**:1179-1188.

Liu, X., A. G. Toxopeus, A. K. Skidmore, X. Shao, G. Dang, T. Wang, and H. H. T. Prins. 2005. Giant panda habitat selection in Foping Nature Reserve, China Journal of Wildlife Management **69**:1623-1632.

Loucks, C. J., L. Zhi, E. Dinerstein, D. Wang, D. Fu, and H. Wang. 2003. The giant pandas of the Qinling Mountains, China: a case study in designing conservation landscapes for elevational migrants. Conservation Biology **17**:558-565.

McKenzie, D. and C. B. Halpern. 1999. Modeling the distributions of shrub species in Pacific northwest forests. Forest Ecology and Management **114**:293-307.

Morain, S. A. 1986. Surveying China's agricultural resources: patterns and progress from space. Geocarto International **1**:15-24.

Myneni, R. B. 2002. Global products of vegetation leaf area and fraction absorbed PAR from year one of MODIS data. Remote Sensing of Environment **83**:214-231.

Myneni, R. B., F. G. Hall, P. J. Sellers, and A. L. Marshak. 1995. The interpretation of spectral vegetation indexes. IEEE Transactions on Geoscience and Remote Sensing **33**:48-486.

Pal, M. and P. M. Mather. 2003. An assessment of the effectiveness of decision tree methods for land cover classification. Remote Sensing of Environment **86**:554-565.

Pan, W., Z. Gao, and Z. Lu. 1988. The giant panda's natural refuge in the Qinling Mountains. Peking University Press, Beijing (in Chinese).

Prenzlel, B. and P. Treitz. 2005. Comparison of function- and structure-based schemes for classification of remotely sensed data. International Journal of Remote Sensing of Environment **26**:543-561.

Purevdorj, T., R. Tateishi, T. Ishiyama, and Y. Honda. 1998. Relationships between percent vegetation cover and vegetation indices. International Journal of Remote Sensing **19**:3519-3535.

Reid, D. G., J. Hu, S. Dong, W. Wang, and Y. Huang. 1989. Giant panda Ailuropoda melanoleuca behaviour and carrying capacity following a bamboo die-off. Biological Conservation **49**:85-104.

Reid, D. G., J. Hu, and Y. Huang. 1991. Ecology of the red panda Ailurus fulgens in the Wolong reserve, China. Journal of Zoology **225**:347-364.

Reid, S., I. A. Diaz, J. J. Armesto, and M. F. Willson. 2004. Importance of native bamboo for understory birds in Chilean temperate forests. The Auk **121**:515-525.

Ren, Y., M.-L. Wang, M. Yue, and Z.-J. Li, editors. 1998. Plants of giant panda's habitat of Qinling Mountains. Shaanxi Science and Technology Press, Xian (in Chinese).

Rettie, W. J., J. W. Sheard, and F. Messier. 1997. Identification and description of forested vegetation communities available to woodland caribou: relating wildlife habitat to forest cover data. Forest Ecology and Management **93**:245-260.

Richards, J. A. and X. Jia. 1999. Remote Sensing Digital Analysis: An Introduction. 3rd Edition edition. Springer-Verlag, Berlin.

Richter, R. 1996. A spatially adaptive fast atmospheric correction algorithm. International Journal of Remote Sensing **17**:1201-1214.

Richter, R. 1998. Correction of satellite imagery over mountainous terrain. Applied Optics **37**:4004-4015.

Rouse, J. W., R. H. Hass, J. A. Schell, and D. W. Deering. 1973. Monitoring vegetation systems in the Great Plains with ERTS. Pages 309-317 in 3rd ERTS symposium. U.S. Government Printing Office, Washington, DC.

Schaller, G. B., J. Hu, W. Pan, and J. Zhu. 1985. The Giant Pandas of Wolong. The University of Chicago Press, Chicago and London.

Simard, M., S. S. Saatchi, and G. D. Grandi. 2000. The use of decision tree and multiscale texture for classification of JERS-1 SAR data over tropical forest. IEEE Transactions on Geoscience and Remote Sensing **38**:2310–2321.

Skidmore, A. K., B. J. Turner, W. Brinkhof, and E. Knowle. 1997. Performance of a neural network: mapping forests using remotely sensed data. Photogrammetric Engineering & Remote Sensing **63**:501-514.

State Forestry Administration. 2006. The Third National Survey Report on Giant Pandas in China. Science Press, Beijing (in Chinese).

Stefanov, W. L., M. S. Ramsey, and P. R. Christenson. 2001. Monitoring urban land cover change: An expert approach to land cover classification of semiarid to arid urban centers. Remote Sensing of Environment **77**:173-185.

Stenback, J. M. and R. G. Congalton. 1990. Using thematic mapper imagery to examine forest understory. Photogrammetric Engineering & Remote Sensing **56**:1285-1290.

Strahler, A. H. 1980. The use of prior probabilities in maximum likelihood classification of remotely sensed data,. Remote Sensing of Environment **10**:135-163.

Taylor, A. H. and Z. Qin. 1987. Culm dynamics and dry matter production of bamboo in the Wolong and Tangjiahe giant panda reserves, Sichuan, China. Journal of Applied Ecology **24**:419-433.

Taylor, A. H. and Z. Qin. 1988. Regeneration patterns in old-growth Abies-Betula forests in the Wolong Natural Reserve, Sichuan, China. Journal of Ecology **76**:1204-1218.

Tian, X. and Q. Liu. 1985. Distribution of Bashania fargesii on the south slope of the Qinling Mountains. Bamboo Research **1**:13-17 (in Chinese).

Townshend, J., C. Justice, W. Li, C. Gurney, and McManus. 1991. Global land cover classification by remote sensing: present capabilities and future possibilities. Remote Sensing of Environment **35**:243-257.

Townshend, P. A. and S. J., Walsh. 2001. Remote sensing of forested wetlands: Application of multipletemporal and multispectral satellite imagery to determine plant community composition and structure in southeastern USA. Plant Ecology **157**: 129-149.

Tucker, C. J., J. R. G. Townshend, and T. E. Goff. 1985. African Landcover classification using satellite data. Science **227**:369-375.

Turner, D. P., W. B. Cohen, R. E. Kennedy, K. S. Fassnacht, and J. M. Briggs. 1999. Relationships between leaf area index and Landsat TM spectral vegetation indices across three. Remote Sensing of Environment **70**:52-68.

Underwood, E. C., S. L. Ustin, and C. M. Ramirez. 2007. A Comparison of Spatial and Spectral Image Resolution for Mapping Invasive Plants in Coastal California. Environmental Management **39**:63-83.

Veblen, T. T. 1982. Growth patterns of chusquea bamboos in the understory of Chilean Nothofagus forests and their influences in forest dynamics. Bulletin of the Torrey Botanical Club **109**:474-487.

Warner, M. 2002. Assessing habitat utilization by neotropical primates: a new approach. Primates **43**:59-71.

Wittich, K. P. and O. Hansing. 1995. Area-averaged vegetative cover fraction estimated from satellite data. International Journal of Biometereology **38**:209-215.

Xu, M., P. Watanachaturaporn, P. K. Varshney, and M. K. Arora. 2005. Decision tree regression for soft classification of remote sensing data. Remote Sensing of Environment **97**:322-336.

Yue, M., G. Dang, and L. Yong. 1999. The basic features of vegetation of Foping Nature Reserve in Shaanxi province. Journal of Wuhan Botanical Research **17**:22-28 (in Chinese).

Chapter 3

Improved understorey bamboo cover mapping using a novel hybrid neural network and expert system

ABSTRACT

The giant panda is an obligate bamboo grazer. Therefore, the availability and abundance of understorey bamboo determines the quantity and quality of panda habitat. However, there is little or no information about the spatial distribution or abundance of bamboo underneath the forest canopy, due to the limitations of traditional remote sensing classification techniques. In this paper, a new method combines an artificial neural network and a GIS expert system in order to map understorey bamboo in the Qinling Mountains of south-western China. Results from leaf-off ASTER imagery, using a neural network and an expert system, were evaluated for their suitability to quantify understorey bamboo. Three density classes of understorey bamboo were mapped, first using a neural network (overall accuracy 64.7%, kappa 0.45) and then using an expert system (overall accuracy 62.1%, kappa 0.43). However, when using the results of the neural network classification as input into the expert system, a significantly improved mapping accuracy was achieved with an overall accuracy of 73.8% and kappa of 0.60 (average z-value=3.35, p=0.001). Our study suggests that combining a neural network with an expert system makes it possible to successfully map the cover of understorey species such as bamboo in complex forested landscapes (e.g., coniferous-dominated and dense canopy forests), and with higher accuracy than when using either a neural network or an expert system.

INTRODUCTION

Bamboo is a grass with a wide distribution range, including tropical, subtropical, and cool-temperate regions on all continents except Europe. It grows in different habitats, from open environments to shaded forests (Soderstrom and Calderon 1979). In southwest China, bamboo is found most frequently underneath the canopy of temperate and subalpine forests (Taylor and Qin 1988), where it supports the giant panda, an endangered species (IUCN 2007). Giant pandas are obligate bamboo grazers and they select habitats primarily on the basis of suitability for foraging (Schaller et al., 1985). Therefore, availability and abundance of understorey bamboo is a key factor in determining the quantity and quality of panda habitat. During the past two decades, many efforts have been made to map and assess panda habitat using traditional ground survey and remote sensing techniques (De Wulf et al., 1988, Liu et al., 2001, Loucks et al., 2003, MOF 1989, State Forestry Administration 2006). All authors note that suitable panda habitat is overestimated, since critical information affecting panda habitat, such as bamboo distribution and its abundance, has not been verified. In these studies, the researchers assume there is a continuous spatial cover of bamboo under the forest canopy. Linderman et al., (2005) estimated that in the Wolong Nature Reserve of China the potential panda habitat decreased by 29-52% after information about bamboo distribution (i.e., presence/absence) was incorporated in the analyses.

The limited information about bamboo distribution and abundance is due to the complexity of bamboo distribution, as it is influenced by humans (clear cutting and fire), as well as by its periodical mass flowering and die-off (Reid et al., 1989). Any ground survey is difficult to extrapolate to larger areas through conventional point-based environmental modelling. The scarcity of extensive, detailed, as well as reliable information about bamboo distribution and its abundance impedes the implementation of panda conservation strategies such as habitat restoration, simply because managers do not know 'what is where'. Consequently, there is a need to develop practical methods for mapping understorey bamboo at local and national levels. As the remaining panda habitat is located in remote and rugged mountain landscapes, remote sensing and geographical information systems (GIS) are potentially an efficient way to acquire habitat data quickly and at low cost.

In a number of studies, mapping understorey vegetation using remote sensing data and traditional classification methods has been attempted. For instance, by utilizing a leaf-on Landsat TM image and an unsupervised classification approach, Stenback and Congalton (1990) detected presence/absence of vegetated understorey for different canopy closures in the Sierran mixed conifer

zone with an overall accuracy of 55 to 69% (kappa 0.08-0.38). The study indicated that the presence of vegetated understorey was more accurately classified in sparse canopy conditions. Ghitter et al., (1995) analysed TM images during leaf-off and leaf-on conditions in central Alberta. They suggested that leaf-off/leaf-on image data could be used to map understorey vegetation in the boreal mixed-wood zone, since an increase in reflectance occurred for areas where the canopy was reduced in density following the phenology of deciduous forests.

Instead of using conventional classifiers and remote sensing data alone, GIS expert systems have been used to predict the presence/absence of understorey species based on a combination of remotely sensed data and available GIS data layers. An expert system is a computer program that simulates the behaviour of human experts to solve problems related to geographic information systems (Stock 1987). For example, using forest type and litter cover derived from a TM image as well as terrain features such as gradient, aspect, and topographic position derived from a DEM, Yang et al., (2006) mapped the presence/absence of matsutake mushrooms under a forest with an overall accuracy of 70% and kappa of 0.36. In another study, based on the relationship between understorey cover abundance and light intensity, Joshi et al., (2006) predicted the presence/absence of an invasive understorey species (*Chromolaena odorata*) in Nepal using a set of GIS data layers such as forest canopy density, grazing intensity, distance from road and forest edge, and obtained an overall mapping accuracy of 74% and kappa of 0.56. This method proved useful for light sensitive understorey plants, but not for shade tolerant species, such as most of the mountainous bamboos. However, all these studies suggest that remote sensing and expert systems may assist when mapping vegetated understorey, in spite of the two-level (i.e., presence/absence) classification scheme and generally low classification accuracies (e.g., overall accuracy <70% or kappa <0.4).

It is well documented that most standard statistical classification techniques, such as maximum likelihood classification based on individual pixels, are often limited in their application and accuracy when classifying complex scenes, due to underlying assumptions made about the data (Atkinson and Tatnall 1997, Foody 1999, Skidmore et al., 1997). This becomes particularly relevant when considering the complex contribution of understorey vegetation. Artificial neural networks (hereafter neural networks), on the other hand, are devised to solve complex nonlinear classification problems and have the ability to recognise complex patterns (Foody 1996). Using neural network algorithms and a leaf-on Landsat TM image, Linderman et al., (2004) mapped the presence/absence of understorey bamboo in a mixed temperate forest with

relatively low canopy cover (average 56% closure), achieving an overall mapping accuracy of 80%. More recently, using the normalised difference vegetation index (NDVI) derived from a winter TM image and a binary decision tree classifier, Wang et al., (2009) mapped evergreen understorey bamboo (*Bashania fargesii*) in a deciduous-dominated temperate forest. A high mapping accuracy for understorey bamboo presence/absence was achieved of 89% (kappa 0.59). In addition, for the first time, three density classes of bamboo (<1%, 1-50%, and >50%) were distinguished with an overall accuracy of 68% (kappa 0.48). In these studies, the use of non-parametric classifiers (i.e., neural network and decision tree) and the leaf-off satellite image improved mapping accuracy. However, to map bamboo underneath a coniferous-dominated and dense forest canopy, more robust quantitative methods were needed to achieve a sufficient level of accuracy.

The objectives of the current study were to combine the advantages of remote sensing and GIS approaches, including the use of leaf-off satellite imagery, with a neural network algorithm and a GIS expert system; to map a semi-evergreen understorey bamboo species, which occurs in a coniferous-dominated subalpine forest; and to improve the mapping accuracy.

STUDY SITE

Description of Study Area
This study was carried out at an elevation of above 2,000 m in the Xinglongling and Tianhuashan giant panda habitats in the Qinling Mountains, an area that has been divided by a national road (No.108) from north to south (since 1970). The study site encompasses the typical summer habitat for pandas. Pandas usually spend 3-4 months a year here, from June to September. Winter habitat is formed by deciduous-dominated forest (below 2,000 m), which was not included in this study. Areas below 2,000 m were therefore masked using a DEM with 30 m spatial resolution. As a result, three nature reserves and two plantations were included in the 443 km² of forest, with the forest being dominated by conifers (Figure 1).

Two vegetation zones were defined in the study area according to Yue et al., (1999). The lower elevation (2,000-2,500 m) is the birch forest zone where *Betula* spp. forms the dominant deciduous tree species. A large number of coniferous species can also be found at this altitude, including pines (*Pinus* spp.) and firs (*Tsuga chinensis*, *Abies* spp.). The higher elevation (2,500-3,000 m) comprises the true coniferous forest zone, where the dominant coniferous tree species is farges

fir (*Abies fargesii*). Usually, at an elevation of 2,000 m, the leaves on canopy trees emerge (or 'leaf-out') at the beginning of May, while leaf-fall is complete by the end of October (Pan et al., 1988).
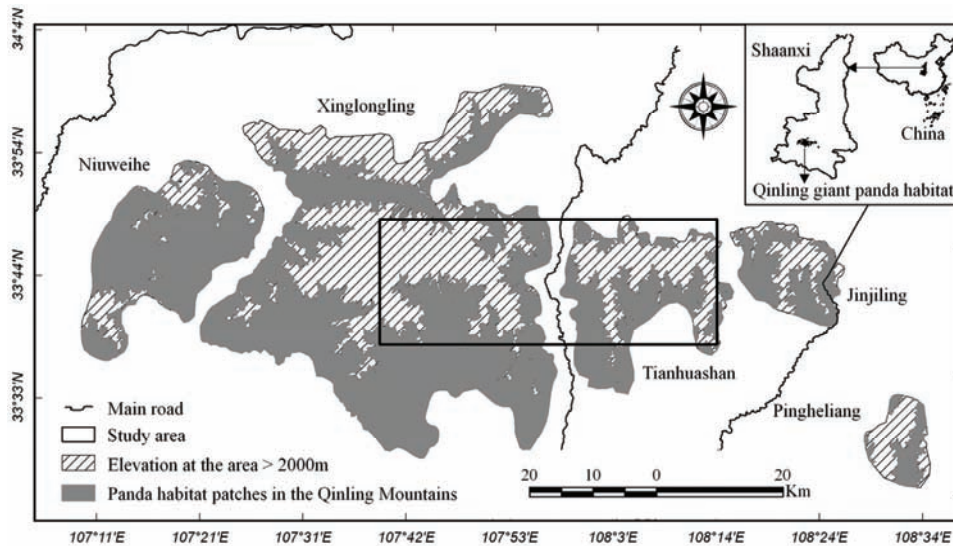
Figure 1 Location of the study area in the Qinling Mountains, China

Target Bamboo Species

Two bamboo species, *Fargesia qinlingensis* and *Fargesia nitida*, comprise almost the entire bamboo biomass in the study area. *F. qinlingensis* is one of the most abundant bamboo species and dominates the understorey of forests at elevations from 2,000 to 3,000 m in the Qinling Mountains, making up the pandas' main food source during the summer season. Due to the similarity in morphology and the spatial overlap between these two bamboo species, the current study treats them as a single species. The new shoots of *F. qinlingensis* regenerate in May and June, and its phenological characteristic such as leaf colour are different to those of the bamboo species at lower altitudes. At the top of the mountains, the bamboo leaves become yellow and senesce but do not fall during the winter season (from November to the beginning of May). The degree of yellowing gradually decreases with elevation. A set of photographs showing the phenological characteristic of *F. qinlingensis* during the leaf-off season (May) and leaf-on season (June) is presented in Figure 2 (a-f). *F. qinlingensis* is shade tolerant and grows well under all conditions, from full sun to full shade. Its culm, or main stem, can grow up to 3.6 m in height and 13 mm in basal diameter. Average culm density is about 80 per m^2.
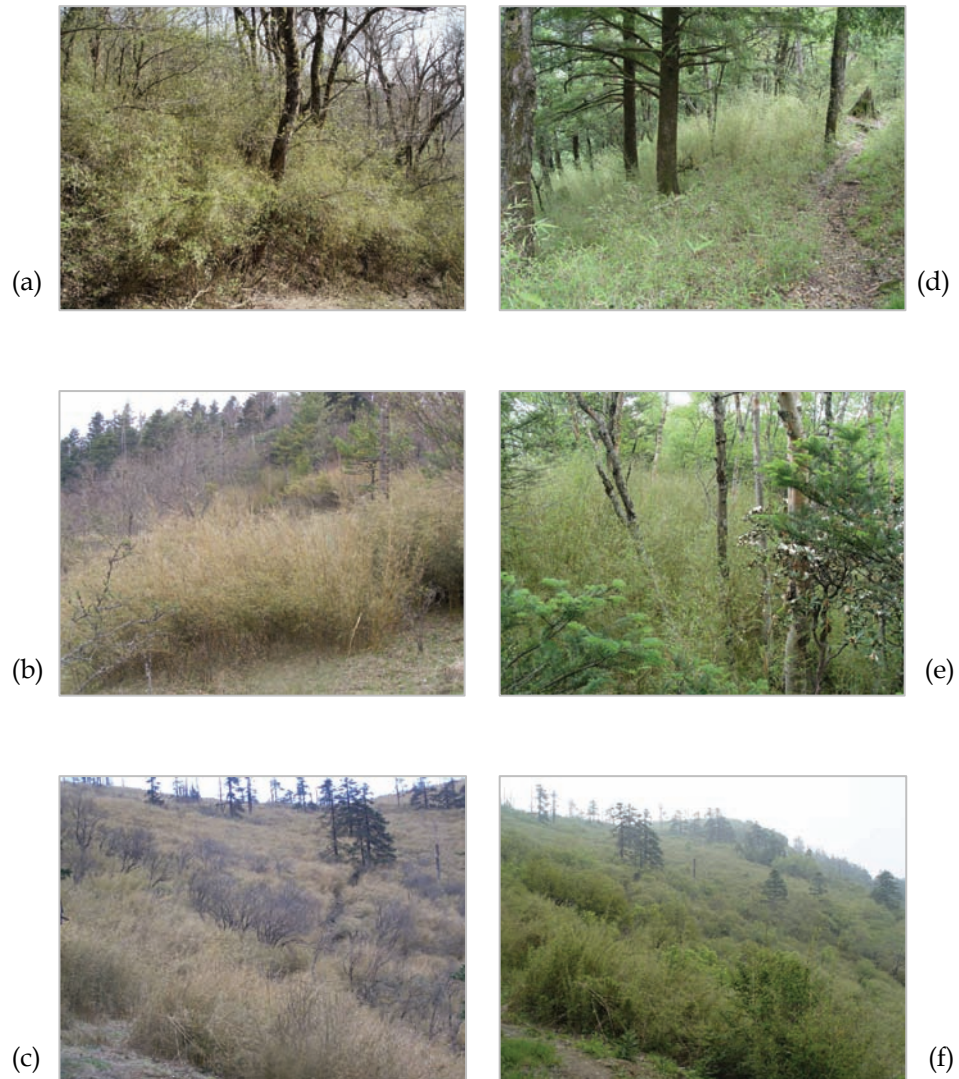
Figure 2 Examples of the phenological characteristics of *F. Qinlingensis* during the leaf-off season (May, photos on the left, arranged from a to c) and leaf-on season (June, photos on the right, arranged from d to f) at an elevation of 2,100 m, 2,300 m, and 2,500 m, respectively, in the Qinling Mountains

DATA ACQUISITION AND PREPARATION

Field Data Collection

The data used in this study were collected during field campaigns in the Qinling Mountains, conducted as part of missions for the Third National Panda Survey between 2001 and 2002. A total of 375 sample plots was carefully selected from the survey database, based on three criteria: 1) the plots were above 2,000 m; 2) the horizontal distance between adjacent plots was at least 300 m to minimise spatial autocorrelation; 3) a strong satellite signal was received by a Garmin 12XL GPS unit, which meant at least four satellites were located well above the horizon. Using the method of Ardö and Pilesjö (1992) the GPS precision was shown to be within 10 meters of the mean latitude and longitude for 95% of observations. Stratified random sampling, based on the terrain position (i.e., valley, mid-slope, and ridge), was adopted in both surveys to ensure the representative habitat types could be collected over the mountainous terrain. The sample plots measured 20 m × 20 m, and were positioned where bamboo cover-abundance was relatively homogeneous over a 60 m × 60 m area. Within the plots, many biotic and abiotic variables were measured such as location, aspect, slope gradient, slope position, tree species, average tree height, vegetation type, bamboo cover-abundance and signs of panda presence (grazing, footprints and faeces). Furthermore, five subplots (1 m × 1 m) were established within each 20 m × 20 m plot to measure the bamboo characteristics in detail, such as total culm density, average height, basal diameter and the proportion of old shoots. A modified Braun-Blanquet cover-abundance scale was used to estimate bamboo cover in the field and assign it to one of the following classes: <1%, 1-24%, 25-49%, 50-74% and 75-100%, following the methods described by Kent and Coker (1992) and State Forestry Administration (2006). In this study only four variables were used, viz., GPS position, bamboo cover-abundance, tree species, and vegetation type. The bamboo cover-abundance was reclassified into three cover classes following previous research (Wang et al., 2009), viz., bamboo absence (<1%), low bamboo cover (1-50%), and high bamboo cover (>50%). Finally, the sample plots of the three cover classes of bamboo were randomly divided into two equal groups, a training set (188 samples) and a test set (187 samples).

ASTER Data and Pre-processing

The timing of acquisition of remote sensing data is critical due to the changing phenology of the canopy and the understorey (Blackburn and Milton 1995, Stenback and Congalton 1990, Wang et al., 2009). To our knowledge ASTER imagery has not been used for mapping understorey plant species. In the present study, we initially used a Landsat TM/ETM+ image to test the new method (i.e., hybrid neural network and expert system) for mapping

understorey bamboo cover in a coniferous-dominated forest, since this study is a continuation of a recent paper published as 'Understorey bamboo discrimination using a winter image (Wang et al., 2009)', of which the TM image was used. However, a cloud-free, snow-free, and leaf-off Landsat TM/ETM+ image is not available between 2001 and 2002. We therefore choose ASTER imagery because it is available, and the spatial resolution and bandwidths of ASTER image, especially the Visible Near Infrared (VNIR) and the Short Wavelength Infrared (SWIR) spectral range are comparable to those of Landsat TM/ETM+ images (Muukkonen and Heiskanen 2005). In this study, a cloud-free and snow-free ASTER image acquired on 2 May 2002 was obtained from NASA's EOS Data Gateway. This image was selected because in May, based on field knowledge, the phenological state of the deciduous overstorey at high elevation (>2,000 m) is 'leaf-off', while the understorey bamboo is still 'leaf-on'. This image comprised both an ASTER-derived DEM and fifteen orthorectified ASTER calibrated radiance images. Validation testing has shown that the horizontal and vertical accuracy is frequently higher than 25 m root mean square error (RMSE) (http://edcdaac.usgs.gov/aster/AST14DMO.asp). Furthermore, the SWIR band of Landsat TM has been shown to contain key spectral information for the classification of vegetated understorey (Stenback and Congalton 1990b). In this study, three VNIR bands (band 1-3) and two SWIR bands (band 4-5) of the ASTER image were therefore used to map understorey bamboo. To preserve the spectral characteristics of the SWIR bands, the VNIR bands (15 m) were spatially resized using nearest neighbour to match the spatial resolution of the SWIR bands (30 m). Meanwhile, to improve the geometric accuracy, the image was rectified using 35 local ground control points (GCPs). These GCPs were located uniformly across the image using clear features including river junctions, roads and rock outcrops. They were collected in the field using a Trimble Pro XRS differential GPS (in 2005). A second order polynomial transformation model with bilinear interpolation was used to geometrically correct the orthorectified image and DEM, using the ERDAS software package. The resulting images and DEM had a spatial resolution of 30 m and a spatial accuracy (RMSE) of less than 10 m.

Preparation of the GIS data set

Four thematic maps (i.e., vegetation type, elevation, slope gradient and terrain position) have been used earlier to discern the cover-abundance of understorey bamboo (Pan et al., 1988, Ren et al., 1998, Tian 1988). The GIS layers may be checked for collinearity in order to ascertain whether all layers were contributing information to the analysis, and decide whether any layers could be dropped from further analysis. However, as some layers (i.e., vegetation type and terrain position) are categorical, such analysis is not possible using techniques such as principal components analysis (PCA) or factor analysis. We

therefore input all these layers into the GIS expert system, in order to map the three density classes of bamboo. A DEM of the study area was used to deduce elevation, slope gradient and terrain position. The slope gradient was calculated using standard GIS algorithms (Skidmore 1990). Terrain position is a more complicated variable to estimate, but it has been shown to be important in determining the distribution of vegetation species (Skidmore 1989a). An improved version of the algorithm described in Skidmore (1990) was implemented, using Interactive Data Language (IDL), to calculate the terrain position (i.e., ridge, upper mid-slope, mid-slope, lower mid-slope and gully) of each cell in the regular grid. This algorithm located ridges and stream lines from geographic principles, and then interpolated mid-slopes using a modified Euclidean distance measure.

Seven major vegetation types (i.e., pure bamboo forest, meadow-shrub-rock, fir-dominated forest, deciduous hardwood, mixed fir-hardwood, mixed pine-hardwood and pine-dominated forest) have been recognised by Yue et al., (1999) in the study area. To map difficult mountainous vegetation types from ASTER images, artificial neural networks were recommended (Foody 1996, Moody et al., 1996) for mixed pixels, since they are unlikely to be modelled well by a statistical classifier (e.g., maximum likelihood classifier). It was realised that even when using neural networks, a problem remains in how to separate the two different coniferous forests (i.e., fir and pine) which have similar spectral characters, but occur at different altitude zones. Therefore, an elevation threshold (2,300 m), based on local knowledge, was introduced to address this potential misclassification, using a knowledge-based classifier. The sample plots with the seven vegetation types were randomly divided into two equal groups which resulted in 190 samples for training and 185 samples for testing. The rules of the classifier were expressed as follows: IF elevation is greater than 2,300 m, THEN all pine-dominated forest and mixed pine-hardwood must be classified as fir-dominated forest and mixed fir-hardwood. While on the other hand, IF elevation is less than 2,300 m, THEN all fir-dominated forest and mixed fir-hardwood must be classified as pine-dominated forest and mixed pine-hardwood.

METHOD

Artificial Neural Networks

In this study, a three-layer feed forward error-back propagation neural network (Skidmore et al., 1997) was implemented in IDL in order to classify the highly mixed forest types as well as to predict three cover classes of understorey

bamboo. The algorithm minimised the root mean square error between the observed and the predicted values (Atkinson and Tatnall 1997) in search of system parameters to increase accuracy and avoid overtraining of the neural network. The neural network (with the sub samples of 190 sites, seven vegetation types, and five ASTER bands) was trained and the best combination of optimum learning rate and momentum to minimize the RMSE was empirically established (Skidmore et al., 1997). The optimal results were obtained with a learning rate of 0.2, a momentum of 0.7 and one hidden layer. The RMSE stabilised after approximately 10,000 epochs. In all, 20 iterations of 10,000 epochs were performed, and the best iteration selected based on RMSE. For mapping understorey bamboo, using the neural network, a sub sample of 188 sites with three cover classes of bamboo and five ASTER bands was trained. The optimal results were obtained with a learning rate of 0.2, a momentum of 0.7 and one hidden layer. The RMSE stabilised after approximately 15,000 epochs. Finally, 20 iterations of 15,000 epochs were performed, and the best iteration was selected based on RMSE.

GIS Expert System
The expert system approach used here was described in detail by Skidmore (1989b) and the same terminology has been used. Bayesian theory was the core statistical method of the expert system used as inference engine. In this case, the expert system was used to infer the most likely bamboo cover class at a given cell, based on the available GIS database layers and the rules. In other words, the research question to be answered by the expert system was: 'which bamboo cover occurs at a given location in the forest?' Each available GIS data layer is a piece of evidence used by the expert system to infer the most probable bamboo cover that would occur at a given grid cell. A priori probabilities for all the items of evidence were incorporated into the inferencing process using a Bayesian (statistical) rule-based approach. The decision as to which bamboo cover would represent the cell location was made by selecting the hypothesis (three density classes of bamboo) with the highest probability. A contextual check was then made by expert system to ascertain whether the adjacent pixels had been classified into bamboo covers that were ecologically valid for the grid cell being considered. If the target grid cell was not similar to the adjacent grid cells, then the cells adjacent to target cell form weighting factors to recalculate target cell. The expert system developed for this study used forward chaining with a complete enumeration of the data (i.e., a blind search terminated by running out of evidence). The expert system algorithm was programmed using IDL by the Department of Nature Resources at the International Institute for Geo-information Science and Earth Observation, the Netherlands. The rules are the most subjective aspect of an expert system (Forsyth 1984). In an ideal situation, rules may be derived statistically; but often this is not possible. Thus a

Table 1 Expert system rules

Environmental variable		Bamboo cover		
		High	Low	Non-bamboo
Vegetation type	Bamboo forest	0.8	0.1	0.1
	Shrub-Meadow-Rock	0.1	0.1	0.9
	Fir-dominated forest	0.7	0.2	0.1
	Deciduous hardwood	0.3	0.3	0.3
	Mixed fir-hardwood	0.5	0.4	0.1
	Mixed pine-hardwood	0.3	0.4	0.3
	Pine-dominated forest	0.1	0.3	0.7
Elevation (m)	2,000 – 2,100	0.2	0.6	0.2
	2,100 - 2200	0.2	0.6	0.2
	2,200 – 2,300	0.4	0.4	0.2
	2,300 – 2,400	0.6	0.3	0.1
	2,400 – 2,500	0.8	0.1	0.1
	2,500 – 2,600	0.8	0.1	0.1
	2,600 – 2,700	0.8	0.1	0.1
	2,700 – 3,000	0.5	0.3	0.2
Slope (degree)	< 5	0.3	0.4	0.3
	6 - 20	0.4	0.4	0.2
	21 - 30	0.4	0.4	0.2
	31 - 40	0.4	0.4	0.2
	> 41	0.2	0.3	0.5
Terrain position	Valley	0.5	0.4	0.1
	Lower mid-slope	0.6	0.3	0.1
	Mid-slope	0.7	0.2	0.1
	Higher mid-slope	0.6	0.2	0.2
	Ridge	0.5	0.2	0.3

rule is a heuristic estimate based on the 'feeling' or 'knowledge' of experts. Rules concerning environmental relationships cannot normally be expressed with absolute certainty (i.e., true or false). In other words, a rule is placed somewhere on a continuum between true (probability of 1) and false (probability of 0), depending on how sure we are that the rule is true (or false). In this study, the selection of environmental variables and formulation of rules was based on the availability of the data and the integration of knowledge from several sources, including: (a) literature (Pan et al., 1988, Ren et al., 1998, Tian 1988); (b) knowledge acquired through discussion with seven experienced local researchers, and (c) personal field observations. Where there was disagreement between different sources, a subjective decision was made based on field

knowledge. As mentioned before, four data layers (i.e., vegetation type, elevation, slope, and terrain position) were used by the expert system to predict the three density classes of understorey bamboo, based on these rules. The rules and their associated probabilities are detailed in Table 1.

A hybrid Neural Network and Expert System
For a land use and land cover classification scheme to be effective, managers usually request it to be of 'operational accuracy'. This means having an overall mapping accuracy greater than 85% (Anderson et al., 1976), although the usefulness of this standard is unclear (Foody 2002, Fuller et al., 2003). In general, a kappa value of less than 0.40 indicates poor performance of a classifier, 0.40 to 0.59 indicates moderate performance; 0.60 to 0.74 indicates good performance; while a kappa value of 0.75 or higher suggests a very good to excellent classifier performance (Mather 1999).

In this study a hybrid classification method for remote sensing data was used, incorporating both a neural network and an expert system, to increase the mapping accuracy compared to methods using either a neural network or an expert system. The expert system is used to correct misclassifications created by the neural network. For example, the neural network misclassified 'high cover' with 'low cover' for bamboo forest. This was 'corrected' by limiting the amount of low bamboo cover at high elevations, using the rule-based probabilities (see Table 1). In this case, the understorey bamboo classification results derived from the neural network served as input to the GIS expert system. Figure 3 illustrates the structure of the hybrid neural network and expert system. In order to select which GIS data layers provided additional information for the classification, all layers were initially used with equal weighting.
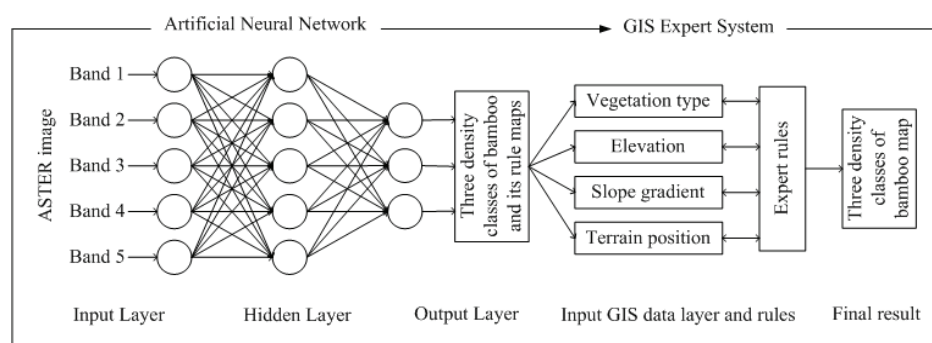
Figure 3 Construction of the hybrid neural network and expert system

Accuracy Assessment
Accuracy assessment of the classified maps (i.e., vegetation type and bamboo cover maps) was summarised using overall accuracy, producer's accuracy, user's accuracy, errors of commission and omission (Jensen 1986), as well as kappa coefficient (Cohen 1960). The kappa coefficient represents the proportion of agreement obtained after removing the chance effect (Congalton 1991, Foody 1992). The kappa statistic and its variance were used to statistically compare the classification accuracies of the maps, using z-tests (Congalton 1991, Skidmore 1999). A z-value greater than or equal to 1.96 indicates a statistically significant difference at 95% confidence between two kappa statistics, which corresponds to a two-sided P value less than or equal to 0.05. The larger z-values result in smaller P values implying more statistically significant results.

RESULTS

Producing the Highest Accuracy Map for the Vegetation Type
Table 2 presents the z-values, overall mapping accuracies and kappa coefficients of the vegetation type maps produced by the three methods: maximum likelihood classifier, artificial neural network, and integrated neural network and knowledge-based classifier. The results show that the highest mapping accuracy was achieved by the integrated neural network and knowledge-based classification with an overall mapping accuracy of 71.7% and kappa of 0.66 (Figure 4). A kappa z-test for pair-wise comparisons showed the integrated neural network and knowledge-based classifier was more accurate than the other two methods (average z-value=3.07, p=0.002) (Table 2).

Table 2 The z-statistic comparing the performance of the three classifiers for vegetation type mapping with overall accuracy (OA) and Kappa coefficient in the last two columns. Significantly different accuracies with confidence of 95% (z-value >1.96) are indicated by*

Classifiers	Maximum likelihood	Neural network	Neural network & Knowledge-based	OA	Kappa
Maximum likelihood	-			52.0	0.42
Neural network	2.07*	-		63.0	0.54
Neural network & Knowledge-based	4.11*	2.03*	-	71.7	0.66

Understorey Bamboo Cover Mapping and its Accuracy Comparison
The three density classes of understorey bamboo maps produced by the three methods (i.e., neural network, expert system, and hybrid neural network and expert system), are shown in Figure 5 (a, b and c, respectively). Error matrices detail the overall map accuracy for the three methods (Table 3), and show that the highest mapping accuracy was achieved with an overall accuracy of 73.8% and kappa of 0.60 using the hybrid neural network and expert system method. A kappa z-test for pair-wise comparison proved that the accuracy derived from the hybrid neural network and expert system method was significantly higher than the accuracies produced by neural network and expert system respectively (average z-value=3.35, p<0.001) (Table 4). However, there was no significant difference in accuracy between the neural network and the expert system method (z=0.41, p=0.682).

Table 3 Error matrices of the neural network, expert system, and hybrid neural network and expert system for three density classes of understorey bamboo mapping, including overall accuracy (% acc.), kappa coefficient, omission error (OE), producer's accuracy (PA), commission error (CE) and user's accuracy (UA)

Classifiers	Bamboo cover	High cover	Low cover	Non-bamboo	CE	UA
Neural network	High cover	22	2	1	12	88
	Low cover	27	58	20	45	55
	Non-bamboo	3	13	41	28	72
	OE	58	21	34	% acc. 64.7	
	PA	42	80	66	Kappa: 0.45	
Expert system	High cover	47	21	16	44	56
	Low cover	5	49	26	39	61
	Non-bamboo	0	3	20	13	87
	OE	10	33	68	% acc. 62.1	
	PA	90	67	32	Kappa: 0.43	
Hybrid neural network and expert system	High cover	40	5	3	17	84
	Low cover	11	62	23	35	65
	Non-bamboo	1	6	36	16	83
	OE	23	15	42	% acc. 73.8	
	PA	77	85	58	Kappa: 0.60	

Table 4 The z-statistic comparing the performance of the three classifiers for three density classes of understorey bamboo mapping with overall accuracy (OA) and kappa coefficient in the last two columns. Significantly different accuracies with confidence of 95% (z-value >1.96) are indicated by *

Classifiers	Neural network	Expert system	Hybrid neural network & expert system	OA	Kappa
Neural network	-			64.7	0.45
Expert system	0.41	-		62.1	0.43
Hybrid neural network & expert system	3.14*	3.56*	-	73.8	0.60
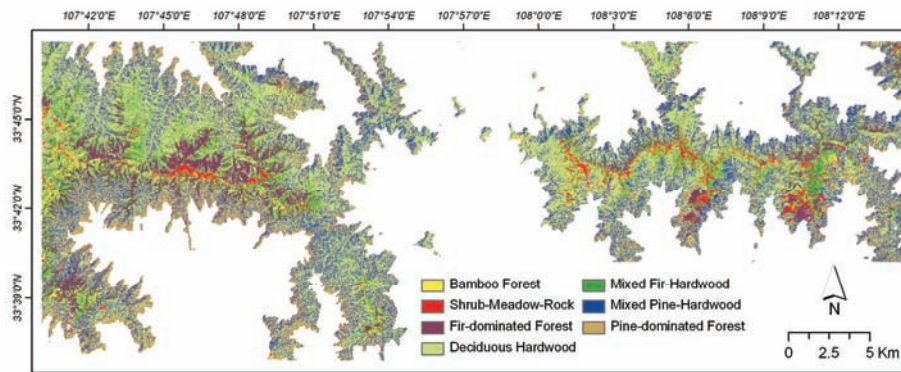
Figure 4 The vegetation type map produced by the integrated neural network and knowledge-based classifier
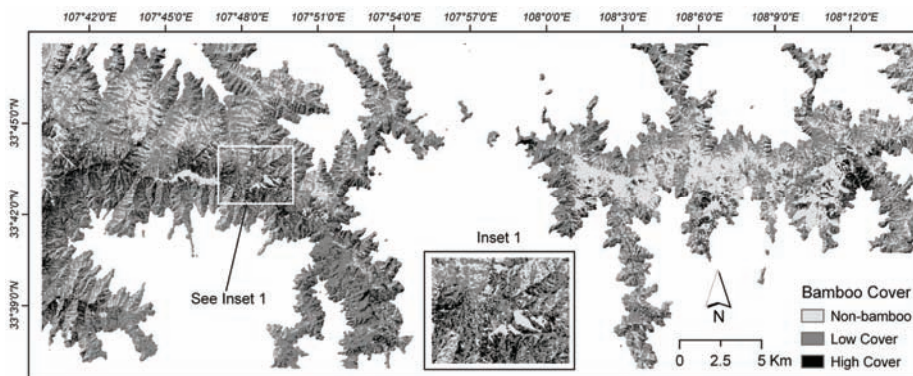
（a）
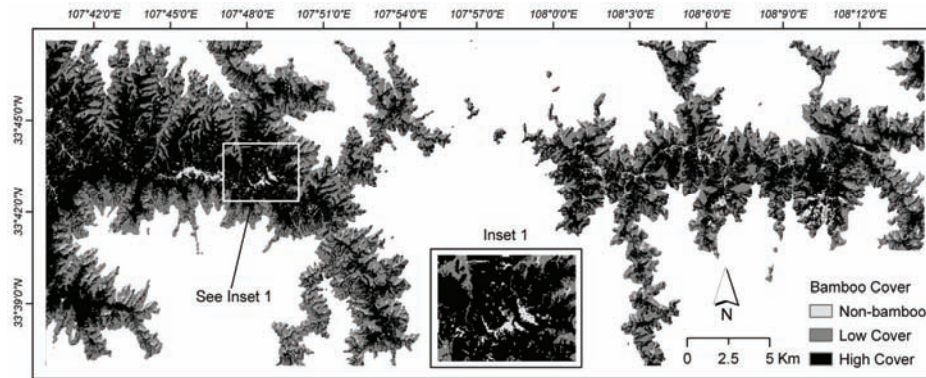
(b)
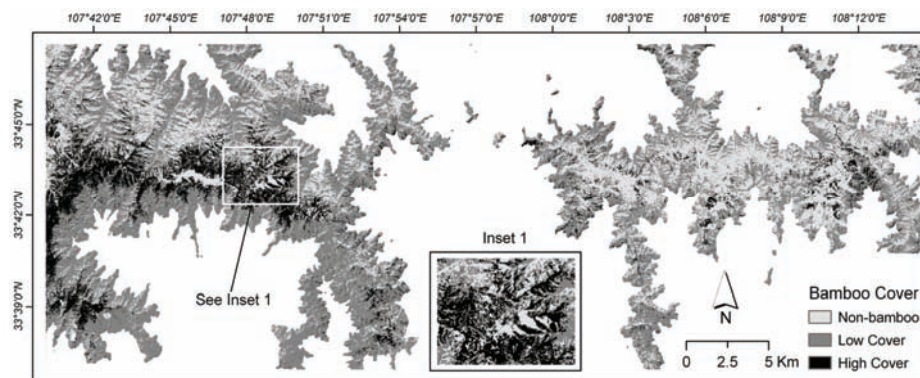
(c)

Figure 5 Three density classes of understorey bamboo produced by (a) the neural network; (b) the expert system; and (c) the hybrid neural network and expert system.

DISCUSSION

Using a leaf-off image and a hybrid neural network and expert system to map three cover classes of understorey bamboo, higher accuracy maps were generated compared with an artificial neural network method or a GIS expert system alone. Not only was the overall accuracy higher (73.8% versus 64.7%), but also the kappa statistics improved (0.60 versus 0.45). A z-test showed that the maps produced by the hybrid neural network and expert system had a

51

significantly higher accuracy than the other two methods, separately. The vegetation type layer and DEM layers used in the expert system provided additional information that complemented the spectral information. Use of this information resulted in better discrimination of three density classes of understorey bamboo which might otherwise have been difficult to classify. Previous studies such as Skidmore (1989), Schmidt et al., (2004), Vaiphasa et al., (2006), and Nangendo et al., (2007) also observed the advantage of using additional data layers when using an expert system.

Why did the hybrid neural network and expert system method produce higher accuracy maps of three density classes of understorey bamboo than the other two methods? To answer this question, we should explain the accuracy contributions of the individual methods (i.e., neural network and expert system), as the hybrid method was designed to combine the advantages of these two methods. Looking at the individual classes in Table 3, it can be seen that there is a big difference in the producer's accuracy of non-bamboo as well as high bamboo cover between the neural network and expert system. The neural network yielded a higher producer's accuracy of non-bamboo area compared to the expert system (66% versus 32%), and conversely, the expert system generated a higher producer's accuracy than the neural network in classifying the high bamboo cover area (90% versus 42%). The higher accuracy of the neural network in mapping non-bamboo area may have had two reasons: (1) leaf-off satellite images were used, which previously was demonstrated to be best for understorey bamboo discrimination (Wang et al., 2009); (2) neural networks are more likely to discern the complex variability in signatures produced by varying canopy and understorey conditions, and may do so more efficiently than traditional classifications (Atkinson and Tatnall 1997, Foody and Arora 1997,Linderman et al., 2004). In contrast, the lower accuracy of the expert system method in mapping non-bamboo areas was most likely caused by the spatial distribution of the bamboo which does not seem to follow clear trends relative to overstorey or abiotic factors (Linderman et al., 2004, Reid et al., 1989). In this study, seven local experts indicated that the prediction of bamboo presence/absence was relatively independent of environmental factors (e.g., elevation, slope and terrain position), except for vegetation types (see Table 2). The lack of correlation between the spatial distribution of bamboo and environmental factors may have been partly due to the unique episodic and synchronized die-offs of large areas of bamboo (Keeley and Bond 1999, Reid et al., 1989).

The expert system method appeared to be more efficient than the neural network method in distinguishing the density of bamboo cover. The expert system method produced a higher map accuracy with dense bamboo cover;

indeed, previous studies have reported that the cover-abundance of bamboo *F. qinlingensis* increased with elevation (Pan et al., 1988, Ren et al., 1998, Tian 1988), and this characteristic was successfully captured in the rules by our local experts (Table 1). The neural network method, however, failed to separate the high bamboo and low bamboo cover classes efficiently (see Table 3). This may have been due to the spectral confusion of these two bamboo cover classes, caused by the inverse relationship between bamboo leaf greenness and altitude during the overstorey leaf-off season (see Figure 2).

Thus, it is clear that both methods (i.e., neural network and expert system) have inherent disadvantages and advantages for classifying the cover-abundance of understorey bamboo. The hybrid neural network and expert system method, however, addressed these difficulties efficiently by using the expert rules and Bayesian method. Consequently, the area misclassified as dense bamboo by the neural network method was modified by the expert system. Simultaneously, the correctly classified non-bamboo areas, as distinguished by the neural network, were retained. To our knowledge, this study represents the first successful mapping of three density classes of understorey bamboo. The method proposed in this research has the potential to provide a practical approach to classifying understorey vegetation and generating information about the quantity and spatial distribution of understorey species in mountainous forest.

CONCLUSIONS

In this study, a novel method for mapping three density classes of understorey bamboo, namely hybrid neural network and expert system has been presented. The main innovation of the hybrid neural network and expert system lies in the use of a Bayesian expert system to correct the estimation of bamboo cover produced by the neural network. Four additional GIS data layers have been included: vegetation cover type, elevation, slope and terrain position. Rules (or knowledge) provided by the experienced local experts have been integrated by the expert system. In other words, the advantages of both remote sensing and GIS classification approaches have been combined to map understorey species. Our experimental results attest to the effectiveness of the proposed technique and show a statistically significant improvement over using either the neural network or the expert system method alone. In addition, for the first time, three density classes of understorey bamboo have been mapped with an overall accuracy of 73.8% and kappa of 0.60, which is a good result (Mather 1999). This approach may also be used for a range of applications, particularly to map cover-abundance of understorey species in complex forested landscapes.

REFERENCES

Anderson, J., E. Hardy, J. Roach, and R. Witmer. 1976. A land-use/land-cover classification system for use with remote sensor data. Washington, DC.

Ardö, J. and P. Pilesjö. 1992. On the accuracy of the global positioning system - A test using a hand-held receiver. International Journal of Remote Sensing **13**:3229-3233.

Atkinson, P. M. and A. R. L. Tatnall. 1997. Neural networks in remote sensing. International Journal of Remote Sensing **18**:699-709.

Blackburn, G. A. and E. J. Milton. 1995. Seasonal variations in the spectral reflectance of deciduous tree canopies. International Journal of Remote Sensing **16**:709-720.

Cohen, I. 1960. A coefficient agreement of nominal scales. Educational and Psychological Measurement **20**:37-46.

Congalton, R. G. 1991. A review of assessing the accuracy of classifications of remotely sensed data. Remote Sensing of Environment **37**:35-46.

De Wulf, R. R., R. E. Goossens, J. R. Mackinnon, and S. C. Wu. 1988. Remote Sensing for wildlife management: giant panda habitat mapping from LANDSAT MSS images. Geocarto International **1**:41-50.

Foody, G. M. 1992. On the compensation of chance agreement in image classification accuracy assessment. Photogrammetric Engineering and Remote Sensing **58**:1459-1460.

Foody, G. M. 1996. Relating the land-cover composition of mixed pixels to artificial neural network classification output. Photogrammetric Engineering and Remote Sensing **62**:491-499.

Foody, G. M. 2002. Status of land cover classification accuracy assessment. Remote Sensing of Environment **80**:185-201.

Foody, G. M. and M. K. Arora. 1997. An evaluation of some factors affecting the accuracy of classification by an artificial neural network. International Journal of Remote Sensing **18**:799-810.

Forsyth, R. 1984. Expert System: Principles and Case Studies. Chapman and Hall, London.

Fuller, R. M., G. N. Smith, and B. J. Devereux. 2003. The characterization and measurement of land cover change through remote sensing: problems in operational applications? International Journal of Applied Earth Observation **4**:243-253.

Ghitter, G. S., R. J. Hall, and S. E. Franklin. 1995. Variability of Landsat Thematic Mapper data in boreal deciduous and mixed-wood stands with conifer understory International Journal of Remote Sensing **16**:2989-3002.

IUCN. 2007. 2007 IUCN Red List of Threatened Species. Gland, Switzerland.

Jensen, J. R. 1986. Introductory Digital Image Processing - A Remote Sensing Perspective. Prentice-Hall, New Jersey.

Joshi, C., J. De Leeuw, J. Van Andel, A. K. Skidmore, D. Lekhak Hari, I. Van Duren, and N. Norbu. 2006. Indirect remote sensing of a cryptic forest understory invasive species. Forest Ecology and Management **225**:245-256.

Keeley, J. E. and W. J. Bond. 1999. Mast flowering and semelparity in bamboos: The bamboo fire cycle hypothesis. The American Naturalist **154**:383-391.

Kent, M. and P. Coker. 1992. Vegetation Description and Analysis - A Practical Approach. John Wiley, New York.

Linderman, M., S. Bearer, L. An, Y. C. Tan, Z. Y. Ouyang, and J. G. Liu. 2005. The effects of understory bamboo on broad-scale estimates of giant panda habitat. Biological Conservation **121**:383-390.

Linderman, M., J. G. Liu, J. Qi, L. An, Z. Y. Ouyang, J. Yang, and Y. C. Tan. 2004. Using artificial neural networks to map the spatial distribution of understory bamboo from remote sensing data. International Journal of Remote Sensing **25**:1685-1700.

Liu, J. G., M. Linderman, Z. Y. Ouyang, L. An, J. Yang, and H. M. Zhang. 2001. Ecological degradation in protected areas: the case of Wolong Nature Reserve for giant pandas. Science **292**:98-101.

Loucks, C. J., Z. Lu, D. Eric, D. J. Wang, D. L. Fu, and H. Wang. 2003. The giant pandas of the Qinling Mountains, China: a case study in designing conservation landscapes for elevational migrants. Conservation Biology **17**:558-565.

Mather, P. M. 1999. Land cover classification revisited. Pages 7-16 *in* P. M. Tate and N. J. Tate, editors. Advances in remote sensing and GIS analysis. Wiley, Chichester.

Moody, A., S. Gopal, and A. H. Strahler. 1996. Sensitivity of neural networks to subpixel land-cover mixtures in coarse resolution satellite data. Remote Sensing of Environment **58**:329-343.

Muukkonen, P. and J. Heiskanen. 2005. Estimating biomass for boreal forests using ASTER satellite data combined with standwise forest inventory data. Remote Sensing of Environment **99**:434-447.

Nangendo, G., A. K. Skidmore, and H. v. Oosten. 2007. Mapping East African tropical forests and woodlands - A comparison of classification. ISPRS Journal of Photogrammetry and Remote Sensing **61**:393-404.

Pan, W., Z. S. Gao, and Z. Lu. 1988. The Giant Panda's Natural Refuge in the Qinling Mountains. Beijing University Press, Beijing (in Chinese).

Reid, D. G., J. C. Hu, S. Dong, W. Wang, and Y. Huang. 1989. Giant panda *Ailuropoda melanoleuca* behaviour and carrying capacity following a bamboo die-off. Biological Conservation **49**:85-104.

Ren, Y., M. L. Wang, and Z. J. Li. 1998. Plants of Giant Panda's Habitat of Qinling Mountains Shaanxi Science and Technology Press, Xi'an (in Chinese).

Schaller, G. B., J. C. Hu, W. S. Pan, and J. Zhu. 1985. The Giant Panda of Wolong. The University of Chicago Press, Chicago.

Schmidt, S. K., A. K. Skidmore, H. E. Kloosterman, H. Van Oosten, L. Kumar, and M. A. J. Janssen. 2004. Mapping costal vegetation using an Expert System and hyperspectral imagery. Photogrammetric Engineering and Remote Sensing **70**:703-716.

State Forestry Administration. 2006. The 3rd National Survey Report on Giant Panda in China Science Press, Beijing (in Chinese).

Skidmore, A. K. 1989a. A comparison of techniques for calculating gradient and aspect from a gridded digital elevation model. International Journal of Geographical Information Systems **3**:323-334.

Skidmore, A. K. 1989b. An expert system classifies Eucalypt forest types using Landsat Thematic Mapper data and a digital terrain model. Photogrammetric Engineering and Remote Sensing **55**:1449-1464.

Skidmore, A. K. 1990. Terrain position as mapped from a gridded digital elevation model. International Journal of Geographical Information Science **4**:33-49.

Skidmore, A. K., W. Brinkhof, and B. J. Turner. 1997. Performance of neural networks for forest mapping from GIS and remotely sensed data. Photogrammetric Engineering and Remote Sensing **63**:501-514.

Soderstrom, T. R. and C. E. Calderon. 1979. A commentary on bamboos (Poaceae: Bambusoideae). Biotropica **11**:161-172.

Stenback, J. M. and R. G. Congalton. 1990. Using thematic mapper imagery to examine forest understory. Photogrammetric Engineering and Remote Sensing **56**:1285-1290.

Stock, M. 1987. AI and expert systems: an overview. AI Application **1**:9-17.

Taylor, A. H. and Z. S. Qin. 1988. Regeneration patterns in old-growth *Abies-Betula* forests in the Wolong Natural Reserve, Sichuan, China. Journal of Ecology **76**:1204-1218.

Tian, X. Q. 1988. Bamboo resource and its relationship to giant panda in Foping Nature Reserve. Bamboo Research **1**:13-17 (in Chinese).

Vaiphasa, C., A. K. Skidmore, and W. F. d. Boer. 2006. A post-classifier for mangrove mapping using ecological data. ISPRS Journal of Photogrammetry and Remote Sensing **61**:1-10.

Wang, T. J., A. K. Skidmore, A. G. Toxopeus, and X. H. Liu. 2009. Understory bamboo discrimination using a winter image. Photogrammetric Engineering and Remote Sensing. 75 (1): 37-47.

WWF and MOF. 1989. National Conservation Management Plan for the Giant Panda and its Habitat WWF, Hong Kong.

Yang, X. F., A. K. Skidmore, D. R. Melick, Z. K. Zhou, and J. C. Xu. 2006. Mapping non-wood forest product (matsutake mushrooms) using logistic regression and a GIS expert system. Ecological Modelling **197**:208-218.

Yue, M., G. D. Dang, and L. J. Yong. 1999. The basic features of vegetation of Foping Nature Reserve in Shaanxi Province. Journal of Wuhan Botanical Research **17**:22-28 (in Chinese).

Chapter 4

Displaying remotely sensed vegetation dynamics along natural gradients for ecological studies

ABSTRACT

Normalized difference vegetation index (NDVI) datasets are growing in popularity to represent vegetation dynamics in ecological studies. Because of its multidimensional nature, it is difficult to visualise the spatial and temporal components of NDVI datasets simultaneously. This study presents a method to display vegetation dynamics as captured by the NDVI along natural gradients and to visualise and test correlations between vegetation phenology and animal movement.

INTRODUCTION

Remote sensing data are increasingly being used for ecological studies (Pettorelli et al., 2005). The normalized difference vegetation index (NDVI), in particular, is useful because it shows spatial and temporal trends in vegetation dynamics, productivity and distribution (Reed et al., 1994, Nemani et al., 2003). Consequently, the NDVI is growing in popularity as a tool to investigate the interaction between vegetation and animal activity, including migration (Boone et al., 2006, Ito et al., 2006).

Until this century, the AVHRR and SPOT sensors were the only instruments providing data to construct NDVI time series at an almost-daily resolution. The 1 km spatial resolution of these datasets limits their applicability for all but continental and global ecological studies. Now, however, MODIS and MERIS data can be used to produce NDVI time series of almost-daily resolution at a spatial resolution as high as 250 or 300 m, making them useful for local and regional studies. Derived datasets for monitoring regional vegetation activity, for example, may be validated with in situ observations of vegetation phenology (Delbart et al., 2006, Beck et al., 2007). Hence, time series are well suited to represent the dynamics of vegetation activity in ecological studies, and compare them, for example, to animal migration and movement.

Displaying NDVI time series and relating them to ecological phenomena is challenging, as the datasets are typically multidimensional, quantifying vegetation activity in space, as well as through time. The most common approach is to exclude either the spatial or the temporal component of the data in the visualisation. A single time series of the NDVI may, for example, be shown to exemplify the data (e.g., Stockli and Vidale 2004), or a map depicting a 'time-slice' of the data may represent the NDVI in space at a given moment in time (e.g., Pettorelli et al., 2005). Alternatively, a parameter derived from the NDVI time series, such as a principal component or the estimated start of the growing season, may be mapped (e.g., Naizot et al., 2004, Karlsen et al., 2007) or plotted against a geographical gradient (e.g., Zhang et al., 2003). While these approaches are complementary, none represents the temporal and spatial patterns in an NDVI dataset simultaneously.

Since its first use, colour palettes have been applied to map the NDVI. Occasionally, colour palettes have been used to represent NDVI values along axes other than a geographical grid: Stockli and Vidale (2004) displayed the NDVI along a time axis with daily resolution and a range of 1 year versus an axis with yearly resolution. This allowed them to display interannual and seasonal variability in the NDVI and the start and end of the growing season in

a single figure. Dye and Tucker (2003) displayed annual vegetation index (VI) patterns in colour along a latitudinal gradient and Anyamba and Tucker (2005) displayed them along a longitudinal gradient. In these latter two examples, colour bars represent the annual trajectory of the NDVI in a single stratum of, respectively, latitude and longitude.

Here, the method of displaying NDVI along spatial and temporal dimensions simultaneously is developed further. It is applied to a mountainous area to show how the vegetation greenness changes in time and with altitude. Using the movement data of radio tracked giant pandas in the area in addition illustrates how the display method facilitates visualising correlations between vegetation phenology and other biotic factors, in this case seasonal animal movement.

STUDY AREA AND MODIS NDVI DATA

The Foping Biosphere Reserve is located in south-western China and between altitudes of 1,000 and 2,900m (see Figure 1). The area is mostly forested with understorey vegetation dominated by bamboo species and has the highest population density of giant pandas in the world (State Forestry Administration 2006).

MODIS NDVI data (MOD13) over part of the Foping Biosphere Reserve were downloaded. The dataset provides 23 NDVI images per year at 16 day interval, where every pixel value is the product of maximum value compositing (Huete et al., 2002). From the 5 year data between 2001 and 2005, the best 1 year time series, consisting of 23 images, was composed as follows: for each pixel and compositing period, the five available NDVI values were extracted and the mean of the three values of highest quality was calculated. If more than three values had the highest quality, the mean NDVI of all these was used. The quality judgement was based on the usefulness index accompanying the MODIS data.

To interpolate the 23 values of the average NDVI time series for display purposes and to reduce noise in the data, the TIMESAT software package and a Savitsky–Golay function were used (Jönsson and Eklundh 2004).
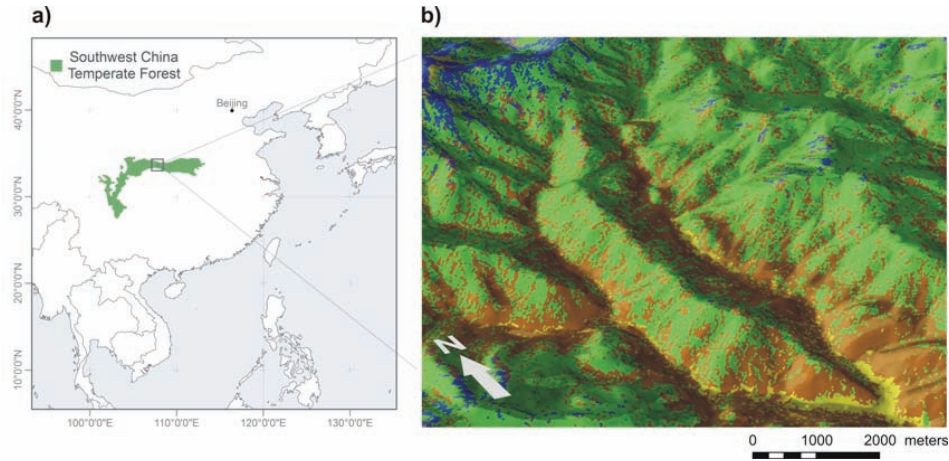
Figure 1 (a) The location of Foping Biosphere Reserve and the southwest China temperate forest it is a part of, in eastern Asia. (b) A vegetation map of Foping Biosphere Reserve (Liu 2001), overlaid on a digital elevation model with a 30m horizontal resolution. Deciduous broadleaf forest is shown in brown, mixed forest in green, evergreen coniferous forest and bamboo meadows in blue and other land cover types yellow

RELATIVE PHENOLOGICAL DEVELOPMENT (RPD)

Changes in NDVI through time reflect phenological development in terrestrial vegetation types ranging from the Arctic to the tropics (Krishnaswamy et al., 2004, Beck et al., 2006). The interpolated NDVI trajectory of each pixel was normalized to cover the range of 0% to 100%, indicating the minimum and maximum NDVI for a given pixel, respectively. Therefore, $RPD_t(NDVI_t–NDVI_{min})/(NDVI_{max}–NDVI_{min})$, where NDVImin is the minimum NDVI for the pixel, NDVImax is the maximum NDVI for the pixel and RPD_t and $NDVI_t$ are the relative phenological development at and NDVI at time t, respectively.

Thus, when viewing the RPD of two pixels at a given time t, one can compare the state of greenness of the two pixels irrespective of their absolute NDVI values. Here, this scale is termed the relative phenological development (RPD).

GIANT PANDA MOVEMENT DATA

The giant panda movement data were gathered between June 1991 and December 1995 from three female and three male individuals equipped with radio collars. The geographical position of the animals was estimated from at least three bearings recorded in the field. As successful registration was not possible every day and for every animal, the number of position estimates varied between animals, from 107 to 465, with a mean of 293.

The first MODIS sensor was launched in 1999, while the giant panda movement datasets are from 1991 to 1995. It was tested whether the 2001 to 2005 average NDVI time series may represent the period 1991 to 1995 by comparing the temperature and precipitation in the two periods, as these are main drivers of plant phenology (Cleland et al., 2007).

COMPATIBILITY OF THE NDVI AND GIANT PANDA MOVEMENT DATA

In general, the 1991 to 1995 period is comparable to the 2001 to 2005 period, although the mean monthly temperature was slightly higher than the 2001 to 2005 maximum in August, November and December (Figure 2(a)). The difference was greatest in November, where the 1991 to 1995 mean was 0.9 °C warmer than the 2001 to 2005 maximum. The mean monthly precipitation in the 1991 to 1995 period was 10mm higher than the 2001 to 2005 maximum in April and 40mm lower than the 2001 to 2005 minimum in September and the driest summers occurred in the former period (Figure 2(b)). Overall, the climate in the period with NDVI observations was somewhat colder in summer and autumn than in the period with giant pandas, and also slightly wetter. The year 2002 was unusual as it saw 210mm of rainfall on 9 June (Hou et al., 2006). However, when excluding the year 2002 from the NDVI data composition as described in §2, the average NDVI values for the 23 images did not change by more than 0.02. Hence, the NDVI is generally representative of the years with giant panda observations.

VISUALISATION

Vegetation activity, estimated using the NDVI time series, was displayed in the Foping Biosphere Reserve along an altitudinal gradient. Annual NDVI trajectories were stratified by altitude and plotted along axes of time and altitude (Figure 3(a)). To facilitate the comparison of phenological development

at different altitudes and across vegetation types, the plot was coloured according to the RPD. Thus, bands of similar colour in the figure can be regarded as vegetation in similar phenological stages, allowing for differences between vegetation types, because of the normalization in the RPD calculation (for non-normalized phenological indices, see Krishnaswamy et al., (2004) and Das et al., (2006). The figure clearly shows how the period of dormancy lengthens and the growing season shortens towards higher altitudes; at the lowest altitudes, the dormancy period continues until April, while it continues until May at the highest altitudes. This concurs with the ground observations of Wang et al., (2009) that in the Foping Biosphere Reserve, canopy trees leaf out in mid April to late May and leaf fall is complete by mid October to early November. After dormancy, the vegetation reaches maximum greenness in the course of about 1 month at the lowest altitudes, increasing to almost 2 months on the mountain peaks. In the middle of summer and the middle of winter, the average NDVI in the area is constant across the altitude gradient in the area. The length of near-maximum greenness lasts for more than 4 months in the lowlands, but for only 3 months on the mountain plateaus and tops.
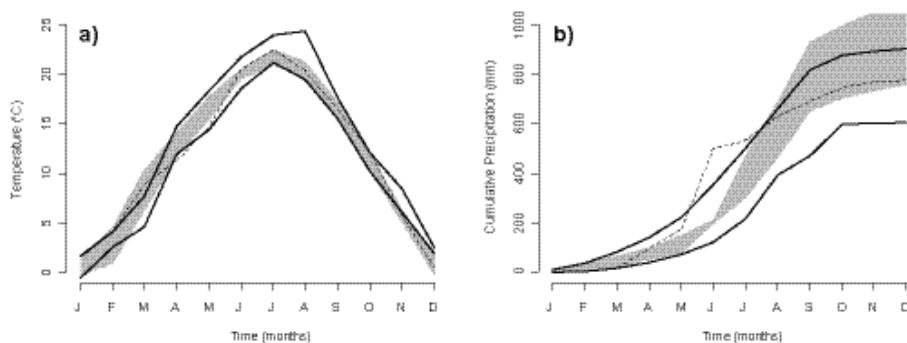
Figure 2 Range of (a) monthly temperatures and (b) cumulative precipitation in Foping from 1991 to 1995, when giant panda location data were collected (lines), and from 2001 to 2005, when MODIS NDVI data were collected (shaded area, excluding 2002). The year 2002 (dashed line) was unusual, because it saw very high rainfall (210 mm) on 9 June. The meteorological station was moved to a new location in July 2001. Therefore, all temperature recordings from this date onwards were adjusted downwards to correct for the 260m difference in altitude of the two locations, assuming a lapse rate of 6.5 °C/km
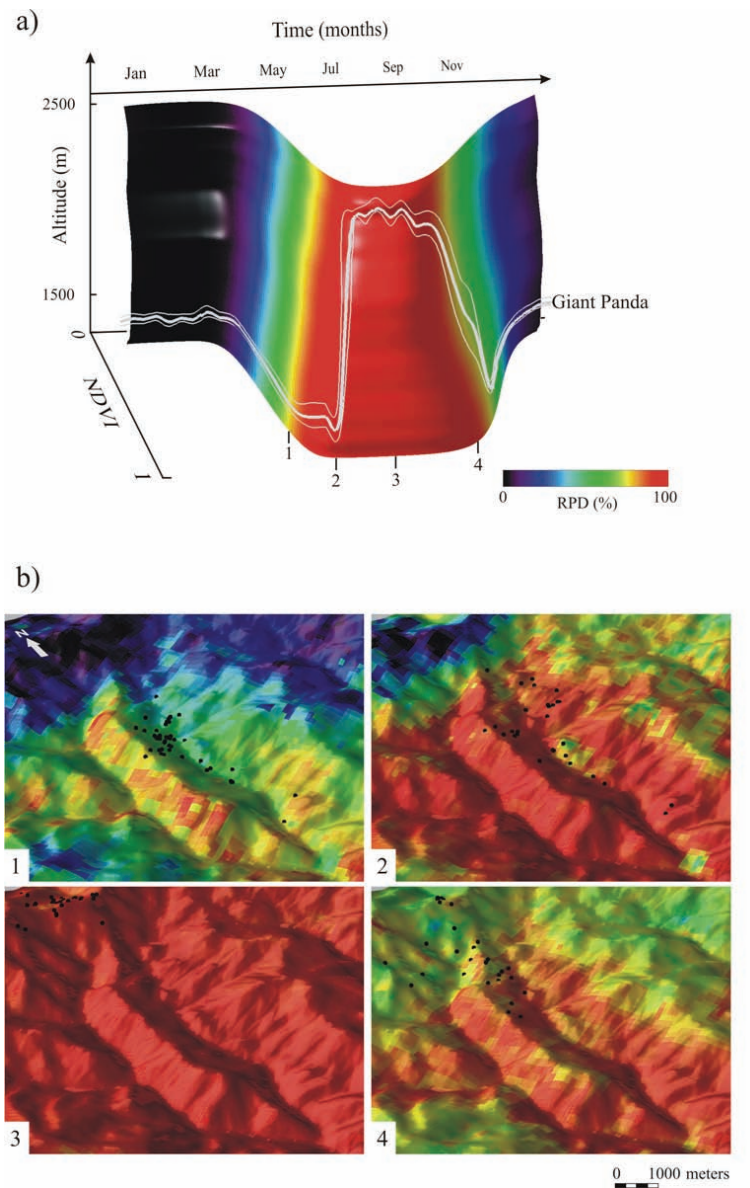
Figure 3 (a) Summarized phenology of the Foping biosphere reserve as detected by MODIS NDVI after processing with TIMESAT. The RPD is a rescaled version of the NDVI. The solid white line shows the average altitudinal movement of six radio tracked giant pandas and the thin white lines indicate the standard error of the average. (b) Time-slices of RPD during early spring, late spring, summer and early autumn, with the positions of the radio tracked giant pandas during a 10 day period indicated by black dots

The altitudinal movement of the giant pandas in the area shows a striking correlation with the phenological development of the area. In spring, the animals move rapidly to higher altitudes when the vegetation reaches its peak greenness. In autumn, the gradual movement of the animals to lower altitudes coincides with the onset of vegetation senescence from the highlands to the valleys.

In addition, the RPD was mapped during early spring, late spring, summer and early autumn and showed the giant panda locations in the corresponding periods (Figure 3(b)). The maps were overlaid on a shaded digital elevation model of the area. Together, they further illustrate how the phenological development correlates with altitude and strongly indicate that phenological development drives the giant panda movement. The display methods described here provide a useful exploratory tool when relating vegetation activity, as monitored in remote sensing, to other ecological phenomena.

REFERENCES

Anyamba, A. and C. J. Tucker. 2005. Analysis of Sahelian vegetation dynamics using NOAA-AVHRR NDVI data from 1981-2003. Journal of Arid Environments **63**:596-614.

Beck, P. S. A., C. Atzberger, K. A. Hogda, B. Johansen, and A. K. Skidmore. 2006. Improved monitoring of vegetation dynamics at very high latitudes: A new method using MODIS NDVI. Remote Sensing of Environment **100**:321-334.

Beck, P. S. A., P. Jönsson, K. A. Hogda, S. R. Karlsen, L. Eklundh, and A. K. Skidmore. 2007. A ground-validated NDVI dataset for monitoring vegetation dynamics and mapping phenology in Fennoscandia and the Kola peninsula. International Journal of Remote Sensing **28**:4311-4330.

Boone, R. B., S. J. Thirgood, and J. G. C. Hopcraft. 2006. Serengeti Wildebeest migratory patterns modeled from rainfall and new vegetation growth. Ecology **87**:1987-1994.

Cleland, E. E., I. Chuine, A. Menzel, H. A. Mooney, and M. D. Schwartz. 2007. Shifting plant phenology in response to global change. Trends in Ecology & Evolution **22**:357-365.

Das, A., J. Krishnaswamy, K. S. Bawa, M. C. Kiran, V. Srinivas, N. S. Kumar, and K. U. Karanth. 2006. Prioritisation of conservation areas in the Western Ghats, India. Biological Conservation **133**:16-31.

Delbart, N., T. Letoan, L. Kergoat, and V. Fedotova. 2006. Remote sensing of spring phenology in boreal regions: A free of snow-effect method using NOAA-AVHRR and SPOT-VGT data (1982-2004). Remote Sensing of Environment **101**:52-62.

Dye, D. G. and C. J. Tucker. 2003. Seasonality and trends of snow-cover, vegetation index, and temperature in northern Eurasia. Geophysical Research Letters **30**:1405.

Hou, J., C. Wang, Y. Lu, Z. Ning, and J. Du. 2006. Activity of typhoons and extreme rainstorms in Shaanxi Province. Journal of Tropical Meteorology **22**:203-208 (in Chinese).

Huete, A., K. Didan, T. Miura, H. Yoshioka, L. Ferreira, X. Goa, and K. Batchily, , . 2001. Validation of the MODIS vegetation indices over a global set of test sites: preliminary results. Remote Sensing of Environment **83**:195-213.

Ito, T. Y., N. Miura, B. Lhagvasuren, D. Enkhbileg, S. Takatsuki, and A. J. Tsunekawa, Z.,. 2006. Satellite tracking of Mongolian gazelles (Procapra gutturosa) and habitat shifts in their seasonal ranges. Journal of Zoology **269**:291-298.

Jonsson, P. and L. Eklundh. 2004. TIMESAT - a program for analyzing time-series of satellite sensor data. Computers & Geosciences **30**:833-845.

Karlsen, S. R., I. Solheim, K. A. Hogda, F. E. Wielgolaski, H. Tomimervik, and P. S. A. Beck. 2007. Variability of the start of the growing season in Fennoscandia,1982-2002. International Journal of Biometeorology **51**:513-524.

Krishnaswamy, J., M. C. Kiran, and K. N. Ganeshaiah. 2004. Tree model based eco-climatic vegetation classification and fuzzy mapping in diverse tropical deciuduous ecosystems using multi-season NDVI. International Journal of Remote Sensing **25**:1185-1205.

Liu, X. H. 2001. Mapping and modelling the habitat of giant pandas in Foping Nature Reserve, China. PhD thesis. Wageningen University, Wageningen.

Naizot, T., Y. Auda, A. Dervieux, J. Thioulouse, and M. F. Bellan. 2004. Une nouvelle analyse multi-temporelle d'images satellitales, les rsidus de l'Analyse en Composantes Principales. Un cas d'tude: une srie d'images Landsat Thematic Mapper de la Camargue, France International Journal of Remote Sensing **25**:1925-1938.

Nemani, R. R., C. D. Keeling, H. Hashinoto, W. M. Jolly, S. C. Piper, C. J. Tucker, R. B. Myneni, and S. W. Running. 2003. Climate-driven increases in global terrestrial net primary production from 1982 to 1999. Science **300**:1560-1563.

Pettorelli, N., J. O. Vik, A. Mysterud, J.-M. Gaillard, C. J. Tucker, and N. C. Stenseth. 2005. Using the satellite-derived NDVI to assess ecological responses to environmental change. Trends in Ecology & Evolution **20**:503-510.

Reed, B. C., J. F. Brown, D. Vanderzee, T. R. Loveland, J. W. Merchant, and D. O. Ohlen. 1994. Measuring phenological variability from satellite imagery. Journal of Vegetation Science **5**:703-714.

State Forestry Administration. 2006. Third National Survey Report on Giant Pandas in China Science Press, Beijing (in Chinese).

Stockli, R. and P. L. Vidale. 2004. European plant phenology and climate as seen in a 20-year AVHRR land-surface parameter dataset. International Journal of Remote Sensing **10**:3303-3330.

Wang, T. J., A. K. Skidmore, A. G. Toxopeus, and X. H. Liu. 2009. Understory bamboo discrimination using a winter image. Photogrammetric Engineering & Remote Sensing. **75**: 37-47

Zhang, J., W. Dong, C. Fu, and L. Wu. 2003. The influence of vegetation cover on summer precipitation in China: a statistical analysis of NDVI and climate data. Advances in Atmospheric Sciences **20**:1002-1006.

Giant Panda (*Ailuropoda melanoleuca*)
Photograph: Yange Yong

Golden Takin (*Budorcas taxicolor bedfordi*)
Photograph: Yange Yong

Chapter **5**

Altitudinal migration of sympatric giant panda and golden takin in relation to plant phenology and bamboo abundance

ABSTRACT

Giant pandas (*Ailuropoda melanoleuca*) and golden takins (*Budorcas taxicolor bedfordi*) occur sympatrically throughout the southern part of the Qinling Mountains in China. Both species have the habit of altitudinal migration in a mixed forest-bamboo landscape. Although previous studies have reported that the migration patterns of giant pandas and golden takins appear different, little is known about these differences in relation to their food quality and quantity. In this study, we use radio-telemetry data from six giant pandas and three golden takin groups to determine if differences in their migration patterns are related to satellite-derived plant phenology (a surrogate of food quality) and bamboo abundance (a surrogate of food quantity). Our results indicate that the altitudinal migration pattern of the golden takin is linked to the early spring green-up and late autumn senescence. The migration pattern of the giant panda, however, is related to the late spring green-up and early autumn senescence, with the spring migration of giant pandas following the peak of bamboo shooting which occurs about three weeks later than the overall greening of the landscape. The short duration of uphill and downhill migrations of the giant panda may be attributable to the sparseness of the bamboo forest at intermediate elevations in the study area, and the consequent lack of forage for giant pandas. At intermediate elevations plant species diversity and density is high, however, providing varied forage for golden takins, and therefore encouraging their relatively early and slower ascent in spring and late descent in autumn. In other words, the altitudinal migration patterns of both the giant panda and the golden takin follow the phenological development of plants in the study area, and the difference between them appears to be attributable to the difference in the phenology of bamboo and non-bamboo plants, and thus the abundance and quality of food available to these two species.

INTRODUCTION

Altitudinal migration is exhibited by numerous species in many different mountainous regions throughout the world (Festa-Bianchet 1988, Geist 1971, Igota et al., 2004, Mysterud 1999, Oosenbrug and Theberge 1980). An understanding of the causes of animal migration may yield valuable insights into the variables that determine life histories, habitat requirements, and foraging strategies of species and individuals (Richter and Cumming 2006). Altitudinal migration may be a strategy for animals to optimize living conditions throughout the year (Fryxell and Sinclair 1988, Pettorelli et al, 2007). Traditionally, these conditions are either interpreted as the availability of abundant and high-quality food (Albon and Langvatn 1992, Hanley 1997, White 1983), or relevant environmental factors such as favourite temperatures, less snow depth, less predation, or the combination of the factors (Festa-Bianchet 1988, Mysterud et al., 2007, Nelson 1995, Pan et al., 1988). We were interested in how ecological factors affect patterns of altitudinal migration. In particular, we focused on how food availability (i.e., food quality and quantity) might cause differences in migration patterns between species, because previous studies have suggested that increased access to highly nutritious and abundant forage is one of the most important driving forces in the evolution of migration of large herbivores (Fryxell and Sinclair 1988, Mysterud et al., 2001).

Giant pandas (*Ailuropoda melanoleuca*) and golden takins (*Budorcas taxicolor bedfordi*) are both large red-listed mammals, and occur sympatrically throughout the southern part of the Qinling Mountains in China (IUCN 2007, Pan et al., 1988, Wu et al., 1990). Many observers have reported that both species have the habit of altitudinal migration in a mixed forest-bamboo landscape in the Foping Nature Reserve (Liu et al., 2002, Pan et al., 1988, Wu et al., 1990, Yong et al., 1994, Zeng et al., 2008). Giant pandas migrate in spring from their winter range at low elevations to their summer range at high elevations and back in autumn (Liu et al., 2002). Golden takins, however, have a more complicated migration pattern. In addition to their spring and autumn migration, they move to intermediate elevations for winter (Zeng et al., 2008). Golden takins and giant pandas both differ in the timing and the rate of their altitudinal migrations. Golden takins spend more time on their uphill and downhill trek than giant pandas do (Zeng et al., 2008). Moreover, giant pandas leave for their summer habitat later and return to their winter habitat earlier than golden takins (Liu et al., 2002). Three drivers of the migration of these two species have been suggested (Pan et al., 1988, Yong et al., 1994, Zeng et al., 2008): (1) to seek more abundant or nutritious forage, (2) to search for optimum temperature conditions, or (3) to escape insect harassment. However, there is no quantitative research testing these hypotheses, as continuous field observations

of environmental conditions are not easily available. Here, we focus on food quality and quantity, using remote sensing to estimate them, and examine the role they might play in the altitudinal migrations of these two sympatric species.

Crude protein content and digestibility of plants peak early in the growing season, and then rapidly decline as vegetation matures (Crawley 1983, Van Soest 1983). Higher forage quality is therefore associated with early phenological stages when new green leaves dominate biomass (Crawley 1983, Prins and Ydenberg 1985, Van Soest 1983). Temperature is one of the key factors determining plant growth and is generally negatively correlated with elevation (Tang and Fang 2006). Hence, in a mountain environment, plants at lower elevations tend to reach spring and summer phenological phases earlier than plants at higher elevations (Beck et al., 2007). The considerable spatial and temporal variation in plant quality is thus a direct result of seasonal changes at different elevation-climate zones. Plant phenology is therefore a good proxy for plant quality (Laycock and Price 1970) and it is frequently described as the driving force in habitat use by vertebrate herbivores (Albon and Langvatn 1992, Fryxell 1991). However, high food quality does not always translate into high food abundance. According to classical theories on optimal foraging, a forager should maximize energetic gains and minimize energetic costs of foraging (MacArthur and Pianka 1966). Under these conditions, animals will spend most time in habitats which are not only richest in food quality, but also highest in food abundance, and the selection of habitat is likely to reflect both these aspects of food availability.

Giant pandas are old carnivores, which evolved into obligate bamboo grazers (Wei et al., 1999). Pandas meet their dietary requirements by consuming large quantities of bamboo daily to compensate for its low digestibility (approximately 20-26% of digestible energy in bamboo leaves and 40-44% in shoots (Dierenfeld et al., 1982, Schaller et al., 1985). Therefore, generally, continuous dense bamboo forest with a high production of bamboo shoots provides the best feeding habitat for wild giant pandas. The golden takin, however, is a forest-dwelling herd-forming ungulate with generalist foraging habits, feeding on more than 160 species of plants, including mosses, ferns, herbs, shrubs and trees in the Qinling Mountains (Zeng et al., 2001). Although the diet of golden takins can vary over the seasons, it consists primarily of twigs, shoots, young stems and leaves of plants (Zeng et al., 2001). However, plant diversity tends to be low and seedlings, saplings and young trees are scarce when dense bamboo dominates the understory (Taylor and Qin 1988, Veblen et al., 1977, Yue et al., 1999). Hence, the areas of dense bamboo, favoured by giant pandas, potentially form poor golden takin habitat (Zeng et

al., 2001).We therefore predict that the spatial-temporal variation in plant phenology and bamboo abundance explains differences in the migration patterns of giant pandas and golden takins.

The ability to examine animal migration responses to environmental factors has often been hampered by a rather limited understanding of animal habitats. Indeed, it is difficult to obtain spatially continuous information on plant quality and abundance by using traditional field survey methods at large temporal and spatial scales (Skidmore and Ferwerda 2008). The rapidly increasing use of satellite remote sensing data in ecological studies has recently changed this situation (Beck et al., 2008, Kerr and Ostrovsky 2003). Remote sensing generates a remarkable array of ecologically valuable measurements, which include details on habitats (land cover classification) and their biophysical properties (vegetation biomass and vegetation phenology). The normalized difference vegetation index (NDVI), in particular, is useful, because it shows spatial and temporal trends in vegetation productivity and distribution (Reed et al., 1994, Nemani et al., 2003). Therefore, changes in NDVI are a good proxy for vegetation dynamics (Justice et al., 1985, Myneni et al., 1997, Nemani et al., 2003), and have been used extensively for monitoring vegetation phenology (Beck et al., 2006, Lloyd 1990, Feed et al., 1994, White et al., 1997). As a result, NDVI is a useful tool for investigating the interaction between vegetation and animal activity, including migration (Boone et al., 2006, Ito et al., 2006).

The aim of this study is to examine the differences in altitudinal migration between giant pandas and golden takins in relation to spatiotemporal variations in their food quality and quantity. Satellite-derived plant phenology and bamboo abundance were adopted as surrogate measures of forage quality and quantity, respectively, for these two species.

MATERIALS AND METHODS

Study site
The study was conducted in the Foping Nature Reserve (Figure 1). This reserve is located on the southern slopes of the Qinling Mountains in southwest China (33°32´-33°45´N, 107°40´-107°55´E). It covers an area of 294 km² and elevation ranges from about 1,000 to 2,900 m. Local weather records from 1957 to 2000 (Foping station No. 57134, elevation 1,087 m), show an annual mean temperature of 11.5°C. The lowest average monthly temperature is -3°C, which occurs in January while the highest average monthly temperature is 28°C, which occurs usually in July. Annual rainfall is approximately 930 mm and mainly concentrated in July, August and September. The first snowfall usually

occurs in November at the highest elevations and about a month later at lower elevations (below 1,500 m). Snow begins to melt in early March and has completely melted at higher elevations by late March.
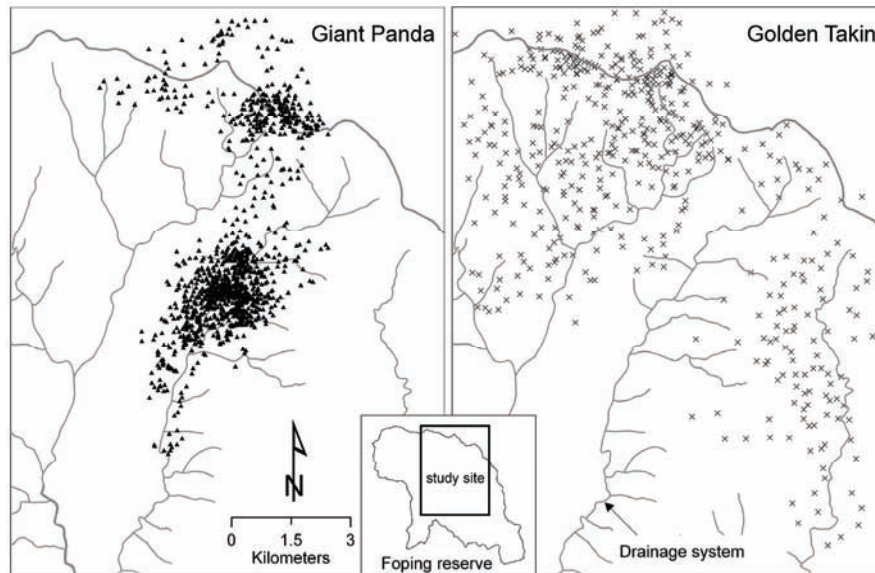
Figure 1 Location of the study site in the Foping Nature Reserve, and the distribution of radio-tracked giant pandas (solid triangle) and golden takins (cross) during 1992-1996

The vegetation varies with elevation, and forest accounts for 96 percent of the total land area in the reserve. According to Ren et al., (1998), the major forest types are broadleaf deciduous forest (below 2,000 m), mixed coniferous and deciduous forest (2,000-2,500 m) and coniferous forest (above 2,500 m), with some interspersed subalpine shrubs and meadows at the top of the mountains (above 2,600 m). These forest types occupy 31%, 59%, 6% and 2% of the total reserve, respectively (Liu 2001). The dominant overstorey tree species are *Quercus* spp., *Populus* spp., *Betula* spp., *Acer* spp., *Pinus* spp., Tsuga chinensis and *Abies fargesii*. Two bamboo species, *Bashania fargesii* (below 2,000 m) and Fargesia qinlingensis (above 2,000 m), dominate the forest understory and form the principal food source for the giant pandas in the study area. Other common understory species include *Lespedeza* spp., *Abelia* spp., *Litsea* spp., *Rosa* spp., *Lonicera* spp., *Spiraea* spp., *Rhododendron* spp., *Carex* spp. and *Kobresia* spp.

Foping Nature Reserve was established in 1978, and is dedicated to the conservation of the giant panda and its habitat. It is one of the few Chinese reserves with intact ecosystems, and is renowned for having the highest density of giant pandas in China. An estimated 76 giant pandas and 480 golden takins live in the reserve (State Forestry Administration 2006, Zeng et al., 1998). Other herbivores that coexist with giant pandas and golden takins are serow (*Capricornis sumatraensis*), goral (*Naemorhedus goral*), musk deer (*Moschus berezovskill*), tufted deer (*Elaphodus cephalophus*) and Chinese muntjac deer (*Muntiacus reevesi*). Large predators such as wolf and tiger once occurred in the region but are now considered to be functionally extinct. Dholes (*Cuon alpinus*) and occasionally leopards (*Panthera pardus*) are still found in the study area, but the size of their populations remains uncertain.

No roads were constructed in the reserve until 2000. About 300 local people resided within the nature reserve during 1998. They were concentrated in five village groups along the river valleys, where the elevation is below 1,500 m. The major land-use activity is farming.

Collection of animal movement data using radio-telemetry
Six giant pandas (3 males and 3 females) and three golden takins (1 male and 2 females) were fitted with radio collars (MOD-500, Telonics Inc. Mesa, AZ, USA) and tracked for different periods (Liu et al., 2002, Zeng et al., 2008). Tracking of giant pandas started in January 1992 and ended in December 1995, while golden takin were tracked from July 1995 to August 1996. The golden takin is gregarious and their group composition can vary over time. The three groups of golden takin with one radio-collared individual each had an average size of about 10 individuals (Zeng et al., 2002). As the locational data showed that the three radio-collared individuals did not meet each other, it was assumed that we were able to obtain information on the movements of approximately 30 individuals through these collared individuals.

A total of 59 and 38 receiving towers across the radio tracking region were used to monitor the giant pandas and golden takins, respectively. The collared animals were located using a tracking system consisting of a TR-2 receiver and a 2-element directional H-antenna. Data were collected daily, and locations calculated by triangulation (White and Garrott 1990). At least 3 signal bearings from different towers were used to form an error polygon. The centre of the polygon represented the animal's location. We used these locations when the associated error polygons measured less than 1 ha. As a result, we obtained 1437 radio-telemetry locations for giant pandas and 487 locations for golden takins (see Figure 1). We subsequently extracted altitudinal data by overlaying the coordinates of animals on a digital elevation model (DEM) with a 25 m

horizontal resolution. Because altitudinal migration patterns of giant pandas and golden takins become visible at a 10-day scale, rather than at a monthly or seasonal scale, we divided each month into three 10-day periods (TD) (Liu et al., 2002, Zeng et al., 2008). The first, second and the last 10 days of the month were used as time units (i.e., 36 TDs per year).

Mapping of plant phenology using MODIS NDVI

Changes in NDVI through time reflect phenological development in vegetation (Beck et al., 2006, Krishnaswamy et al., 2004). Moderate Resolution Imaging Spectroradiometer (MODIS) data can be used to produce NDVI time series at a spatial resolution of up to 250 m, making them useful for local and regional studies. For this study, MODIS 250 m NDVI data (MOD13Q1) over part of Foping Nature Reserve were downloaded. The dataset provides 23 NDVI images per year at 16 day intervals, where every pixel value is produced by maximum value compositing of near-daily data (Huete et al., 2002). From the data collected in the 5 years between 2001 and 2005, the best 1 year time series, consisting of 23 images, was composed, i.e., for each pixel and compositing period, the five available NDVI values were extracted and the mean of the three values of highest quality, based on the quality flags provided in the MOD13Q1 product, was calculated. To interpolate the 23 values of the average NDVI time series for display purposes and to reduce noise in the data, the TIMESAT software package and a Savitsky-Golay function were used (Jönsson and Eklundh 2004). The interpolated NDVI trajectory of each pixel was normalized to cover the range of 0% to 100%, indicating the minimum and maximum NDVI for a given pixel, respectively, and producing the Relative Phenological Development (RPD) metric:

$$RPD_t = (NDVI_t - NDVI_{min})/(NDVI_{max} - NDVI_{min}) \tag{1}$$

where $NDVI_{min}$ and $NDVI_{max}$ are the minimum and maximum NDVI for the pixel, respectively, and $NDVI_t$ is the NDVI at time t. Thus, when viewing the RPD of two pixels at a given time t, one can compare the state of greenness of the two pixels irrespective of their absolute NDVI values. Annual RPD trajectories were plotted along axes of time and altitude (Beck et al., 2008).

Compatibility of the NDVI and animal movement data

The first MODIS sensor was launched in 1999, while the datasets on the movement of the radio-collared giant pandas and golden takins were from 1992 to 1996. We tested whether the 2001 to 2005 average MODIS-NDVI time series may be considered representative of the period 1992 to 1996 by comparing the Global Inventory Monitoring and Modelling Study (GIMMS) NDVI dataset of the two periods. The GIMMS-NDVI dataset is available on a bimonthly basis

from July 1981 to present with a spatial resolution of 8 km (http://www.landcover.org/data/gimms/). Previous studies have shown that the GIMMS-NDVI dataset is comparable with MODIS-NDVI data (Tucker et al., 2005). Foping Nature Reserve is covered by three GIMMS pixels, which were averaged and concatenated into two datasets covering 1992-1996 and 2001-2005. These datasets were then processed using TIMESAT software (Jönsson and Eklundh 2004), as described above for the MODIS-NDVI from 2001-2005. The average GIMMS-NDVI values for the two periods are shown in Figure 2, and their differences were tested using a paired t-test. The result shows that there was no significant difference in the mean NDVI values between the 24 images of GIMMS 1992-1996 and those of GIMMS 2001-2005 (t-test, t=1.02, df=8, p=0.39). In another study, Beck et al., (2008) analyzed the mean monthly temperature and cumulative precipitation for these two periods, which gave results similar to those of the NDVI comparison. We therefore concluded that the NDVI between 2001 and 2005 is representative of the 1992 to 1996 period.
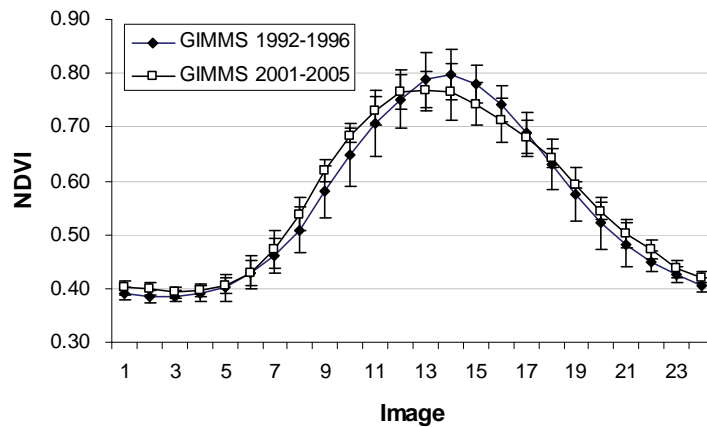
Figure 2 Comparison of annual NDVI trajectories over Foping Reserve during two periods using GIMMS-NDVI datasets. The *x*-axis represents NDVI images, two per month, starting on January 1. Each point in the figure represents a 5-year mean NDVI value with the standard deviation shown as a vertical bar

Estimation of seasonal activity ranges of the two species

Based on the elevation data for the six giant pandas and three golden takins (Figure 3), as well as previous studies (Liu et al., 2002, Zeng et al., 2008), we partitioned the radio-telemetry locations of giant pandas and golden takins into four seasonal activity ranges, being a winter non-migration range, a spring migration range, a summer non-migration range and an autumn migration range (Table 1). We then generated 95% space-use contours for the four

seasonal activity ranges for each species with the Hawths Analysis Tools for ArcGIS software (Beyer 2004), which uses an extension of the fixed kernel density estimator (KDE). Fixed KDE is one of the most commonly applied space-use estimators in wildlife studies and has been used to estimate animal home ranges (Worton 1989), interactions (Millspaugh et al., 2004) and resource selection (Marzluff et al., 2004, Millspaugh et al., 2006), amongst others.
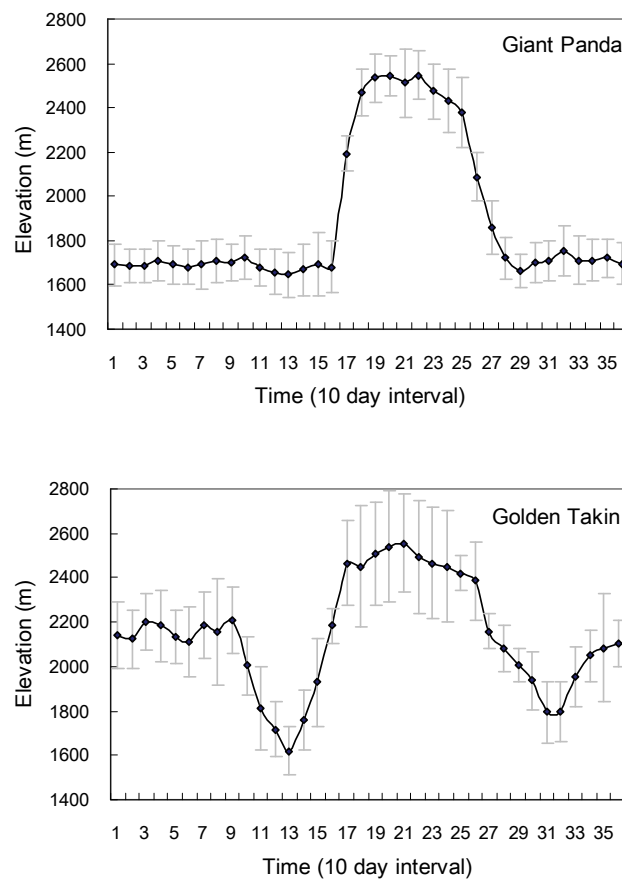
Figure 3 Average elevation and standard deviation (grey bars) per 10 day interval for six giant pandas and three golden takins

Table 1 Elevations and times for determining the four seasonal activity ranges of giant panda and golden takin

Seasonal activity ranges		Winter non-migration	Spring migration	Summer non-migration	Autumn migration
Giant Panda	Elevation (m)	< 2000	2000-2300	> 2300	2000-2300
	Time (TDs)	28-16	17	18-24	25-27
Golden Takin	Elevation (m)	2000-2300	1400-2300	> 2300	1600-2300
	Time (TDs)	34-9	10-16	17-25	26-33

Classification of bamboo abundance from remote sensing images

Remote sensing can be used to map the distribution of land cover over large areas. However, most attempts to map the density of understory vegetation such as bamboo have not been successful (De Wulf et al., 1988, Morain 1986). In the Foping Nature Reserve, the overstorey is composed of varying degrees of deciduous and coniferous cover. These typically limit spectral information from the understory bamboo reaching a space- or airborne sensor, thus restricting traditional remote sensing classification approaches. However, recently Wang et al., (2009) successfully classified three density classes of understory bamboo (i.e., dense, sparse, and non-bamboo) at a 30 m resolution, based on leaf-off Landsat TM and ASTER images and a hybrid neural network and expert system. The resulting maps of understory bamboo density had an overall accuracy of 73%. To examine the difference in the proportion of dense bamboo forest between the seasonal activity ranges of the two species, a z-test for two proportions is applied.

RESULTS

Altitudinal migration and plant phenology

Figure 4 presents altitudinal migration patterns of giant pandas and golden takins against a background of relative phenological development (RPD) of vegetation throughout the year. It shows how the period of dormancy lengthens, and the growing season shortens, towards higher altitudes. At the lowest altitudes, the dormancy period continues till April, but lasts till May at the highest altitudes. After dormancy, the vegetation reaches near-maximum greenness in the course of about one and half months at the lowest altitudes, while on the mountain peaks maximum greenness occurs about two months after winter dormancy. The length of near-maximum greenness lasts for more

than four months at lower elevations, but for only two months on the mountain plateaus and tops at higher elevations.
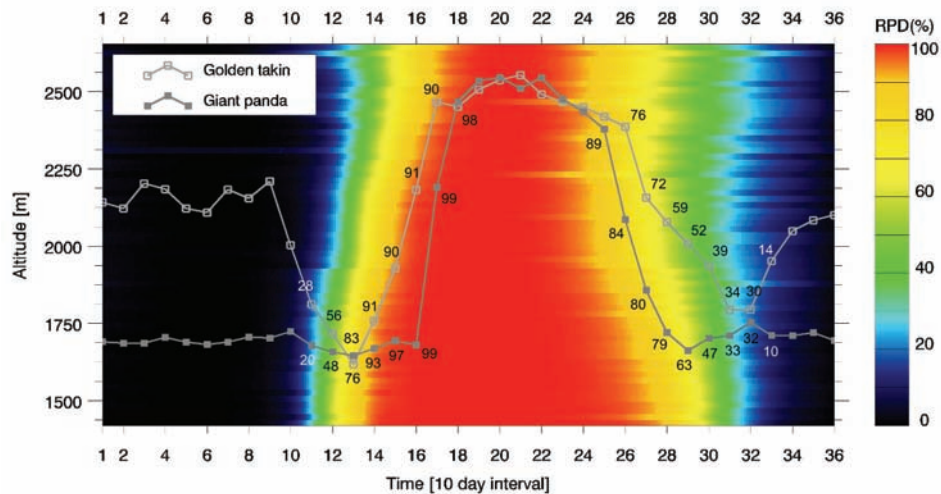
Figure 4 Altitudinal migration patterns of the giant panda (solid squares) and the golden takin (open squares) as estimated from the average elevations of radio-tracking data. The movement is shown against a background of the vegetation's relative phenological development (RPD) throughout the year, where each interval represents a period of 10 days. The RPD is estimated using the satellite-based NDVI and ranges from 0% for minimum greenness to 100% for maximum greenness. Key migration times are tagged with RPD values for both the giant panda (above the solid squares) and the golden takin (below the open squares) to show the differences of altitudinal migration in response to vegetation phenology,

Altitudinal migration of giant pandas and golden takins in response to plant phenology (i.e., RPD) are different (Figure 4). Between days 110 and 130, golden takins descend from the intermediate elevations to the lowest elevations, coinciding with an increase in RPD from 28% to 83%. In the same period, giant pandas show a slight downhill-movement while RPD in their habitat increases from 20% to 76%. Statistical comparison of the mean RPD shows that the golden takins migrate to the areas with advanced plant phenology earlier than giant pandas during their early-spring migration (t-value=2.86, df=182, p=0.005). From day 140 to day 170, the golden takins gradually ascend to high elevations followed a practically constant RPD gradient (RPD=±90%). In contrast to golden takins, the giant pandas stay at low elevations until the start of the peak

growing season around day 150 and then take only a week to move up to high elevations. Statistical comparison of the mean RPD shows that the golden takins migrate upwards while the vegetation is in earlier phenological stages than the giant pandas do (t-value=-10.00, df=134, p=0.000). During early-autumn migration, when golden takins start to leave their summer habitat, around day 260, the RPD at high elevation is about 76%. The golden takins gradually descend to the lowest elevation, where the RPD has decreased to 34% by day 310. The giant pandas only spend about four weeks (day 250-280) descending from their high-elevation summer habitat to their low-elevation winter habitat where the RPD are 89% and 79%, respectively. Based on the mean RPD during autumn (day 250-300), the golden takins follow later phenological stages of the vegetation, compared to the giant pandas (t-value=-2.57, df=175, p=0.0111). During the late-autumn migration, the golden takins reach low elevations where the RPD values are close to 30% around day 320, about a month later than the pandas do. After a week at the lowest elevations, the takins ascend to intermediate elevations for overwintering.

Seasonal activity ranges and bamboo abundance
The seasonal space-use of giant pandas and golden takins is different, based on the distribution of their seasonal activity ranges (Figure 5): in winter and spring their activity ranges are distinct, while in summer and autumn they overlap. Throughout the year, however, the takins are more dispersed than the pandas.

Figure 6 shows the proportion of dense bamboo forest within the four seasonal activity ranges of giant pandas and golden takins. On average, the proportion of dense bamboo forest in the four seasonal activity ranges of giant pandas is higher than in that of golden takin (40% vs. 23%, z-value=30.42, α=0.05). The difference is bigger in winter and summer (Figure 6a and 6c), which are the non-migratory seasons, than in spring and autumn, which are the migratory seasons (Figure 6b and 6d). The proportions of dense bamboo forest are lower in the two migration ranges than in the two non-migratory ranges, and the difference is most outspoken in the giant panda ranges (28% vs. 45%, z-value=20.1, α=0.05 for giant pandas; 21% vs. 31%, z-value=31.30, α=0.05 for golden takins). In the golden takin ranges, the difference was due to the higher proportion of the dense bamboo forest in the summer range (31%), which overlaps with the giant panda summer range, compared to the autumn, spring and winter ranges (about 21%).
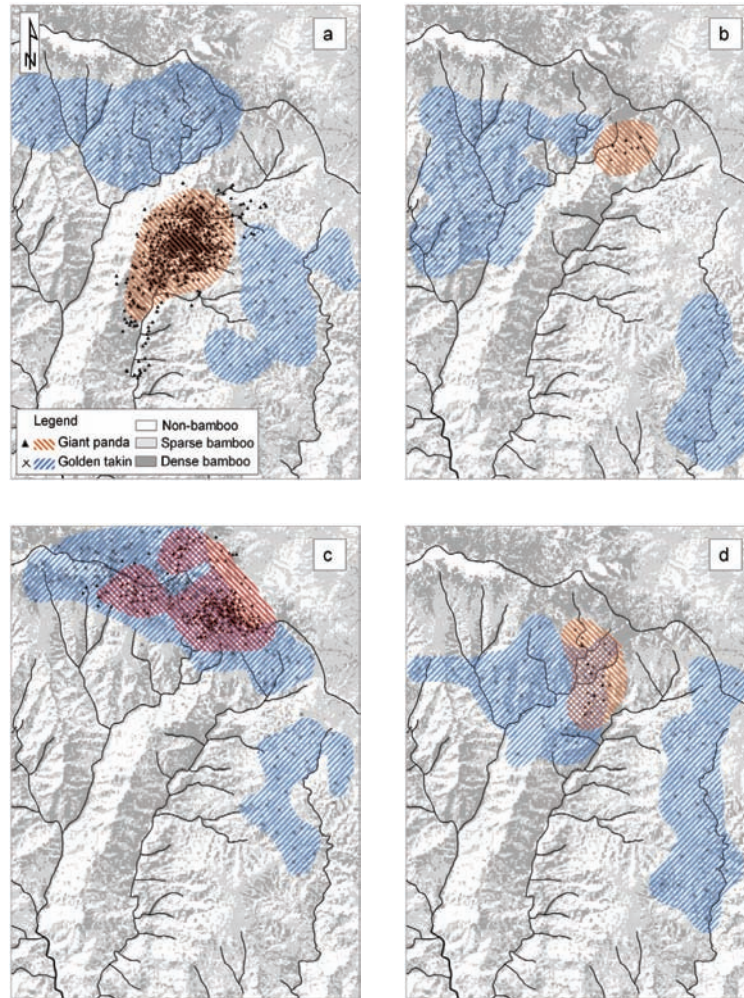
Figure 5 Seasonal activity ranges of giant pandas and golden takins, in winter (a), during spring migration (b), in summer (c) and during autumn migration (d). The ranges were estimated by applying a fixed kernel density estimator on radio-telemetry data. The background map shows the bamboo abundance in the study area
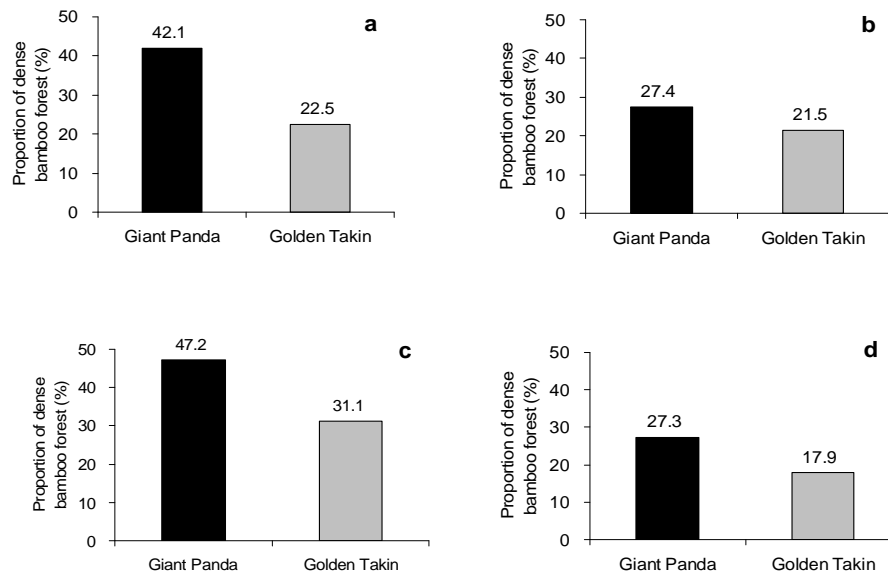
Figure 6 Proportion of dense bamboo forest in four seasonal activity ranges: (a) winter range, (b) spring migration range, (c) summer range, and (d) autumn migration range of the giant panda and the golden takin

DISCUSSION

Both giant pandas and golden takins respond to the "green wave" of vegetation phenology during their altitudinal migration in spring, but in distinct ways. The migration of the golden takin is linked to the early spring and late autumn phenological stages (i.e., early spring green-up and late autumn senescence), while the migration pattern of the giant panda, is related to the late spring and early autumn phenological stages (i.e., late spring green-up and early autumn senescence). This migratory behaviour of the golden takin is consistent with the hypothesis that the altitudinal migration of most generalist herbivores is in response to the first greening of vegetation in spring and follows late senescence in autumn (Albon and Langvatn 1992, Nicholson et al., 1997, Mysterud 1999). The contrasting result for the giant panda appears to be a consequence of its particular foraging behaviour, focused uniquely on the bamboo resource.

Unlike golden takins, giant pandas are specialists, which eat bamboo almost exclusively. Giant pandas show marked seasonal preferences for certain parts of the bamboo plants (Schaller et al., 1985). They prefer leaves over stems during most of the year but favour bamboo shoots when available. Nutrient analysis shows that the shoot is the most digestible part of bamboo (Schaller et al., 1985), as well as offering the highest calorific intake at 34,020 KJ/day (Pan et al., 1988). In the Foping Nature Reserve, the two bamboo species (*Bashania fargesii* and *Fargesia qinlingensis*) differ from the general vegetation in their annual cycle of shoot production. Their peak shooting periods occur three weeks later than the overall greening of the landscape. The shooting season of *Bashania fargesii* occurs from mid-April to the beginning of June, and peaks in May (Tian 1989), and the shooting season of *Fargesia qinlingensis*, which only grows above 2000 m, occurs from the beginning of June to the end of July, and peaks from mid-June to mid-July (Pan et al., 1988, Tian 1989). The shoots of *Fargesia qinlingensis* have just become available when the panda arrives at its high-elevation summer habitat in the middle of June. Our field observations also confirmed that giant pandas mainly consume the shoots of *Fargesia qinlingensis* from the middle of June to the end of July (Yong et al., 1994). As the shoots of *Fargesia qinlingensis* lignify in August, the giant pandas switch to eating leaves, and gradually descend to their winter habitats. The timing of the giant panda's spring and autumn migrations corresponds closely the start and end of maximum availability of bamboo shoots at high elevations in our study area. We therefore suggest that the sprouting and aging of palatable and digestible bamboo shoots may be the main driving force behind the migration of giant pandas.

Because golden takins are generalists, the phenological change of their forage is better represented by satellite-derived plant phenology, than bamboo phenology is. Satellite analysis of plant phenology is fundamentally different from traditional ground-based observations. The capacity of satellite sensors to detect important phenological events such as budding, flowering and fruiting is limited by the ground resolution of the sensors and the effects of other vegetation and soil background characteristics (Reed et al., 1994). Satellite sensors measure broad-scale changes in the landscape, that may not be associated with phenological events of specific plants, especially when they occur in the understorey (e.g., bamboo shooting), but can be descriptive of general vegetation phenological changes. Therefore, the altitudinal migration of golden takins has a more explicit relationship with the NDVI-derived change in vegetation phenology than the migration of giant pandas does.

The cover of dense bamboo forest is consistently higher in the giant panda activity range than in the golden takin activity range. Bamboo cover in the giant

panda's migration ranges is lower than in its summer or winter activity ranges, but still higher than in the golden takins migration ranges. Because bamboo is poor in nutrients, strong preference for habitats with a high bamboo density is vital to pandas, as it reduces the pandas' energy expenditure while foraging (Reid and Hu 1991). The migration pattern of giant pandas in the present study indicates that the animals avoid areas of low-bamboo density. Collared giant pandas only took one to three weeks to pass through sparse bamboo habitats during their spring and autumn migration, but spent about eight and three months, respectively, in their bamboo-rich winter and summer habitats. By contrast, golden takins are not as reliant on bamboo as giant pandas are. Besides bamboo, the golden takin usually feeds on herbs, shrubs and young trees. It therefore prefers habitats with a greater proportion of open-land and with a lower bamboo density (Zeng et al., 2001). This was demonstrated again in the present study, where the golden takins occupied a habitat with less dense bamboo forest than the giant pandas did, especially in their spring and autumn migration ranges. Moreover, the golden takin spends more time migrating than the giant panda does, which presumably resulted in prolonged access to abundant and high quality food.

In sum, the relatively fast up- and downhill movement of the giant panda may be attributed to the sparseness of the bamboo forest at intermediate elevations in the study area, and the consequent lack of forage for the giant panda. At these elevations, the diversity and density of plant species is high, providing varied forage for the golden takin, and therefore encouraging their relatively slow ascent and descent in spring and autumn, respectively. Our results suggest that the altitudinal migration patterns of both the giant panda and the golden takin follow the phenological development, and thus quality of their forage plants, and that the differences in migration are attributable to the differences in phenology and abundance of bamboo and non-bamboo plants.

REFERENCES

Albon, S. D. and R. Langvatn. 1992. Plant phenology and the benefits of migration in a temperate ungulate. Oikos **65**:502-513.

Baker, R. R. 1978. The evolutionary ecology of animal migration. Hodder & Stoughton, London.

Beck, P. S. A., C. Atzberger, K. A. Hogda, B. Johansen, and A. K. Skidmore. 2006. Improved monitoring of vegetation dynamics at very high latitudes: a new method using MODIS NDVI. Remote Sensing of Environment **100**:321-334.

Beck, P. S. A., T. J. Wang, A. K. Skidmore, and X. H. Liu. 2008. Displaying remotely sensed vegetation dynamics along natural gradients for ecological studies. International Journal of Remote Sensing **29**:4277-4283.

Beyer, H. L. 2004. Hawth's Analysis Tools for ArcGIS. Available at: www.spatialecology.com/htools.

Boone, R. B., S. J. Thirgood, and J. G. C. Hopcraft. 2006. Serengeti wildebeest migratory patterns modeled fromrainfall and new vegetation growth. Ecology **87**:1987-1994.

Crawley, M. J. 1983. Herbivory: the dynamics of animal-plant interactions. Blackwell Scientific, Oxford, U.K.

Dierenfeld, E. S., H. F. Hintz, J. B. Robertson, P. J. Van Soest, and O. T. Oftedal. 1982. Utilization of bamboo by the giant panda. Journal of Nutrition **112**:636-641.

Festa-Bianchet, M. 1988. Seasonal range selection in bighorn sheep: conflicts between forage quality, forage quantity, and predator avoidance. Oecologia **75**:580-586.

Fryxell, J. M. 1991. Forage quality and aggregation by large herbivores. American Naturalist **138**:478-498.

Fryxell, J. M. and A. R. E. Sinclair. 1988. Causes and consequences of migration by large herbivores. Trends in Ecology and Evolution **3**:237-241.

Geist, V. 1971. Mountain sheep: a study in behaviour and evolution. University of Chicago, Chicago.

Hanley, T. A. 1997. A nutritional view of understanding and complexity in the problem for diet selection by deer (*Cervidae*). Oikos **79**:209-218.

Huete, A., K. Didan, T. Miura, E. P. Rodriguez, X. Gao, and L. G. Ferreira. 2002. Overview of the radiometric and biophysical performance of the MODIS vegetation indices. Remote Sensing of Environment **83**:195-213.

Igota, H., M. Sakuragi, H. Uno, K. Kaji, M. Kaneko, R. Akamatsu, and K. Maekawa. 2004. Seasonal migration patterns of female sika deer in eastern Hokkaido, Japan. Ecological Research **19**:169-178.

Ito, T. Y., N. Miura, B. Lhagvasuren, D. Enkhbileg, S. Takatsuki, and A. J. Z. Tsunekawa. 2006. Satellite tracking of Mongolian gazelles (*Procapra gutturosa*) and habitat shifts in their seasonal ranges. Journal of Zoology **269**:291-298.

IUCN. 2007. 2007 IUCN Red List of Threatened Species. World Conservation Union, Gland, Switzerland.

Jönsson, P. and L. Eklundh. 2004. TIMESAT - a program for analyzing time-series of satellite sensor data. Computers & Geosciences **30**:833-845.

Justice, C. O., J. R. G. Townshend, B. N. Holben, and C. J. Tucker. 1985. Analysis of the phenology of global vegetation using meteorological satellite data. International Journal of Remote Sensing **6**:1271-1318.

Kerr, J. T. and M. Ostrovsky. 2003. From space to species: ecological applications for remote sensing. Trends in Ecology and Evolution **18**:299-305.

Krishnaswamy, J., M. C. Kiran, and K. N. Ganeshaiah. 2004. Tree model based eco-climatic vegetation classification and fuzzy mapping in diverse tropical deciudous ecosystems using multi-season NDVI. International Journal of Remote Sensing **25**:1185-1205.

Laycock, W. A. and D. A. Price. 1970. Factors influencing forage quality, environmental influences on nutritional value of forage plants. Pages 37-47 *in* Range and wildlife habitat evaluation - a research symposium. USDA Forest Service Miscellaneous Publication No.1147.

Liu, X. H. 2001. Mapping and modelling the habitat of giant pandas in Foping Nature Reserve, China. PhD thesis. Wageningen University, Wageningen, The Netherlands.

Liu, X. H., A. K. Skidmore, T. J. Wang, Y. G. Yong, and H. H. T. Prins. 2002. Giant panda movements in Foping nature reserve, China. Journal of Wildlife Management **66**:1179-1188.

Lloyd, D. 1990. A phenological classification of terrestrial vegetation cover using shortwave vegetation index imagery. International Journal of Remote Sensing **11**:2269-2279.

MacArthur, R. H. and E. R. Pianka. 1966. On optimal use of a patchy environment. The American Naturalist **100**:603-609.

Marzluff, J. M., J. J. Millspaugh, P. Hurvitz, and M. A. Handcock. 2004. Relating resources to a probabilistic measure of space use: forest fragments and Stellar's jays. Ecology **85**:1411-1427.

Millspaugh, J. J., R. A. Gitzen, B. J. Kernohan, M. A. Larson, and C. L. Clay. 2004. Comparability of three analytical techniques to asses joint space use. Wildlife Society Bulletin **32**:148-157.

Millspaugh, J. J., R. M. Nielson, L. McDonald, J. M. Marzluff, R. A. Gitzen, C. D. Rittenhouse, M. W. Hubbard, and S. L. Sheriff. 2006. Analysis of resource selection using utilization distributions. Journal of Wildlife Management **70**:384-395.

Morain, S. A. 1986. Surveying China's agricultural resources: patterns and progress from space. Geocarto International **1**:15-24.

Myneni, R. B., C. D. Keeling, C. J. Tucker, G. Asrar, and R. R. Nemani. 1997. Increased plant growth in the northern high latitudes from 1981 to 1991. Nature **386**:698-702.

Mysterud, A. 1999. Seasonal migration pattern and home range of roe deer (*Capreolus capreolus*) in an altitudinal gradient in southern Norway. Journal of Zoology **247**:479-486.

Mysterud, A., C. Iversen, and G. Austrheim. 2007. Effects of density, season and weather on use of an altitudinal gradient by sheep. Applied Animal Behaviour Science **108**:104-113.

Mysterud, A., R. Langvatn, N. G. Yoccoz, and N. C. Stenseth. 2001. Plant phenology, migration and geographical variation in body weight of a large herbivore: the effect of a variable topography. Journal of Animal Ecology **70**:915-923.

Nelson, M. E. 1995. Winter range arrival and departure of white-tailed deer in northeastern Minnesota. Canadian Journal of Zoology **73**:1069-1076.

Nemani, R. R., C. D. Keeling, H. Hashimoto, W. M. Jolly, S. C. Piper, C. J. Tucker, R. B. Myneni, and S. W. Running. 2003. Climate-driven increases in global terrestrial net primary production from 1982 to1999. Science **300**:1560-1563.

Nicholson, M. C., R. T. Bowyer, and J. G. Kie. 1997. Habitat selection and survival of mule deer: tradeoffs associated with migration. Journal of Mammalogy **78**:483-504.

Oosenbrug, S. M. and J. B. Theberge. 1980. Altitudinal movements and summer habitat preferences of woodland caribou in the Kluane ranges, Yukon territory. Arctic **33**:59-72.

Pan, W. S., Z. S. Gao, and Z. Lu. 1988. The giant panda's natural refuge in the Qinling Mountains. Beijing University Press, Beijing (in Chinese).

Pettorelli, N., F. Pelletier, A. V. Hardenberg, M. Festa-Bianchet, and S. D. Cote. 2007. Early onset of vegetation growth vs. rapid green-up: impacts on juvenile mountain ungulates. Ecology **88**:381-390.

Prins, H. H. T. and F. van Langevelde. 2008. Assembling a diet from different places. Pages 129-158 *in* H. H. T. Prins and F. van Langevelde, editors. Resource ecology: spatial and temporal dynamics of foraging. Springer, Dordrecht.

Prins, H. H. T. and R. C. Ydenberg. 1985. Vegetation growth and a seasonal habitat shift of the barnacle goose (*Branta leucopsis*). Oecologia **66**:122-125.

Reed, B. C., J. F. Brown, D. Vanderzee, T. R. Loveland, J. W. Merchant, and D. O. Ohlen. 1994. Measuring phenological variability from satellite imagery. Journal of Vegetation Science **5**:703-714.

Reid, D. G. and J. C. Hu. 1991. Giant panda selection between *Bashania faberi* habitats in Wolong Reserve, Sichuan, China. Journal of Applied Ecology **28**:228-243.

Ren, Y., M. L. Wang, M. Yue, and Z. J. Li. 1998. Plants of giant panda's habitat of Qinling Mountains. Shaanxi Science and Technology Press, Xi'an (in Chinese).

Richter, H. V. and G. S. Cumming. 2006. Food availability and annual migration of the straw-colored fruit bat (*Eidolon helvum*). Journal of Zoology **268**:35-44.

Schaller, G. B., J. C. Hu, W. S. Pan, and J. Zhu. 1985. The giant pandas of Wolong. University of Chicago Press, Chicago.

Skidmore, A. K. and J. G. Ferwerda. 2008. Resource distribution and dynamics: mapping herbivore resources. Pages 57-77 *in* H. H. T. Prins and F. van Langevelde, editors. Resource ecology: spatial and temporal dynamics of foraging. Springer, Dordrecht.

State Forestry Administration. 2006. The third national survey report on giant pandas in China. Science Press, Beijing (in Chinese).

Tang, Z. Y. and J. Y. Fang. 2006. Temperature variation along the northern and southern slopes of Mt. Taibai, China. Agricultural and Forest Meteorology **139**:200-207.

Taylor, A. H. and Z. S. Qin. 1988. Regeneration patterns in old-growth *Abies-Betula* forests in the Wolong Natural Reserve, Sichuan, China. Journal of Ecology **76**:1204-1218.

Tian, X. Q. 1989. Shooting and growth of *Bashania fargesii*. Bamboo research **8**:400-407 (in Chinese).

Tucker, C. J., J. E. Pinzon, M. E. Brown, D. A. Slayback, E. W. Pak, R. Mahoney, E. F. Vermote, and N. E. Saleous. 2005. An extended AVHRR 8-km NDVI dataset compatible with MODIS and SPOT vegetation NDVI data. International Journal of Remote Sensing **26**:4485-4498.

Van Soest, P. J. 1983. Nutritional ecology of the ruminant. Second edition edition. Cornell University Press, New York.

Veblen, T. T., D. H. Ashton, F. M. Schlegel, and A. T. Veblen. 1977. Distribution and dominance of species in the understorey of a mixed evergreen-deciduous *Nothofagus* forest in south-central Chile. Journal of Ecology **65**:815-830.

Wang, T. J., A. K. Skidmore, and A. G. Toxopeus. 2009a. Improved understorey bamboo cover mapping using a novel hybrid neural network and expert system International Journal of Remote Sensing **30**: 965-981.

Wang, T. J., A. K. Skidmore, A. G. Toxopeus, and X. H. Liu. 2009b. Understorey bamboo discrimination using a winter image. Photogrammetric Engineering and Remote Sensing **75**: 37-47.

Wang, X. Z., Y. L. Song, Z. G. Zeng, H. S. Gong, and N. X. Zhao. 2005. Characteristics of birth-site and early mother-infant relationship of the golden takin. Acta Zoologica Sinica **51**:748-752 (in Chinese).

Wei, F. W., Z. J. Feng, Z. W. Wang, and M. Li. 1999. Feeding strategy and resource partitioning between giant and red pandas. Mammalia **63**:417-430.

White, C. G. and R. A. Garrott. 1990. Analysis of wildlife radiotracking data. Academic Press, San Diego, California.

White, M. A., P. E. Thornton, and S. W. Running. 1997. A continental phenology model for monitoring vegetation responses to interannual climatic variability. Global Biogeochemical Cycles **11**:217-234.

White, R. G. 1983. Foraging patterns and their multiplier effects on prodcutivity of northern ungulates. Oikos **40**:377-384.

Worton, B. J. 1989. Kernel methods for estimating the utilization distribution in home-range studies. Ecology **70**:164-168.

Wu, J. Y., Y. P. Han, H. Qu, S. X. Liu, X. M. Zhu, J. X. Jia, J. Y. Liu, and L. Zhang. 1990. The Chinese Takin. China Forestry Publishing House, Beijing (in Chinese).

Yong, Y. G., K. W. Wang, and T. J. Wang. 1994. Movement habits of the giant pandas in Foping. Acta Theriologica Sinica **14**:9-14 (in Chinese).

Yue, M., Y. Ren, G. D. Dang, and T. Q. Gu. 1999. Species diversity of higher plant communities in Foping National Reserve. Chinese Biodiversity **7**:263-269 (in Chinese).

Zeng, Z. G., A. K. Skidmore, Y. L. Song, T. J. Wang, and H. S. Gong. 2008. Seasonal altitudinal movements of golden takin in the Qinling Mountains of China. Journal of Wildlife Management **72**:611-617.

Zeng, Z. G., Y. L. Song, and H. S. Gong. 1998. Population size and age structure of golden takin in Foping Nature Reserve. Acta Theriologica Sinica **18**:241-246 (in Chinese).

Zeng, Z. G., Y. L. Song, W. Q. Zhong, H. S. Gong, J. Zhang, and G. D. Dang. 2001. Food habits of golden takin. Chinese Journal of Zoology **36**:36-44 (in Chinese).

Zeng, Z. G., W. Q. Zhong, Y. L. Song, J. S. Li, and F. Guo. 2002. Group size, composition and stability of golden takin in Shaanxi Foping Nature Reserve, China. Folia Zoologica **51**:289-298.

Zhu, X. J., D. G. Lindburg, W. S. Pan, K. A. Forney, and D. J. Wang. 2001. The reproductive strategy of giant pandas (*Ailuropoda melanoleuca*): infant growth and development and mother-infant relationships. Journal of Zoology **253**:141-155.

Chapter **6**

Characterizing the spatial distribution of giant pandas in the fragmented forest landscape

ABSTRACT

Although forest fragmentation has been recognized as one of the major threats to the population of the wild giant panda, little is known about the relationship between forest fragmentation and the spatial distribution of wild giant pandas. This study examines the effects of forest fragmentation on the distribution of the entire wild giant panda population. To quantify the fragmentation of forests, eight fragmentation metrics, with the highest loadings following a factor analysis and derived from MODIS 250 m EVI multi-temporal data, were selected. A forward stepwise logistic regression was then applied to explore the relationship between panda distribution and forest fragmentation. It was found that patches of forest occupied by giant pandas were significantly larger, closer together and more contiguous than patches where giant pandas were not recorded, indicating that giant pandas appear sensitive to patch size and isolation effects associated with forest fragmentation. Forest fragmentation occurs least in the Qinling Mountains and most in the Xiangling and Liangshan regions. Using the selected landscape metrics, the logistic regression model predicted the distribution of giant pandas with an overall accuracy of 72.5% (kappa 0.45). However, when a knowledge-based control for elevation and slope was applied to the regression, the overall accuracy of the model improved to 77.6% (kappa 0.55). These findings imply that the design of effective conservation areas for wild giant pandas must include large and dense forest patches, which are adjacent to other similar patches.

INTRODUCTION

The giant panda (*Ailuropoda melanoleuca* David, 1869) is one of the world's most endangered mammals as well as arguably the world's most recognized flagship species. Fossil evidence suggests that the giant panda occurred widely in warm temperate and subtropical forests over much of eastern and southern China (Hu et al., 1985). Today, wild pandas are restricted to temperate montane forests across five separate mountain regions where bamboo dominates the forest understorey. According to the third national giant panda survey conducted between 2000 and 2002, the number of giant panda individuals increased in the last decades, but their distribution is discontinuous, with 24 isolated populations (State Forestry Administration 2006).

Forest fragmentation and degradation have been hypothesized to be causing a decline in the wild giant panda population and its habitat (Hu et al., 1985, Hu 2001). However, little is known about the distribution pattern of giant pandas at a national level (Hu 2001, Lindburg and Baragona 2004) and no quantitative or systematic studies have attempted to address giant panda distribution in relation to fragmentation of forested landscapes (e.g., forest patch size, patch isolation and aggregation), certainly not covering the entire distribution range of the wild giant panda.

Landscape structural variables (i.e., landscape metrics) are easily obtainable from remote sensing over large areas and their calculation is less demanding than collecting detailed data on species distribution (Groom et al., 2006). A large number of landscape metrics have been proposed to quantify landscape patterns based on land cover derived from remotely sensed data (O'Neill et al., 1988, Hulshoff 1995, Skinner 1995, Gustafson 1998), and an increasing number of studies use landscape metrics to predict the distribution of species (Bissonette 1997, Dufour et al., 2006). Because most landscape metrics are scale-dependent and landscape elements are species-specific (Cain et al., 1997, Saura 2004), appropriate land cover classes and spatial resolution are critical when linking the response variable of species to landscape metrics (Turner et al., 1989, Taylor et al., 1993, Hamazaki 1996, Frohn 1998, Corsi et al., 2000, Wu et al., 2000, Saura 2004). When choosing a data source for land cover classification, data availability and spatial resolution are two important issues. High spatial resolution (e.g., 30m) sensors, such as Landsat Thematic Mapper (TM), have a relatively narrow swath width and revisit the same area infrequently making their acquisition and interpretation expensive and time-consuming. It is also difficult to acquire sufficient images for a large area. The time-series of 16-day composite Moderate Resolution Imaging Spectroradiometer (MODIS) 250 m Enhanced Vegetation Index (EVI) images, with a broad geographical coverage

(swath width 2,330 km), intermediate spatial resolution and high temporal resolution, offers a new option for large area land cover classification (Bagan et al., 2005, Liu and Kafatos 2005, Xavier et al., 2006, Wardlow et al., 2007). EVI is designed to minimize the effects of atmospheric and soil background (Huete et al., 2002), and is responsive to canopy density (Gao et al., 2000).

The aim of this paper is to understand how the distribution of the entire giant panda population relates to forest fragmentation, and to propose a modelling approach in comprehension and simplification of analysis of panda spatial distribution at the landscape scale. Specific research questions include: (1) Which landscape metrics characterize fragmentation of forests occupied by giant pandas? (2) What are the relationships between the distribution of giant pandas and forest fragmentation? (3) Which proportion of the distribution of the giant panda may be explained by landscape metrics?

MATERIALS AND METHODS

Study area

The study area (Figure 1) incorporates 45 administrative counties in the provinces of Shaanxi, Gansu and Sichuan in China, which cover the entire giant panda distribution area, and were fully sampled during the third national panda survey (State Forestry Administration 2006). The total area encompasses about 160,000 km², with an elevation of 560 m to 6,500 m. The study area includes all mountain ranges with panda distribution along the eastern edge of the Qinghai-Tibetan Plateau: Qinling, Minshan, Qionglai, Xiangling (including Greater Xiangling and Lesser Xiangling), and Liangshan (Hu 2001). The northernmost area where the giant panda occurs at present is the Qinling region (Hu 2001), which is covered with deciduous broadleaf and subalpine coniferous forests (Ren et al., 1998). The density of giant pandas is highest in the Qinling Mountains (State Forestry Administration 2006). The Minshan and Qionglai regions, with a cool and humid climate, include the largest extant panda habitat in China (Hu 2001). The Xiangling and Liangshan regions form the southernmost panda distribution area, dominated by evergreen broadleaf forests and coniferous forests (China Vegetation Compiling Committee 1980).

Environmental and species data

Remote sensing data preparation

Three 12-month (January to December) time-series of 16-day composite MODIS 250 m EVI data (MOD13Q1 V004) for 2001-2003 were created for the study area. Each time-series consisted of 23 dimensions (16-day composite period), and

four tiles (h26v05, h26v06, h27v05, and h27v06) of the MODIS data were required to cover the study area. For each dimension, the EVI data were downloaded (http://edcimswww.cr.usgs.gov/pub/imswelcome), extracted by tile, mosaicked, reprojected from the Sinusoidal to the Albers Equal Area Conic projection, using a nearest neighbour operator, and subset to the study area. To diminish noise caused mainly by remnants of clouds, a clean and smooth 12-month time-series of EVI (23 dimensions) was reconstructed from previous three 12-month EVI time-series by employing an adaptive Savitzky–Golay smoothing filter, using the TIMESAT package (Jönsson and Eklundh 2004). The resulting smoothed 12-month time-series was then transformed into principal components (PCs) using a Principal Component Analysis (Byrne et al., 1980, Richards 1984) to reduce data volume. The first five PCs (accounting for 99.1% of variance in the smoothed EVI time-series) were retained for further land-cover characterization.
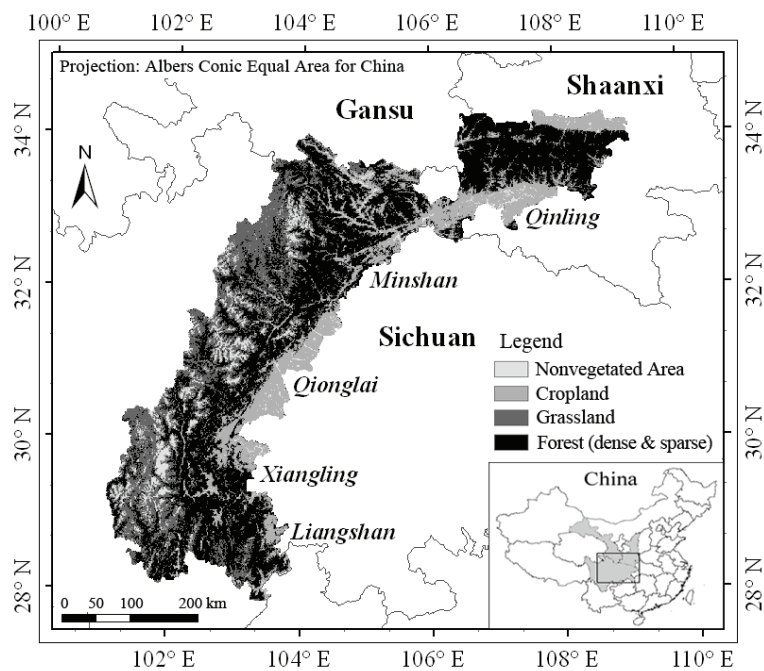
Figure 1 Map of the study area delineated in bold black polygon with four land cover types. Land cover types were classified from MODIS 250 m EVI time-series from 2001 to 2003

Ancillary data used in this study included the National Land Cover Map of China (NLCD-2000), a digital elevation model (DEM) and the Bio-Climatic Division Map of China. The NLCD-2000 Map, developed from hundreds of

95

Landsat TM images (30 m resolution) acquired in 1999 and 2000 for all of China (Liu et al., 2003a), was geometrically reprojected to form a mosaic with a pixel size of 250 m. This database was used to extract reference data for land cover classification. The DEM was clipped from the Shuttle Radar Topography Mission (SRTM) 90 m (http://www2.jpl.nasa.gov/srtm) seamless digital topographic data and resampled to 250 m using a nearest neighbour operator. The Bio-Climatic Division Map of China was originally vector data, which was generated based on annual mean precipitation, cumulated temperature, and humidity index, as described in Liu et al. (2003b). This dataset was rasterized with a pixel size of 250 m to improve land cover classification. All data were geometrically rectified and geo-referenced based on the MODIS 250 m EVI data to ensure proper mutual registration and geographic positioning.

Land cover characterization

As giant pandas prefer dense forests (Hu et al., 1985, Hu 2001), land cover in the study area was classified into five categories (i.e., dense forest, sparse forest, grassland, cropland, and non-vegetated area) (Table 1) by using a combination of ISODATA and Neural Network classifiers in ENVI 4.3 (ITT Industries Inc. 2006). Reference data for land cover classification (5991 pixels for training and 2112 pixels for accuracy assessment) were derived from NLCD-2000 map using a simple random sample stratified by land cover type. Considering the spatial resolution of MODIS data, samples falling in land cover patches with a size less than 500 ha were discarded to ensure the reliability of reference data. Land cover classification accuracy was assessed using a confusion matrix as cross-tabulations of the mapped class vs. the reference class (Story and Congalton 1986, Congalton 1991, Congalton and Green 1999). The resulting land cover map (overall accuracy 84%, kappa 0.8), with a grain size of 250 m, was used for further computation of the landscape metrics.

Giant panda presence-absence data

Based on previous studies, models using both presence and absence data predicted the distribution of forest species with higher accuracy than methods utilizing presence data only, particularly when species occupied available habitats proportionally to their suitability, making absence data reliable and useful to enhance model calibration (Hirzel et al., 2001, Brotons et al., 2004). Giant panda occurrence data (n=1,450) used in this study were collected via an exhaustive survey (see Note 1) throughout the study area (Loucks and Wang 2004, State Forestry Administration 2006), thus for our purposes we considered the panda absent from the locations if no evidence of presence was found during the survey. It is applicable to generate randomly distributed panda pseudo-absences and ameliorate the data set towards true absences via the approach proposed in Zaniewski et al., (2002) and Olivier and Wotherspoon (2006), which species absence samples were generated

by buffering species presence data. Firstly 3000 points were randomly sampled within the dense forest and sparse forest, with a minimum distance of 3 km between points (based on the maximum territory size of the giant panda which is around 30 km^2 (Hu 2001, Pan 2001)), and a minimum distance of 3 km to forest edges. Then three criteria were used to extract panda absence data: (1) with an elevation lower than 4000 m or a slope less than 50º (Hu 2001); (2) located outside a 3-km buffer zone of panda occurrence points; and (3) with a minimum distance of 3 km to the boundary of buffer zones. In total, 1300 points were selected as panda absence points. Further, 1300 panda presence points were randomly selected from panda occurrence points. Moran's *I* statistic (Moran's *I*=0.03, z=1.91, p>0.05) showed that spatial autocorrelation between the independent variables was not significant for panda presence-absence data.

Note1: The third national giant panda survey was conducted via a dragnet investigation approach. The whole investigation area was plotted out with an average size of 2 km^2. Each plot was throughout investigated. In total 11,174 plots were investigated (http://assets.panda.org/downloads/pandasurveyqa.doc).

Table 1 Description of the land cover classification categories used in this study and extracted reference data for each land cover class

Land cover class	Description	Number of pixels	
		Training	Testing
Dense forest	Natural or man-made forest with canopy cover greater than 30%	1890	646
Sparse forest	Lands covered by trees with canopy cover less than 30% or shrub	1587	529
Grassland	Lands covered by herbaceous plant with coverage greater than 20%	901	330
Cropland	Lands for agriculture	927	333
Non-vegetated area	Non-vegetated lands, including built-up, water body, bare land, ice/snow areas, etc.	686	274

Statistical analysis of landscape metrics

Metrics computation

Initially a total of 26 class-level landscape metrics (see Table 1) were computed for the dense forest class and the combination of dense and sparse forest classes respectively using the raster version of FRAGSTATS 3.3 (McGarigal and Cushman 2002). The raster version of FRAGSTATS computes metrics using a moving square window and creates a continuous landscape metric surface for statistical analysis. To choose an appropriate scale (i.e., the size of the moving window in

this study), the effect of different moving window radiuses on metrics computation outputs were examined. Firstly a random sample of 10 points within the study area were created, 26 metrics were then calculated for each point with eight different moving window radiuses (1.25 km, 1.5 km, 2 km, 2.5 km, 3 km, 3.5 km, 4 km, 5 km). The values of the metrics were plotted against the radiuses of the moving window to determine at what radii the majority of curves would become asymptotic. It was evident that the values for nearly all metrics leveled out at 3-3.5 km (see Figure 2). Therefore, a moving window radius of 3 km was chosen as the appropriate scale for calculating landscape metrics. After computation, metric values of overlaying panda presence and absence samples were extracted.

Table 2 Landscape metrics selected in this study

Metric (Acronym)	Description
Largest Patch Index (LPI)	The area (m²) of the largest patch of the corresponding patch type divided by total landscape area (m²).
Landscape Shape Index (LSI)	The total length of edge (or perimeter) involving the corresponding class, given in number of cell surfaces, divided by the minimum length of class edge.
Patch Density (PD)	The number of the corresponding patches divided by total landscape area (m²).
Percentage of Landscape (PLAND)	The sum of the areas (m²) of all patches of the corresponding patch type, divided by total landscape area (m²).
Edge Density (ED)	The sum of the lengths (m) of all edge segments involving the corresponding patch type, divided by the total landscape area (m²).
Mean Patch Area (AREA)	The sum of the areas (m²) of all patches of the corresponding patch type, divided by the number of patches of the same type.
Radius of Gyration Distribution (GYRATE)	The mean distance (m) between each cell in the patch and the patch centroid.
Contiguity Index (CONTIG)	The average contiguity value for the cells in a patch minus 1, divided by the sum of the template values minus 1.
Fractal Dimension Index (FRAC)	The sum of 2 times the logarithm of patch perimeter (m) divided by the log of patch area (m²) for each patch of the corresponding patch type, divided by the number of patches of the same type.
Perimeter Area Ratio (PARA)	The ratio of the patch perimeter (m) to area (m²).
Shape Index (SHAPE)	Patch perimeter divided by the minimum perimeter possible for a maximally compact patch of the corresponding patch area.
Core Percentage of Landscape (CPLAND)	The sum of the core areas of each patch (m²) of the corresponding patch type, divided by total landscape area (m²).
Disjunct Core Area Density (DCAD)	The sum of number of disjunct core areas contained within each patch of the corresponding patch type, divided by total landscape area (m²).
Disjunct Core Area Distribution	The sum of the corresponding patch type, of the corresponding patch metric values, divided by the number of patches of the

(DCORE)	same type.
Core Area Index (CAI)	The patch core area (m²) divided by total patch area (m²).
Core Area (CORE)	The sum of the core areas of each patch of the corresponding patch type, divided by the number of patches of the same type.
Patch Cohesion Index (COHESION)	1 minus the sum of patch perimeter divided by the sum of patch perimeter times the square root of patch area for patches of the corresponding patch type, divided by 1 minus 1 over the square root of the total number of cells in the landscape.
Connectance Index (CONNECT)	The number of functional joinings between all corresponding patches, divided by the total number of possible joinings between all patches of the corresponding patch type.
Euclidian Nearest Neighbour Index (ENN)	The distance (m) to the nearest neighboring patch of the same type, based on shortest edge-to-edge distance.
Proximity Index (PROX)	The sum of patch area divided by the nearest edge-to-edge distance squared (m²) between the patch and the focal patch of all patches of the corresponding patch type whose edges are within a specified distance (m) of the focal patch.
Aggregation Index (AI)	The number of like adjacencies involving the corresponding class, divided by the maximum possible number of like adjacencies involving the corresponding class.
Clumpy Index (CLUMPY)	The proportional deviation of the proportion of like adjacencies involving the corresponding class from that expected under a spatially random distribution.
Landscape Division Index (DIVISION)	1 minus the sum of patch area (m²) divided by total landscape area (m²), quantity squared.
Interspersion Juxtaposition Index (IJI)	Minus the sum of the length (m) of each unique edge type involving the corresponding patch type divided by the total length (m) of edge (m) involving the same type, multiplied by the log of the same quantity.
Percentage of Like Adjacencies (PLADJ)	The number of like adjacencies involving the focal class, divided by the total number of cell adjacencies involving the focal class.
Splitting Index (SPLIT)	The total landscape area (m²) squared divided by the sum of patch area (m²) squared.
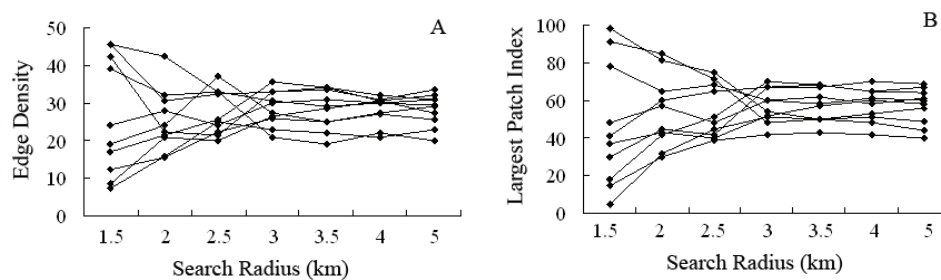
Figure 2 Example of two landscape metric values plotted against seven different search radii of moving window: (A) Edge Density (ED), (B) Largest Patch Index (LPI)

Metrics reduction analysis

To obtain a set of redundancy-free metrics for the panda distribution modelling, a two-tailed partial correlation analysis with control for the effect of elevation was employed to eliminate highly correlated metrics and therefore reduce multicollinearity. Of the pairs of metrics with correlation coefficients $\geq |0.9|$, we retained metrics that are commonly used in the literature (Riitters et al., 1995, Griffith et al., 2000). With these remaining metrics, a multivariate factor analysis was performed (Riitters et al., 1995, Cain et al., 1997) and non-correlated factors were extracted using a principal components method with orthogonal rotations. These were retained by the Kaisers rule of thumb that the eigenvalue of the factor should be greater than 1.0 (Bulmer 1979). For each retained factor, the metric with highest absolute loading was assumed to be representative and included in further statistical analysis.

Significance testing

Because some metrics did not meet the assumption of homogeneity of variances and some were non-normally distributed, the relationships between selected landscape metrics and panda distribution were further tested using the nonparametric Mann-Whitney *U* test. Metrics with a significant difference were used for further model building. Furthermore, a post-hoc test of the overall ANOVA test was conducted to determine how the fragments of forests occupied by giant pandas in the five mountain ranges differ by employing the Games-Howell test. The Games-Howell test is considered to be robust when sample sizes and variances are not equal across compared groups (Field 2005).

Characterizing the giant panda distribution with selected metrics

Logistic regression analysis

The binomial logistic regression, a common statistical method used to estimate occurrence probabilities in relation to environmental predictors (Mladenoff et al., 1995, Hosmer and Lemeshow 2000), was employed to delineate the relation between panda presence-absence and the selected metrics. Stepwise model-fitting with forward selection was used to construct models with a 'good' fit to the data, where 'good' is defined as a variable with the most significant change in deviance at each stage being incorporated into the model until no other variables were significant at $p<0.05$. The panda presence-absence samples were randomly split into two parts, one for model building (n=2,000), another for model evaluation (n=600). All statistical analyses were conducted in SPSS 15 (SPSS Inc. 2006).

Spatial implementation of logistic regression model

As the logistic regression model was built using landscape metrics, whereas the distribution of the giant panda is in reality limited by a range of environmental conditions such as topographical features, the model may overestimate panda distribution regardless of environmental tolerances or preferences of the giant panda. Hence, a knowledge-based control was developed by integrating the logistic regression model with elevation and slope to mitigate the risk of over-prediction, as described below:

$$P_i' = P_i \times C_{ele} \times C_{slope} \tag{1}$$

where P_i' is refined probability, P_i is the probability estimated by logistic regression model, C_{ele} is the conditional probability related to elevation, and C_{slope} is the conditional probability related to slope. The knowledge-based rules for control were formulated using knowledge from several sources including (1) literature (Hu 2001, Pan et al., 2001); (2) discussion with specialists; (3) knowledge acquired from field observations; and (4) analyses of the third national panda survey data. These are summarized in Table 3. The logistic regression model with knowledge-based control was spatially implemented in ERDAS IMAGINE 9.1 (Leica Geosystems Geospatial Imaging 2005).

Table 3 Conditional probabilities of elevation and slope in the five mountain regions for knowledge-based control of logistic regression model

Terrain factors		Conditional probability				
		Qinling	Minshan	Qionglai	Xiangling	Liangshan
Elevation	< 1200 m	0.10	0.01	0.01	0.01	0.01
	1200 m ~ 2000 m	1.00	0.50	0.50	0.10	0.10
	2000 m ~ 2500 m	1.00	1.00	1.00	1.00	1.00
	2500 m ~ 3000 m	0.80	1.00	1.00	1.00	1.00
	3000 m ~ 3500 m	0.01	0.80	0.80	0.80	0.80
	> 3500 m	0.01	0.10	0.10	0.50	0.50
Slope	< 10º	0.80	0.70	0.70	0.40	0.60
	10º ~ 40º	1.00	1.00	1.00	1.00	1.00
	40º ~ 50º	0.20	0.60	0.60	0.10	0.10
	> 50º	0.01	0.10	0.10	0.01	0.01

Model evaluation

Model performance was evaluated on the basis of presence and absence. Thus the Receiver Operating Characteristic (ROC) procedure was used to determine the threshold defining absence and presence (Thuiller et al., 2003, Pearson 2004). The ROC procedure plots sensitivity (defined as the proportion of correctly

predicted sites of panda presence compared to the total number of panda presence sites in testing samples) against specificity (defined as the proportion of correctly predicted sites of panda absence compared to the total number of panda absence sites in testing samples) at a series of thresholds. In this study, the threshold value at which these two curves cross (Fielding and Bell 1997) was applied to the conversion of discrete panda presence/absence map from probability values (i.e., 0 to 1) produced by the logistic regression model. The performance of the model was assessed using overall accuracy, sensitivity and specificity, the kappa coefficient and Z-test. The kappa coefficient and its variance (Congalton 1991, Skidmore et al., 1996) were computed and the effect of the knowledge-based control was examined using a Z-statistic (Congalton 1991).

RESULTS

Representative metrics for quantifying forest fragmentation

Eight landscape metrics were selected (from 26 metrics) as representative of forest fragmentation based on the Kaisers rule of thumb that the eigenvalue of the factor should be greater than 1 in factor analysis (Table 4). Four of the selected metrics measure patterns of dense forest: edge density (ED), largest patch index (LPI), patch proximity (PROX), and patch clumpiness (CLUMPY), and four metrics measure patterns of the combination of dense and sparse forest: average patch area (AREA), edge density (ED), patch proximity (PROX), and clumpiness (CLUMPY). In general, these metrics measure three aspects of forest heterogeneity: patch area/edge (ED, LPI, and AREA), patch connectivity (PROX), and patch aggregation (CLUMPY). Multicollinearity between metrics was tested and shown not to be problematic (i.e. Variance-Inflation Factors <5, and tolerance >0.2 (Sokal and Rohlf 1995)).

Table 4 Factor analyses for metrics measuring the dense forest and metrics measuring the combination of dense and sparse forest. Factors were retained by the rule of eigenvalue >1.0. Factor loadings >|0.8| are underlined, and factor loadings <|0.3| are not presented. Metrics in bold are selected for statistical analysis and model building

Metrics measuring dense forest	Factor				Metrics measuring combination of dense and sparse forest	Factor			
	1st	2nd	3rd	4th		1st	2nd	3rd	4th
ED		0.92			**AREA**	0.94			
LPI	0.91				**ED**		0.95		
LSI	-0.46	0.79			LSI		0.49	0.72	
PD	-0.80				PD	-0.49	-0.56	0.41	

	1	2	3	4
CONTIG	0.87			
SHAPEX	0.73	0.42		
DCAD		0.74		0.31
DCORE	0.61	-0.48		
ENN	-0.67			
PROX				0.89
SPLIT			-0.79	
IJI		0.53		
CLUMPY			0.90	
AI	0.75		0.53	
CONNECT				0.88
COHESION	0.56	0.35	0.63	
Eigenvalue	6.19	4.28	2.35	1.51
% of variance	38.69	26.75	14.69	9.44
% of cum. variance	38.69	55.44	70.13	79.57

	1	2	3	4
PLAND	0.68	0.43		
CONTIG	0.81			
SHAPE		0.80		
CPLAND	0.45			
DCAD		0.71	0.38	
DCORE	0.62		-0.51	
ENN	-0.60			-0.31
PROX		0.90		
SPLIT			-0.76	
IJI		0.68		
CLUMPY			0.86	
AI		0.54		0.53
CONNECT	0.49		0.81	
COHESION		0.43		0.52
Eigenvalue	8.18	2.82	1.70	1.39
% of variance	45.43	15.67	9.44	7.71
% of cum. variance	45.43	61.11	70.54	78.25

Extraction Method: Principal Components Method.
Rotation Method: Varimax with Kaiser Normalization.

Giant panda distribution related to forest fragmentation

The results of the Mann-Whitney *U* test show that six out of the eight metrics were significantly different (at $p < 0.05$) for forests with pandas present and those with pandas absent (Table 5), demonstrating that these six metrics are important factors determining the distribution of giant pandas. The patches of dense forest occupied by giant pandas were larger, closer together and more contiguous than those where panda were not recorded. However, giant pandas were not sensitive to patch proximity and clumpiness patterns of the combination of dense and sparse forest.

The metrics calculated for plots occupied by giant pandas in the five mountain regions were to some extent heterogeneous, with subtle distinctions between the five regions (Table 6). The results of the Games-Howell test revealed that forest fragmentation occurs least in the Qinling Mountains and most in the Xiangling and Liangshan regions, and that patterns of forest fragmentation in the Minshan and Qionglai regions are similar, as shown in Table 6.

Table 5 Summary statistics and the results of nonparametric Mann-Whitney *U* test of eight metrics for the forest patches with pandas present and those with pandas absent

Forest type	Metrics	Mean ± S.D.		U
		Presence (n=1000)	Absence (n=1000)	
Dense forest	ED	21.6 ± 6.2	12.4 ± 5.9	-24.6*
	LPI	54.1 ± 17.5	33.4 ± 21.4	-20.3*
	PROX	16.2 ± 10.9	9.9 ± 7.4	-12.8*
	CLUMPY	0.4 ± 0.2	0.6 ± 0.3	-16.2*
Combination of dense and sparse forest	AREA	91.5 ± 84.1	104.3 ± 90.3	-14.8*
	ED	14.0 ± 0.8	16.6 ± 2.1	-11.3*
	PROX	8.1 ± 6.3	10.12 ± 8.6	-9.3
	CLUMPY	0.4 ± 0.2	0.4 ± 0.2	-10.7

* Difference is significant at the 0.05 level.

Table 6 Statistics on mean differences of each of the eight metrics from pair-wise multiple comparisons of the panda presence in the five mountain regions

LPI of dense forest

	Qinling	Minshan	Qionglai	Xiangling
Minshan	4.21			
Qionglai	10.8*	6.12*		
Xiangling	14.5*	9.82*	3.73	
Liangshan	17.1*	12.8*	6.58*	2.79

ED of dense forest

	Qinling	Minshan	Qionglai	Xiangling
Minshan	-6.64*			
Qionglai	-6.82*	-0.15		
Xiangling	-8.97*	-2.64*	-2.33	
Liangshan	-8.63*	-1.32	-1.34	0.95

PROX of dense forest

	Qinling	Minshan	Qionglai	Xiangling
Minshan	-6.15*			
Qionglai	-2.18	2.03		
Xiangling	-4.98*	-0.83	-2.86	
Liangshan	0.18	4.35*	2.29	5.17

CLUMPY of dense forest

	Qinling	Minshan	Qionglai	Xiangling
Minshan	0.16*			
Qionglai	0.12*	-0.04*		
Xiangling	0.14*	-0.01	0.02	
Liangshan	0.08*	-0.07*	-0.04	-0.06

*Games-Howell test, the mean difference is significant at the 0.05 level.

AREA of the combination of dense and sparse forest

	Qinling	Minshan	Qionglai	Xiangling
Minshan	106*			
Qionglai	82*	-24*		
Xiangling	114*	7.3	31*	
Liangshan	67*	-39*	-15	-46*

ED of the combination of dense and sparse forest

	Qinling	Minshan	Qionglai	Xiangling
Minshan	-3.54*			
Qionglai	-3.51*	0.03		

Xiangling	-3.87*	-0.13	-0.16	
Liangshan	-3.94*	-0.13	-0.16	0.01

PROX of the combination of dense and sparse forest

	Qinling	Minshan	Qionglai	Xiangling
Minshan	3.24*			
Qionglai	2.19*	-1.05		
Xiangling	4.51*	1.27	2.32*	
Liangshan	-0.96	-4.20*	-3.16*	-5.48*

CLUMPY of the combination of dense and sparse forest

	Qinling	Minshan	Qionglai	Xiangling
Minshan	0.18*			
Qionglai	0.18*	0.01		
Xiangling	0.21*	0.02	0.02	
Liangshan	0.19*	0.05	0.02	0.03

*Games-Howell test, the mean difference is significant at the 0.05 level.

The logistic regression model and its performance

Of the six representative metrics, three metrics were significant at p<0.01 when included in a forward stepwise logistic regression model (Table 7). A threshold of 0.52 was selected for transforming continuous probabilities of panda occurrence to discrete panda presence/absence map (Figure 3). The logistic regression model predicted the panda presence with an overall accuracy of 72.5% and kappa 0.45 (Table 8). By applying a knowledge-based control for slope and elevation to the model, the overall accuracy and kappa increased to 77.6% and 0.55 respectively (Table 8). It is noticeable that the predicted areas of panda presence shrank mainly in the Qionglai, Xiangling, and Liangshan ranges when using a knowledge-based control (Figure 4). The Z-test for kappa coefficients shows that the accuracy of the modelling was significantly improved (at p<0.05) by applying the knowledge-based control.

Table 7 Parameter estimates of the logistic regression model. Significance of coefficients was assessed using the Wald statistic

Parameter	Coefficient	Standard Error	Wald Statistic	*P*
ED of dense forest	0.151	0.0102	219.922	<0.001
LPI of dense forest	0.097	0.0023	273.478	<0.001
CLUMPY of dense forest	-1.489	0.333	20.031	<0.001
Constant	-4.289	0.316	184.316	<0.001

Table 8 Statistics for evaluation of logistic regression model performance

Logistic regression model	Overall accuracy	Sensitivity	Specificity	Kappa	Kappa variance	Z
Without knowledge-based control	72.5%	83.7%	61.3%	0.45	0.00031	4.12
With knowledge-based control	77.6%	81.0%	74.2%	0.55	0.00028	(P<0.05)
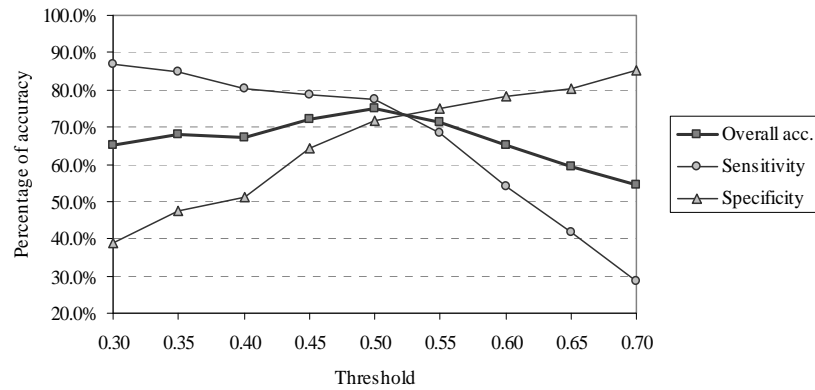
Figure 3 Sensitivity and specificity plotted against threshold for defining decision thresholds. The threshold is assigned at the point where the two curves cross, which is 0.52
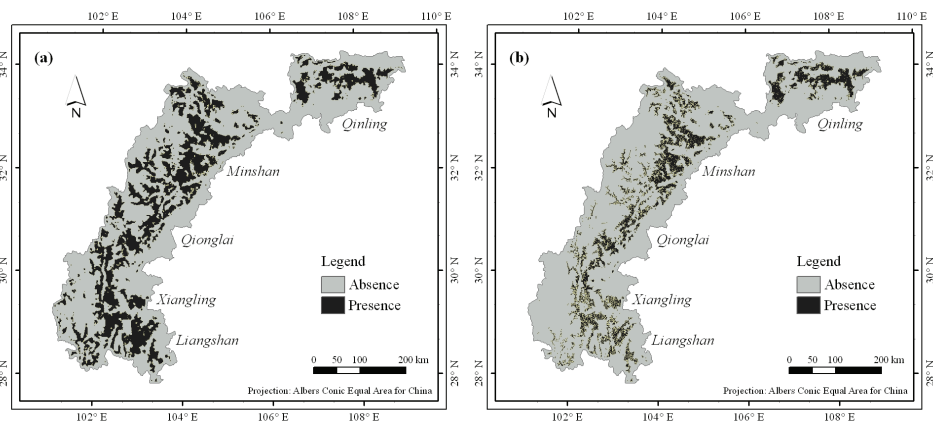
Figure 4 Presence-absence of the giant panda predicted by the logistic regression model (threshold=0.52): (a) without knowledge-based control achieved an overall accuracy of 72.5% (kappa 0.45); (b) with knowledge-based control for elevation and slope achieved an overall accuracy of 77.6% (kappa 0.55). Predicted accuracy of panda presence shrank mainly in the Qionglai, Xiangling, and Liangshan ranges

DISCUSSION

Giant panda distribution related to forest fragmentation
Our results show that dense forest is essential for the survival of giant pandas, and giant pandas are sensitive to the fragmentation of dense forest. Of the eight landscape metrics selected in this study, six metrics were significantly different between areas of panda presence and absence (Table 5), demonstrating that panda distribution is significantly related to forest patch area, edge density, and patch clumpiness. All metrics measuring forest patch size/edge (LPI, ED, and AREA) were significantly different between panda presence and absence, no matter whether the metrics were computed for dense forest solely or the combination of dense and sparse forest. Only the metrics PROX and CLUMPY of dense forest differed significantly between panda presence and absence, indicating that dense forest plays a more important role in determining panda distribution than the sparse forest does.

All of the three metrics (LPI, ED, and CLUMPY) included in the logistic regression model relate to dense forest. These metrics measure the ratio of patch area to patch edge, indicating that the giant panda is sensitive to patch size and isolation effects associated with the fragmentation of dense forest. The giant panda tends to occur in larger, more contiguous patches of dense forest. From the ecological point of view, the preference for larger and less segregated forest patches may relate to panda migration or dispersal, because small or highly segregated patches will increase the cost of migration or dispersal between patch clusters, increasing the chance of being disturbed by human activities as well as by requiring higher energy consumption. It is interesting that the CLUMPY of dense forest, in contrast to metrics LPI and ED, have a negative coefficient in the logistic regression model, implying that giant pandas tend to be appearing in less clumped dense forest patches rather than highly clumped patches. However, the mechanism of this is beyond current horizons and needs closer inspection.

Pairwise multiple comparisons of panda presence in five mountain regions show that there are variations in the patterns of forests across the current panda distribution area. Forests occupied by the giant panda are less fragmented in the Qinling Mountains, and more fragmented in the Xiangling and Liangshan regions. The Qinling Mountains, according to result of the third national giant panda survey, also has the highest population density of giant panda among five ranges (State Forestry Administration 2006). By associating population density with the values of these landscape metrics, it is clear that patch size/edge of dense forest has a positive effect on panda distribution.

Model performance and its factors

Model performance can be affected by various factors, including limitations of the model itself, quality of the data input, and sampling techniques (Morrison 2001). Logistic regression depends on explanatory variables included in the model and may include areas beyond the environmental thresholds of the giant panda (Elton et al., 2001, Morrison 2001). When combined with knowledge-based controls for the effect of elevation and slope, logistic regression accurately predicts the spatial distribution of the giant panda using landscape metrics.

Yet knowledge-based controls require adequate relevant knowledge and a good understanding of the relationship between the species and environmental factors. As the data used in this study were inferred by buffering the panda occurrence points, there is a possibility that the result may be biased by the inclusion of false-absence points. This is a potential problem faced by all such habitat modelling (Morrison 2001), and this problem remains unresolved. Additional searches may be conducted in limited areas in order to provide accurate data on panda absences, and this information may then be used to refine the model, as suggested by Brotons et al., (2004). In addition, the heterogeneity in forest density across the panda distribution area may also increase within-group variance in the training samples, and consequently decrease the power of the model.

Landscape metrics may be sensitive to the level of detail in the categorical map data used as input (Turner et al., 2001). In this study, forests were categorized into dense forest (canopy cover >30%) and sparse forest (canopy cover <30%). This division was adopted as it was used in UNEP-WCMC's forest classification (http://www.unep-wcmc.org/forest/fp_background.htm).It's also ecologically meaningful because giant pandas have a strong preference for forest patches with a high canopy cover. In addition, the presence of understorey bamboo was not considered in the model due to the data being unavailable. The distribution of understorey bamboo is highly correlated with the distribution of forest (Schaller 1987, Ren et al., 1998, State Forestry Administration 2006), so it may be assumed that the exclusion of bamboo information on model output is compensated by the inclusion of the forest cover information.

Implications for panda conservation

Although the selected landscape metrics in the analysis partly explain the distribution of giant pandas, our model has important implications for giant panda conservation in heterogeneous landscape. It allows assessing the relationship between forest fragmentation and response of panda population at

the landscape scale. For a management point of view, such information is important for panda habitat evaluation and new nature reserve/corridor design since there are only around 61% pandas are under protection in panda reserves (State Forestry Administration 2006). In recent years several new nature reserves have been suggested or already established just based on the actual presence of giant pandas acquired from the third national giant panda survey (State Forestry Administration 2006). However, this notion overlooks the availability of suitable habitat and neglects the impact of habitat fragmentation for panda population exchange. Our modelling approach can open prospect in comprehension and simplification of analysis of panda spatial distribution at the landscape scale. For the conservation of the giant panda, the following measures are recommended when designing new nature reserve/corridor:

(1) All of the dense forest patches in current panda distribution regions should be preserved to serve as a source habitat for giant pandas.

(2) Our results show a significant positive relationship between the distribution of giant pandas and the area of forest patches. Therefore, the additional fragmentation of the forest patches in current panda habitat has to stop for the conservation of this endangered species. A large dense forest patch is better than several small aggregated patches for the survival of the giant panda.

(3) Corridors of forest should be established to connect forest patches with one another and with areas currently occupied by giant pandas or existing nature reserve. This will facilitate the migration of giant pandas and population exchange.

(4) To make corridor suitable for the giant panda, it is important to increase the proportion of dense forest patch as well as the degree of patch adjacency, and reforest the region if necessary. This should be carried out following ecological restoration principles, e.g., metapopulation theory. Experiments should first be conducted at sample sites, and then restoration should be expanded to cover the entire corridor.

(5) It is also necessary to reintroduce the giant panda into the areas once occupied by giant pandas in the past and its environment are still similar to current panda habitat.

The realization of the above mentioned recommendation may contribute to the connection of the panda populations living in the isolated forest patches. This connection can support the survival of the giant panda species and the maintenance and conservation of its habitat.

CONCLUSION

This study demonstrates a successful approach for modelling the spatial distribution of the giant panda from multi-temporal MODIS 250 m EVI data and landscape metrics. Eight metrics were selected to quantify forest fragmentation. All metrics were significantly different for the forest patches with pandas present and those with pandas absent. Forest patch size, edge

density, and patch aggregation were found to have significant roles in panda distribution. The selected landscape metrics partly explained the distribution of giant pandas, though a knowledge-based control for elevation and slope significantly improved the explanation. The findings of this study imply that the design of effective conservation areas for the wild giant panda must include large and dense forest patches, which are adjacent to other similar patches.

REFERENCE

Bagan, H., Q. Wang, M. Watanabe, Y. Yang, and J. Ma. 2005. Land cover classification from MODIS EVI times-series data using SOM neural network. International Journal of Remote Sensing **26**:4999-5012.

Bissonette, J. A., editor. 1997. Wildlife and Landscape Ecology: Effects of Pattern and Scale. Springer-Verlag, Berlin.

Brotons, L., W. Thuiller, M. B. Araujo, and A. Hirzel. 2004. Presence-absence versus presence-only modelling methods for predicting bird habitat suitability. Ecography **27**:437-448.

Bulmer, M. G. 1979. Principles of statistics. Dover Publications, INC., New York.

Byrne, G. F., P. F. Crapper, and K. K. Mayo. 1980. Monitoring land-cover change by principal component analysis of multitemporal Landsat data. Remote Sensing of Environment **10**:175-184.

Cain, D. H., K. H. Riitters, and K. Orvis. 1997. A multi-scale analysis of landscape statistics. Landscape Ecology **12**:199-212.

China Vegetation Compiling Committee. 1980. China Vegetation. Science Press, Beijing (in Chinese).

Congalton, R. and K. Green. 1999. Assessing the accuracy of remotely sensed data: Principles and practices. CRC/Lewis Press, Boca Raton.

Congalton, R. G. 1991. A review of assessing the accuracy of classifications of remotely sensed data. Remote Sensing of Environment **37**:35-46.

Corsi, F., J. de Leeuw, and A. K. Skidmore. 2000. Modelling species distribution with GIS. Pages 389-434 *in* L. Boitani and T. K. Fuller, editors. Research Techniques in Animal Ecology: Controversies and Consequences Columbia University Press, New York.

Dufour, A., F. Gadallah, H. H. Wagner, A. Guisan, and A. Buttler. 2006. Plant species richness and environmental heterogeneity in a mountain landscape: effects of variability and spatial configuration. Ecography **29**:573-584.

Elton, C. S., M. A. Leibold, and J. T. Wootton. 2001. Animal Ecology. University of Chicago Press, Chicago.

Field, A. 2005. Discovering statistics using SPSS. Sage Publications, London.

Fielding, A. H. and J. F. Bell. 1997. A review of methods for the assessment of prediction errors in conservation presence/absence models. Environmental Conservation **24**:38-49.

Frohn, R. C. 1998. Remote Sensing for Landscape Ecology : New Metric Indicators for Monitoring, Modeling, and Assessment of Ecosystems. Lewis Publishers, New York.

Gao, X., A. R. Huete, W. G. Ni, and T. Miura. 2000. Optical-biophysical relationships of vegetation spectra without background contamination. Remote Sensing of Environment **74**:609-620.

Griffith, J. A., E. A. Martinko, and K. P. Price. 2000. Landscape structure analysis of Kansas at three scales. Landscape and Urban Planning **52**:45-61.

Groom, G., C. A. Mucher, M. Ihse, and T. Wrbka. 2006. Remote sensing in landscape ecology: experiences and perspectives in a European context. Landscape Ecology **21**:391-408.

Guisan, A, O, Broennimann, R. Engler, M. Vust, N. G. Yoccoz, A. Lehmann, and N. E. Zimmermann. 2006. Using niche-based models to improve the sampling of rare species. Conservation Biology, **20**: 501-511.

Gustafson, E. J. 1998. Quantifying landscape spatial pattern: What is the state of the art? Ecosystems **1**:143-156.

Hamazaki, T. 1996. Effects of patch shape on the number of organisms. Landscape Ecology **11**:299-306.

Hirzel, A.H., V. Helfer, and F. Metral. 2001. Assessing habitat-suitability models with a virtual species. Ecological Modelling **145**: 111-121.

Hosmer, D. W. and S. Lemeshow. 2000. Applied Logistic Regression. Wiley, New York.

Hu, J. C. 2001. Research on the Giant Panda. Shanghai Scientific & Technological Education Publishers, Shanghai (in Chinese).

Hu, J., G. B. Schaller, W. Pan, and J. Zhu. 1985. The giant panda in Wolong. Sichuan Science and Technology Press, Chengdu (in Chinese).

Huete, A., K. Didan, T. Miura, E. P. Rodriguez, X. Gao, and L. G. Ferreira. 2002. Overview of the radiometric and biophysical performance of the MODIS vegetation indices. Remote Sensing of Environment **83**:195-213.

Hulshoff, R. M. 1995. Landscape indices describing a Dutch landscape. Landscape Ecology **10**:101-111.

ITT Industries Inc. 2006. ENVI (Environment for Visualizing Images) Version 4.3. ITT Industries Inc., Boulder, USA.

Jönsson, P. and L. Eklundh. 2004. TIMESAT - a program for analyzing time-series of satellite sensor data. Computers and Geosciences **30**:833–845.

Leica Geosystems Geospatial Imaging, L. 2005. ERDAS IMAGINE 9.1, Norcross, GA, USA.

Lindburg, D. and K. Baragona, editors. 2004. Giant Pandas: Biology and Conservation. University of California Press, Berkeley.

Liu, J., M. Liu, D. Zhuang, Z. Zhang, and X. Deng. 2003a. Study on spatial patterns of land-use change in China during 1995-2000. Science in China **46**: 373-384.

Liu, J. Y., D. F. Zhuang, D. Luo, and X. Xiao. 2003. Land-cover classification of China: integrated analysis of AVHRR imagery and geophysical data. International Journal of Remote Sensing **24**:2485-2500.

Liu, X. and M. Kafatos. 2005. Land-cover mixing and spectral vegetation indices. International Journal of Remote Sensing **26**:3321-3327.

Loucks, C.J. and H. Wang. 2004 Assessing the habitat and distribution of the giant panda: Methods and issue. In: Panda 2000 (eds. D.G. Lindburg and K. Baragona). University of California Press, San Diego.

Mcgarigal, K. and S. A. Cushman. 2002. Comparative evaluation of experimental approaches to the study of habitat fragmentation effects. Ecological Applications **12**: 335-345.

McGarigal, K. and B. J. Marks. 1995. Fragstats: Spatial pattern analysis program for quantifying landscape structure. U.S. Forest service general technical report. In, Portland, OR, USA.

Mladenoff, D. J., T. A. Sickley, R. G. Haight, and A. P. Wydeven. 1995. A regional landscape analysis and prediction of favorate gray wolf habitat in the Northern Great Lakes region. Conservation Biology **9**:279-294.

Morrison, M. L. 2001. A proposed research emphasis to overcome the limits of wildlife-habitat relationship studies. Journal of Wildlife Management **65**:613-623.

O'Neill, R. V., J. R. Krummel, R. H. Gardner, G. Sugihara, B. Jackson, D. L. DeAngelis, B. T. Milne, M. G. Turner, B. Zygmunt, S. W. Christensen, V. H. Dale, and R. L. Graham. 1988. Indices of landscape pattern. Landscape Ecology **1**:153-162.

Pan, W. S., Z. Lu, X. J. Zhu, D. J. Wang, H. Wang, Y. Long, D. L. Fu, and X. Zhou. 2001. A Chance for Lasting Survival. Beijing University Press, Beijing (in Chinese).

Ren, Y., M. L. Wang, M. Yue, and Z. J. Li. 1998. Plants of Giant Panda's Habitat of Qinling Mountains. Shaanxi Science and Technology Press, Xi'an (in Chinese).

Richards, J. A. 1984. Thematic mapping from multitemporal image data using the principal components transformation. Remote Sensing of Environment **16**:25-46.

Richard, J.A. 1984. Thematic mapping from multitemporal image data using the principal components transformation. Remote Sensing of Environment **16**: 25-46.

Riitters, K. H., R. V. O'Neill, C. T. Hunsaker, J. D. Wickham, D. H. Yankee, S. P. Timmins, K. B. Jones, and B. L. Jackson. 1995. A factor analysis of landscape pattern and structure metrics. Landscape Ecology **10**:23-39.

Saura, S. 2004. Effects of remote sensor spatial resolution and data aggregation on selected fragmentation indices. Landscape Ecology **19**:197-209.

Schaller, G. 1987. Bamboo shortage not only cause of panda decline. Nature **327**: 562

Skidmore, A. K., F. Watford, P. Luckananurug, and P. J. Ryan. 1996. An operational GIS expert system for mapping forest soils. Photogrametric Engineering & Remote Sensing **62**:501– 511.

Skinner, C. N. 1995. Change in spatial characteristics of forest openings in the Klamath mountains of northwestern California, USA. Landscape Ecology **10**:219-228.

Sokal, R. R. and F. J. Rohlf. 1995. Biometry: the Principles and Practice of Statistics in Biological Research. W. H. Freeman and Co., New York.

SPSS Inc. 2006. SPSS 15 for Windows. SPSS Inc., Chicago.

State Forestry Administration. 2006. The Third National Survey Report on Giant Panda in China. Science Press, Beijing (in Chinese).

Story, M. and Congalton, R.G. 1986. Accuracy assessment: A user's perspective. Photogrammetric Engineering and Remote Sensing **52**: 397-399.

Taylor, P. D., L. Fahrig, K. Henein, and G. Merriam. 1993. Connectivity is a vital element of landscape structure. Oikos **68**:571-573.

Thuiller, W., J. Vayreda, J. Pino, S. Sabate, S. Lavorel, and C. Gracia. 2003. Large-scale environmental correlates of forest tree distributions in catalonia (ne spain). Global Ecology and Biogeography **12**: 313-325.

Turner, M. G., R. H. Gardner, and R. V. O'Neill. 2001. Landscape Ecology in Theory and Practice : Patterns and Process. Springer, Berlin.

Turner, M. G., R. V. O'Neill, R. H. Gardner, and B. T. Milne. 1989. Effects of changing spatial scale on the analysis of landscape pattern. Landscape Ecology **3**:153-162.

Wardlow, B. D., S. L. Egbert, and J. H. Kastens. 2007. Analysis of time-series MODIS 250 m vegetation index data for crop classification in the U.S. Central Great Plains. Remote Sensing of Environment **108**:290-310.

Wu, J. G., D. E. Jelinski, M. Luck, and P. T. Tueller. 2000. Multiscale analysis of landscape heterogeneity: scale variance and pattern metrics Geographical Information Science **6**:6-19.

Xavier, A. C., B. F. T. Rudorff, Y. E. Shimabukuro, L. M. S. Berka, and M. A. Moreira. 2006. Multi-temporal analysis of MODIS data to classify sugarcane crop. International Journal of Remote Sensing **27**:755-768.

Zaniewski, A. E., A. Lehmann, and J. M. Overton. 2002. Predicting species spatial distributions using presence-only data: a case study of native New Zealand ferns. Ecological Modelling **157**:261-280.

Bamboo (*Fargesia qinlingensis*) in the panda summer habitat

Photograph: Tiejun Wang

Bamboo (*Bashania fargesii*) in the panda winter habitat

Photograph: Baiquan Xiong

Chapter 7

A synthesis:

Remote sensing of giant panda habitat

INTRODUCTION

A variety of ecological applications require data from broad spatial extents that cannot be collected using field-based methods. Remote sensing data and techniques address these needs, which include identifying and detailing the biophysical characteristics of species' habitats, predicting the distribution of species and spatial variability in species richness, and detecting natural and human-caused change at scales ranging from an individual range to the entire world (Kerr and Ostrovsky 2003). The objectives of this study were to develop innovative methods in remote sensing and GIS for estimating the giant panda habitat and forage abundance, and to explain the altitudinal migration and the spatial distribution of giant pandas in fragmented forest landscape. Our research was motivated by the fact that an understanding of the habitat, foraging behaviour and spatial distribution of giant pandas should rest on an understanding of their unique food availability and abundance. Moreover, as the remaining giant panda habitat is located in remote and rugged mountain landscapes with dense and mixed forest which required the survey of an area of about 30,000 km², remote sensing and geographical information systems (GIS) are potentially an efficient way to acquire habitat data quickly and at low cost (De Wulf et al., 1988, MacKinnon and De Wulf 1994, Liu et al., 2001, Loucks et al., 2003). We found that the proposed remote sensing and GIS methods in this thesis are capable of achieving this goal. In this final chapter, we summarize the major research findings relevant to the specific research questions stated in Chapter 1, and discuss the practical relevance of these results in the light of the development and implementation of giant panda conservation strategies.

MAPPING GIANT PANDA FORAGE ABUNDANCE

Seasonal change is a common natural phenomenon occurring on an annual basis especially in temperate forested landscapes. By considering the phenological variation of vegetation growth in temperate regions, more accurate vegetation maps have been obtained (Goodenough et al., 2001, Townsend and Walsh 2001). Because the canopy forest in the giant panda habitat is dominated by deciduous or mixed forest, and the deciduous canopy trees are leafless and do not block the view of ground features, we therefore predict that there is a possibility to map evergreen understorey bamboo species (i.e., the forage of giant panda) using winter (leaf-off) satellite images. Our first research question is:

- Can vegetation indices derived from winter (leaf-off) satellite images be successfully used to predict evergreen understorey bamboo in a

deciduous-dominated or mixed forest? If so, does a statistically significant difference exist in bamboo mapping accuracy between the vegetation index thresholds-based decision tree approach and the traditional multispectral bands-based classifiers?

In Chapter 2, we developed a new approach that combines forest phenology and Landsat vegetation indices to estimate the spatial distribution and coverage of an evergreen understorey bamboo species (*Bashania fargesii*) in the Foping Nature Reserve. It was found that vegetation indices, especially the normalized difference vegetation index (NDVI) derived from leaf-off (winter) images were significantly correlated with percent understorey bamboo cover for both deciduous and mixed coniferous/deciduous forests. Winter NDVI was used to map bamboo coverage using a binary decision tree classifier. A high mapping accuracy for understorey bamboo presence/absence was achieved with an overall accuracy of 89 percent (kappa=0.59). In addition, for the first time, we successfully classified three density classes of bamboo with an overall accuracy of 68 percent (kappa=0.48). These results were compared to three traditional multispectral bands-based methods (mahalanobis distance, maximum likelihood, and artificial neural networks). The highest mapping accuracy was again obtained from winter images. However, the kappa z-test showed that there was no statistical difference in accuracy between the methods. We therefore conclude that winter imagery significantly improves understorey bamboo cover mapping accuracy regardless of the classification methods used; and the winter vegetation indices, especially winter NDVI, can be successfully used to map evergreen understorey bamboo. The simplicity, robustness and availability of NDVI have potential to quickly identify the "hot spots" of understorey bamboo over a large region.

The bamboo species at high elevations, for example, in the Qinling Mountains (above 2,000 m), are not evergreen but are semi-evergreen. At the top of the mountains, the bamboo leaves become yellow and senesce but do not fall during the winter season. The degree of yellowing gradually decreases with elevation. In addition to the coniferous-dominated canopy forests, it makes prediction of understorey bamboo forest extremely difficult. Instead of using conventional classifiers and remote sensing data alone, GIS expert systems have been used to predict the presence/absence as well as cover abundance of understorey plant species based on a combination of remotely sensed data and available GIS data layers in previous studies. Our second research question is:

- Is it possible to develop a new approach, an integrated neural network and expert system algorithm, based on remote sensing and GIS in order

117

to achieve a higher accuracy for mapping evergreen or semi-evergreen understorey bamboo species in a coniferous-dominated forest?

In Chapter 3, we developed a novel method which combines an artificial neural network and a GIS expert system in order to map the semi-evergreen understorey bamboo species in a coniferous-dominated forest. Results from leaf-off ASTER imagery and four thematic maps (i.e., vegetation type, elevation, slope gradient and terrain position), using a neural network and an expert system, were evaluated for their suitability to quantify understorey bamboo. Three density classes of understorey bamboo were mapped, first using a neural network (overall accuracy 64.7%, kappa 0.45) and then using an expert system (overall accuracy 62.1%, kappa 0.43). However, when using the results of the neural network classification as input into the expert system, a significantly improved mapping accuracy was achieved with an overall accuracy of 73.8% and kappa of 0.60 (average z-value=3.35, p=0.001). To our knowledge, this study represents the first successful mapping of three density classes of understorey bamboo. Our study suggests that combining a neural network with an expert system makes it possible to successfully map the cover of understorey bamboo in a coniferous-dominated and dense canopy forests, and with higher accuracy than when using either a neural network or an expert system. This approach may also be used for a range of applications, particularly to map cover abundance of understorey species in complex forested landscapes.

The presence and abundance of understorey bamboo is a key factor in giant pandas habitat assessment, but it has normally been assumed to have a constant cover over space and time. The direct result of this research is an improved understanding of the distribution pattern of understorey bamboo abundance in the Qinling Mountains as well as other forests in central China. On the basis of these results, a more accurate assessment and modelling for suitable giant panda habitat can be achieved.

TESTING ALTERNATIVE HYPOTHESES EXPLAINING ALTITUDINAL MIGRATION IN SYMPATRIC SPECIES

Remote sensing data are increasingly being used for ecological studies (Pettorelli et al., 2005). The normalized difference vegetation index (NDVI), in particular, is useful because it shows spatial and temporal trends in vegetation dynamics, productivity and distribution (Reed et al., 1994, Nemani et al., 2003). Consequently, the NDVI is growing in popularity as a tool to investigate the interaction between vegetation and animal activity, including migration (Boone et al., 2006, Ito et al., 2006). Until this century, the NOVA/AVHRR and

SPOT/VGT sensors were the only instruments providing data to construct NDVI time series at an almost-daily resolution. The 1 km spatial resolution of these datasets limits their applicability for all but continental and global ecological studies. Now, however, MODIS data can be used to produce NDVI time series of almost-daily resolution at a spatial resolution as high as 250 m, making them useful for local and regional studies. Our third research question is:

- Does the seasonal movement or altitudinal migration of giant pandas correlate with satellite (MODIS NDVI)-derived plant phenology?

In Chapter 3, we developed a method, namely the relative phenological development (RPD) index, to display phenological development as captured by the 250 m-MODIS NDVI. The radio tracked movement data of giant pandas in the Foping Nature Reserve was taken as an example to test the method. We found that the altitudinal migration of the giant pandas shows a striking correlation with the phenological development of the area. In spring, the animals move rapidly to higher altitudes when the vegetation reaches its peak greenness. In autumn, the gradual movement of the animals to lower altitudes coincides with the onset of vegetation senescence from the highlands to the valleys. The relative phenological development index maps were overlaid on a shaded digital elevation model of the area. Together, they further illustrate how the phenological development correlates with altitude and strongly indicates that phenological development drives giant panda movement. We therefore conclude that the relative phenological development index derived from 250 m-MODIS NDVI is a useful exploratory tool when relating vegetation activity to other ecological phenomena at local and regional scales. And this study has confirmed that the altitudinal migration of giant pandas is correlated with MODIS NDVI-derived plant phenology.

Giant panda and golden takin occur sympatrically throughout the southern part of the Qinling Mountains. Both species have the habit of altitudinal migration in a mixed forest-bamboo landscape. Although previous studies have reported that the migration patterns of these two species appear different, little is known about these differences in relation to their food quality and quantity. Previous studies have suggested that increased access to highly nutritious and abundant forage is one of the most important driving forces in the evolution of migration of large herbivores (Mysterud et al., 2001). As crude protein content and digestibility of plants peak early in the growing season, and then rapidly decline as vegetation matures (Crawley 1983, Van Soest 1983), plant phenology is therefore a good proxy for plant quality (Laycock and Price 1970). However, high food quality does not always translate into high food abundance. In a

giant panda habitat, plant diversity tends to be low and seedlings, saplings and young trees are scarce when dense bamboo dominates the understorey (Taylor and Qin 1988, Yue et al., 1999). Hence, the areas of dense bamboo, favoured by giant pandas, potentially form poor golden takin habitat (Zeng et al., 2001). We therefore predict that the spatial-temporal variation in plant phenology and bamboo abundance explains differences in the migration patterns of giant pandas and golden takins. Our fourth research question is:

- Can satellite-derived plant phenology (a surrogate of food quality) and bamboo abundance (a surrogate of food quantity) explain the differences in altitudinal migration patterns between giant pandas and golden takins?

In Chapter 5, we used radio-telemetry data from six giant pandas and three golden takins to determine if differences in their migration patterns are related to satellite-derived plant phenology and bamboo abundance. The results indicate that the altitudinal migration pattern of the golden takin is linked to the early spring green-up and late autumn senescence. The migration pattern of the giant panda, however, is related to the late spring green-up and early autumn senescence, with the spring migration of giant pandas following the peak of bamboo shooting which occurs about three weeks later than the overall greening of the landscape. The short duration of uphill and downhill migrations of the giant panda may be attributable to the sparseness of the bamboo forest at intermediate elevations in the study area, and the consequent lack of forage for giant pandas. At intermediate elevations plant species diversity and density is high, providing varied forage for golden takins, and therefore encouraging their relatively early and slower ascent in spring and late descent in autumn. In other words, the altitudinal migration patterns of both the giant panda and the golden takin follow the phenological development of plants in the study area, and the difference between them appears to be attributable to the difference in the phenology of bamboo and non-bamboo plants, and thus the abundance and quality of food available to these two species.

To the best of our knowledge, it is the first time anyone has successfully tested the mechanism of altitudinal migration of sympatric species, specifically the giant panda and the golden takin, based on satellite-derived spatially continuous variables. Hence, we believe that this work represents a step forward in the use of remotely sensed data, contribute significantly to the understanding of animal migration behaviour and presents a tool useful to evolutionary biologists and ecologists.

UNDERSTANDING SPATIAL DISTRIBUTION OF GIANT PANDAS IN THE FRAGMENTED FOREST LANDSCAPE

Although forest fragmentation has been recognized as one of the major threats to the population of the wild giant panda, little is known about the relationship between forest fragmentation and the spatial distribution of wild giant pandas. Landscape structural variables (i.e., landscape metrics) are easily obtainable over large areas and their calculation is less demanding than collecting detailed data on species distribution (Groom et al., 2006). As most landscape metrics are scale-dependent and landscape elements are species-specific (Cain et al., 1997, Saura 2004), appropriate land cover classes and spatial resolution are critical when linking the response variable of species to landscape metrics (Turner et al., 1989, Wu et al., 2000). When choosing a data source for land cover classification, data availability and spatial resolution are two important issues. High spatial resolution sensors, such as Landsat TM, have a relatively narrow swath width and revisit the same area infrequently making their acquisition and interpretation expensive and time-consuming. It is also difficult to acquire sufficient images for a large area. A time-series of 16-day composite Moderate Resolution Imaging Spectroradiometer (MODIS) 250 m Enhanced Vegetation Index (EVI) images, with a broad geographical coverage, intermediate spatial resolution and high temporal resolution, offers a new option for large area land cover classification (Xavier et al., 2006). Our fifth research question is:

- Which landscape metrics characterize fragmentation of forests occupied by giant pandas? What are the relationships between the distribution of giant pandas and the forest fragmentation?

In Chapter 6, we examine the effects of forest fragmentation on the distribution of the entire wild giant panda population. To quantify the fragmentation of forests, eight fragmentation metrics, with the highest loadings following a factor analysis and derived from MODIS 250 m EVI multi-temporal data, were selected. All metrics were significantly different for the forest patches with pandas present and those with pandas absent. Forest patch size, edge density, and patch aggregation were found to have significant roles in giant panda distribution. A forward stepwise logistic regression was then applied to explore the relationship between panda distribution and forest fragmentation. We found that the patches of forest occupied by giant pandas were significantly larger, closer together and more contiguous than patches where giant pandas were not recorded, indicating that giant pandas appear sensitive to patch size and isolation effects associated with forest fragmentation. Forest fragmentation occurs least in the Qinling Mountains and most in the Xiangling and Liangshan regions. Using the selected landscape metrics, the logistic regression model

predicted the distribution of giant pandas with an overall accuracy of 69.9% (kappa 0.39). However, when a knowledge-based control for elevation and slope was applied to the regression, the overall accuracy of the model improved to 74.9% (kappa 0.49). We therefore conclude that landscape metrics derived from MODIS 250 m EVI multi-temporal data can be successfully used to characterize the panda spatial distribution in relation to forest fragmentation at a large landscape level.

The findings of this study imply that the design of effective conservation areas for the wild giant panda must include large and dense forest patches, which are adjacent to other similar patches. The remote sensing based approach in this study can be applied to routine habitat monitoring and habitat evaluation for the giant panda at national level.

GENERAL CONCLUSION

Remote sensing is indispensable for ecological and conservation biological applications and will play an increasing important role in the future. For many purposes, it provides the only means of measuring the characteristics of habitats across broad areas and detecting environmental changes that occur as a result of human or natural process. These data are increasingly easy to find and use. Overall, our study has shown the potential of satellite remote sensing to map giant panda habitat and forage (i.e., understorey bamboo) abundance. The results are important for understanding the foraging behaviour and the spatial distribution of giant pandas, as well as the evaluation and modelling of giant panda habitat in order to guide decision-making on giant panda conservation.

REFERENCES

Boone, R. B., S. J. Thirgood, and J. G. C. Hopcraft. 2006. Serengeti Wildebeest migratory patterns modeled from rainfall and new vegetation growth. Ecology **87**:1987-1994.

Cain, D. H., K. Riitters, and K. Orvis. 1997. A multi-scale analysis of landscape statistics. Landscape Ecology **12**:199-212.

Crawley, M. J. 1983. Herbivory: the dynamics of animal-plant interactions. Blackwell Scientific, Oxford, U.K.

De Wulf, R. R., R. E. Goossens, J. R. Mackinnon, and S. C. Wu. 1988. Remote sensing for wildlife management: giant panda habitat mapping from LANDSAT MSS images. Geocarto International **1**:41-50.

Goodenough, D. G., A. S. Bhogall, H. Chen, and A. Dyk. 2001. Comparison of methods for estimation of Kyoto Protocol products of forests from multitemporal Landsat. Pages 764-767 *in* Proceedings of IEEE 2001 International Geoscience and Remote Sensing Symposium, IGARSS'01, July 2001, Sydney.

Groom, G., C. A. Mucher, M. Ihse, and T. Wrbka. 2006. Remote sensing in landscape ecology: Experiences and perspectives in a european context. Landscape Ecology **21**:391-408.

Ito, T. Y., N. Miura, B. Lhagvasuren, D. Enkhbileg, S. Takatsuki, and A. J. Tsunekawa. 2006. Satellite tracking of Mongolian gazelles (Procapra gutturosa) and habitat shifts in their seasonal ranges. Journal of Zoology **269**:291-298.

Kerr, J. T. and M. Ostrovsky. 2003. From space to speceis: ecological applications for remote sensing. TRENDS in Ecology and Evolution **18**:299-305.

Laycock, W. A. and D. A. Price. 1970. Factors influencing forage quality, environmental influences on nutritional value of forage plants. Pages 37-47 *in* Range and wildlife habitat evaluation - a research symposium. USDA Forest Service Miscellaneous Publication No.1147.

Liu, J. G., M. Linderman, Z. Y. Ouyang, L. An, J. Yang, and H. M. Zhang. 2001. Ecological degradation in protected areas: the case of Wolong Nature Reserve for giant pandas. Science **292**:98-101.

Loucks, C. J., Z. Lu, E. Dinerstein, D. J. Wang, D. L. Fu, and H. Wang. 2001. The giant pandas of the Qinling Mountains, China: a case study in designing conservation landscapes for elevational migrants. Conservation Biology **17**:558-565.

Mackinnon, J. R. and R. R. De Wulf. 1994. Designing protected areas for giant pandas in China.*in* R. I. Miller, editor. Mapping the diversity of nature. Chapman & Hall, London.

Mysterud, A., R. Langvatn, N. G. Yoccoz, and N. C. Stenseth. 2001. Plant phenology, migration and geographical variation in body weight of a large herbivore: the effect of a variable topography. Journal of Animal Ecology **70**:915-923.

Nemani, R. R., C. D. Keeling, H. Hashinoto, W. M. Jolly, S. C. Piper, C. J. Tucker, R. B. Myneni, and S. W. Running. 2003. Climate-driven increases in global terrestrial net primary production from 1982 to1999. Science **300**:1560-1563.

Pettorelli, N., J. O. Vik, A. Mysterud, J.-M. Gaillard, C. J. Tucker, and N. C. Stenseth. 2005. Using the satellite-derived NDVI to assess ecological responses to environmental change. TRENDS in Ecology and Evolution **20**:503-510.

Reed, B. C., J. F. Brown, D. Vanderzee, T. R. Loveland, J. W. Merchant, and D. O. Ohlen. 1994. Measuring phenological variability from satellite imagery. Journal of Vegetation Science **5**:703-714.

Saura, S. 2004. Effects of remote sensor spatial resolution and data aggregation on selected fragmentation indices. Landscape Ecology **19**:197-209.

Taylor, A. H. and Z. S. Qin. 1988. Regeneration patterns in old-growth Abies-Betula forests in the Wolong Natural Reserve, Sichuan, China. Journal of Ecology **76**:1204-1218.

Townsend, P. A. and S. J. Walsh. 2001. Remote sensing of forested wetlands: Application of multitemporaI and multispectral satellite imagery to determine plant community composition and structure in southeastern USA. Plant Ecology **157**:129-149.

Turner, M. G., R. V. O'neill, R. H. Gardner, and B. T. Milne. 1989. Effects of changing spatial scale on the analysis of landscape pattern. Landscape Ecology **3**:153-162.

Van Soest, P. J. 1983. Nutritional ecology of the ruminant. Cornell University Press, New York.

Wu, J., D. E. Jelinski, M. Luck, and P. T. Tueller. 2000. Multiscale analysis of landscape heterogeneity: Scale variance and pattern metrics. Geographical Information Science **6**:6-19.

Xavier, A. C., N. Acirc, B. F. T. Rudorff, Y. E. Shimabukuro, L. M. S. Berka, and M. A. Moreira. 2006. Multi-temporal analysis of modis data to classify sugarcane crop. International Journal of Remote Sensing **27**:755-768.

Yue, M., Y. Ren, G. D. Dang, and T. Q. Gu. 1999. Species diversity of higher plant communities in Foping National Reserve. Chinese Biodiversity **7**:263-269 (in Chinese).

Zeng, Z. G., Y. L. Song, W. Q. Zhong, H. S. Gong, J. Zhang, and G. D. Dang. 2001. Food habits of golden takin. Chinese Journal of Zoology **36**:36-44 (in Chinese).

Author's Biography

Wang, Tiejun was born on 8 November 1970 in Shaanxi province, China. He attended Shaanxi Agriculture School in 1986, and received a professional diploma in 1990. After graduation, he started work with the Foping National Nature Reserve as a park ranger and the head of field station. In 1995, he was appointed as a project coordinator to support the implementation of GEF-China Nature Reserve Management Program in Foping. He joined the State Forestry Administration of China in 2000, where he served as an assistant in the Department of Wildlife Conservation. In 2001, he received a joint scholarship from WWF-International and Dutch government to do an MSc in Rural Land Ecology at ITC in the Netherlands. He completed his MSc thesis with distinction in March 2003. He went back to China and was employed by WWF-China, where he served as a project manager at Xi'an office, and a full time consultant for the Species Program in Beijing. In 2005, he awarded an ITC scholarship with partially finial support from WWF-Netherlands and Institute of Zoology of Chinese Academy of Sciences to pursue PhD research at ITC and Wageningen University, which resulted in this thesis.

Publications

1) **Wang, T.J.,** A.K. Skidmore and A.G. Toxopeus (2009) Improved understorey bamboo cover mapping using a novel hybrid neural network and expert system. International Journal of Remote Sensing, 30(4): 965-981.

2) **Wang, T.J.,** A.K. Skidmore, A.G. Toxopeus and X.H. Liu (2009) Understory bamboo discrimination using a winter image. Photogrammetric Engineering & Remote Sensing, 75(1): 37-47.

3) Beck, P.S.A., **T.J. Wang,** A.K. Skidmore and X.H. Liu (2008) Displaying remotely sensed vegetation dynamics along natural gradients for ecological studies. International Journal of Remote Sensing, 29(14): 4277-4283.

4) Zeng, Z.G., A.K. Skidmore, Y.L. Song, **T.J. Wang** and H.S. Gong (2008) Seasonal altitudinal movements of golden takin in the Qinling Mountains of China. Journal of Wildlife Management, 72(3): 611-617.

5) **Wang, T.J.,** A.K. Skidmore, Z.G. Zeng, P.S.A. Beck, Y.L. Si, Y.L. Song, X.H. Liu and H.H.T. Prins (2009) Altitudinal migration of sympatric giant panda and golden takin in relation to plant phenology and bamboo abundance, in review.

6) **Wang, T.J.,** X.P. Ye, A.K. Skidmore and A.G. Toxopeus (2009) Characterizing the spatial distribution of giant pandas in the fragmented forest landscape, in review.

7) Zeng, Z.G., P.S.A. Beck, **T.J. Wang**, A.K. Skidmore, Y.L. Song, H.S. Gong and H.H.T. Prins (2009) Plant phenology and solar radiation drive seasonal movement of golden takins in the Qinling Mountains, China, Journal of Mammalogy, in press.

8) Wu, G.F., Y.L. Liu and **T.J. Wang** (2007) Methods and strategy for modelling daily global solar radiation with measured meteorological data - a case study in Nanchang station, China. Energy Conversion and Management, 48 (9): 2447-2452.

9) Liu, X.H., A.G. Toxopeus, A.K. Skidmore, X.M. Shao, G.D. Dang, **T.J. Wang** and H.H.T. Prins (2005) Giant panda habitat selection in Foping nature reserve, China. Journal of wildlife management, 69(4):1623-1632.

10) Liu, X.H., A.K. Skidmore, **T.J. Wang**, Y.G. Yong and H.H.T. Prins (2002) Giant panda movements in Foping nature reserve, China. Journal of Wildlife Management, 66(4):1179-1188.

11) Bian, M., **T.J. Wang**, Y.F. Liu, T. Fei and A.K. Skidmore (2007) Detection of understory bamboo in giant panda habitats using an indirect remote sensing approach. Acta Ecologica Sinica, 27(11): 4824-4831 (in Chinese).

12) Song, Y.L., G.D. Dang, J.S. Li, **T.J. Wang**, Z.G. Zeng and Zhao, L.G. (2003) Estimating the carrying capacity of the golden takin in Foping National Nature Reserve, Shaanxi, China. Acta Zoologica Sinica, 49(4): 445-450 (in Chinese).

13) **Wang, T.J.** and M.T. Song (2000) A study on the species diversity of amphibians and reptiles in Foping national nature reserve. Cultum Herpetologica Sinica (8): 109-115 (in Chinese).

14) **Wang, T.J.,** Y.G. Yong, X.H. Liu and A.K. Skidmore (2000) The best time for giant panda survey in the Qinling Mountains. Biological Diversity (Hong Kong), 1(1): 26-32 (in Chinese).

15) **Wang, T.J.** (2003) Habitat analysis for giant panda in Laoxiancheng Nature Reserve in the Qinling Mountains, China. MSc thesis, ITC. Enschede, The Netherlands.

ITC Dissertation list

A list of ITC dissertations can be found in:

http://www.itc.nl/research/phd/phd_graduates.aspx

PE&RC PhD Education Certificate

With the educational activities listed below
the PhD candidate has complied with the
educational requirements set by the C.T. de
Wit Graduate School for Production
Ecology and Resource Conservation
(PE&RC) which comprises of a minimum
total of 32 ECTS (= 22 weeks of activities)

Review of Literature (5.0 ECTS)
- Quantification of habitat fragmentation pattern and process for flagship
  species in the Qinling Mountains, China (2004-2005)

Writing of Project Proposal (7 ECTS)
- Quantification of habitat fragmentation pattern and process for flagship
  species in the Qinling Mountains, China (2004-2005)

Post-Graduate Courses (4.2 ECTS)
- Land science: concepts, tools and uncertainties in land use studies and
  landscape dynamics; Wageningen University (2005)
- IDL Basic programming; ITC (2007)
- Advanced statistics course; Wageningen University (2007)

Deficiency, Refresh, Brush-up Courses (1.4 ECTS)
- Basic statistics; PE&RC (2007)

Competence Strengthening / Skills Courses (1.4 ECTS)
- Scientific writing course; ITC (2005)

Discussion Groups/Local Seminars and Other Scientific Meetings (6.8 ECTS)
- Fort-nightly PhD discussion group; ITC (2005-2008)
- PhD and research seminars; ITC (2005-2008)
- PhD day in Tropical Ecology; University of Amsterdam (2008)

PE&RC Annual Meetings, Seminars and the PE&RC Weekend (2.6 ECTS)
- PhD weekend; Wageningen University (2007)
- Research day of department of Natural Resources; ITC (2005-2008)

International Symposia, Workshops and Conferences (5 ECTS)
- FAO/INBAR Global Bamboo Thematic Study Workshop; Beijing (2005)
- Fourth International Symposium on Multispectral Image Processing
  and Pattern Recognition; SPIE, Wuhan (2005)
- XXI ISPRS Conference; Beijing (2008)

Cover Photograph: Dr. Eveline Dungl
Cover design: Yali Si